THE EFFECT OF ADDED SOLID PARTICLES ON ELECTROSTATIC PROBES IN FLAMES

by

Eric Roy Miller

A thesis submitted for the Degree of Doctor of Philosophy in the University of Aston in Birmingham.

April, 1969.

SUMMARY

The work commenced as an experimental investigation of the effect of solid particles on positive ion densities in flames. The studies were carried out on hydrogen-oxygen-nitrogen flames, to which particulate materials were added at a controlled rate. The apparatus used in the production of the flames is described, and also the measuring system, which was a rotating electrostatic probe. The theory underlying the operation of electrostatic probes is discussed, and the particular problems encountered in using probes in high temperature flames are identified. This is followed by an account of the calibration of the rotating probe for the determination of positive ion densities. Measurement of this quantity in particulate flames was prevented by the current spikes resulting from the collision of the probe with solid particles. It is shown that the spikes are caused by thermionic emission of electrons from incandescent particles on the surface of the probe, and that this effect invalidates conventional probe measurements in flames containing solid particles. Analysis of the temperature dependence of the spikes produced by particles of carbon, lanthanum hexaboride, barium oxide and tungsten carbide has enabled the thermionic work functions of these materials to be determined. For barium oxide, a discontinuity in the temperature plot indicates that the work function of the liquid material is being measured. It is suggested that the spikes provide a novel means of determining thermionic work functions in hot gaseous environments.

PREFACE.

This dissertation, which is being submitted for the degree of Doctor of Philosophy in the University of Aston in Birmingham, is an account of work carried out under the supervision of Professor F. M. Page in the Department of Chemistry in the University of Aston, in the period from July 1964 to February 1968. Except where references are given in the text, the work described is original, and neither the whole nor any part has been submitted for a degree at any other university.

I should like to express my gratitude to Professor Page for his continued guidance and encouragement throughout, and to acknowledge helpful discussions with members of the Chemistry and other departments, in particular with Mr. H. Williams. I am grateful to the Ministry of Technology for the award of a Research Assistantship for the duration of the work.

E. R. MILLER.

APRIL 1969.

C O N T E N T S.

1. INTRODUCTION.

It has long been known that flames are conductors of electricity, although until about twenty years ago the subject remained an academic curiosity. Since that time interest has grown rapidly, and a great number of detailed investigations into the nature and properties of ions in flames have been reported. Still more recently there has been a growth of interest in heterogeneous combustion, in which solid or liquid particles suspended in the flame can modify the flame ionisation. This aspect of flame research has been promoted because of its promise of practical assistance with problems in two important technologies, rocketry and the direct generation of electricity.

The present generation of rocket vehicles depends on the chemical energy released from a fuel by combustion. Unfortunately ionisation occurring in the high temperature flame gases can seriously disturb radio communication with the vehicle, communications blackout being particularly serious when the so-called high-energy propellants are used. This term refers to propellant formulations to which light metals, particularly aluminium, have been added, largely to make use of the very high heat of combustion of the metal. This beneficial property carries the corallary that the combustion products will be highly stable, condensed-phase substances, resulting in the case of aluminium in the appearance of micron sized alumina particles in the rocket exhaust. It is found that aluminised propellants are particularly troublesome in regard to communications, and it has been suggested that electron emission from hot alumina particles is contributory to the high levels of iosisation observed.[1]

The other major reason for interest in flames containing condensed

phases is a consequence of the search for more efficient methods of energy conversion. The low efficiency of current methods of electricity generation, caused by inherent thermodynamic restrictions on the operating principles of conventional steam turbine generators, has led to the search for "direct" methods of energy conversion. In this class the concept of magneto hydrodynamic power generation has received much attention, and will almost certainly be the first direct method to come into use, provided that the remaining technological difficulties can be overcome. The method dispenses with the boilers and turbines of conventional power stations, and uses as the armature of a dynamo a highly conducting gas which is driven through a magnetic field. Electrodes, perpendicular to the magnetic field and the direction of gas flow enable current to be removed from the system. The essential requirement of the process is a gas which can be rendered conducting at a temperature which is not excessively high. In hydrocarbon flames, the basis of the open - cycle type of generator, the degree of natural ionisation of the components of the flame gases, i.e. H_2O, N_2, CO_2 etc., is very low, and the required conductivity is only achieved by seeding with materials of low ionisation potential, notably alkali metal salts. Even then acceptable levels of conductivity are only reached at temperatures in excess of 2500°C, when problems of corrosion become severe. An alternative solution to the problem may lie in the addition to the flame of small particles of low work function, which could produce the desired conductivity at lower temperatures. The use of barium oxide[2] and lanthanum hexaboride[3] has been suggested for this purpose.

There have been many theoretical treatments of ionisation in high temperature gases containing solid particles,[1,4-8] and it has been shown that enhancement or suppression of gaseous ionisation may occur, depending on the work function and size of the particles. However, experimental studies on this subject have been few in number, and at the outset the present work was planned as an investigation of the interaction of solid

particles and gaseous ions in laboratory flames of known composition and temperature. There are several experimental methods for studying ionisation in flames, and a brief summary of these at this point would be in order. For small laboratory flames the three most important techniques are

a) mass - spectrometry

b) microwave attenuation

c) electrostatic probes

Mass-spectromety, in which the ions are sampled and analysed according to their mass, is the only method which actually identifies the ions present in the flame. It is particularly useful in the formulation of reaction mechanisms, and its application by Calcote,[9,29] and Knewstubb and Sugden[10], has enabled the main sequence of ionisation reactions in hydrocarbon flames to be established. However, the interpretation of the results is complicated by the uncertainty that ions collected may not have been initially present in the flame, but may have been formed during sampling. Ions are normally sampled through a cooled pinhole inserted into the flame, so that before entering the instrument ions must pass through a cool boundary layer, in which attachment can easily occur. This problem is most severe with flames at atmospheric pressure, and there would be very great practical difficulties in using the technique in dust - laden flames.

Microwave measurements yield a value for the electron concentration in the flame, and are applicable over the range 10^8 - 10^{12} electrons/cm^3. In the most sensitive method, the flame is burned inside a resonant cavity, and the dissipation of microwave energy by the electrons damps its resonance characteristics. This change may be related to the electron concentration in the flame. Microwave techniques have been much used in kinetic studies in flames[11,12], and have been applied to the ionisation produced by carbon particles in flames by Sugden and Thrush[5], and Shuler and Weber.[13]

Woolley[19] has applied the technique to the ionisation of a variety of smokes in flames. The main difficulty with microwave methods is that of obtaining a sufficient degree of spatial resolution. The holes in the cavity walls which allow the passage of the flame enable the electric and magnetic fields to spread into the flame, and the section of flame under observation becomes ill - defined. The best resolution claimed for the method is 3 mm.

An electrostatic probe is an extremely simple device, consisting of a small electrode inserted into the flame. The current drawn by the electrode at various applied potentials is measured, and analysis of the measurements allows the determination of positive ion concentrations, and, with suitable precautions, the electron temperature. The outstanding advantage of probes is their ability to make local measurements, which makes them ideally suited for the production of ion profiles in flames. Probes have been used for this purpose by Calcote[28], and when used in conjunction with mass - spectrometric measurements they enable considerable insight to be gained into the mechanism of ionisation reactions. A major problem with the probe technique lies in the interpretation of the experimental measurements. Until recently there has been no theoretical treatment which applied at the pressures which exist in flames, and probe results have consequently been open to criticism. However a rigorous analysis of positive ion collection by a probe at high pressures has been carried out by Su and Lam[14], and this has been shown by Soundy and Williams to closely fit experimental observations in flames containing gaseous additives.

In view of the advantages of simplicity and high spatial resolution of electrostatic probes, it was decided to employ the technique in this work. Unfortunately it proved impossible to fulfil the original objective of the work, the investigation of the combined effects of particle and gaseous ionisation in flames. It was found that the presence of particles markedly altered the response of the probe in flames, in that a time dependent phenomenon in the form of current spikes was superimposed on the ion current

to the probe. The identification of the origin of this effect formed the major part of the work. It is shown that the spikes are caused by thermionic emission from incandescent particles which strike the probe. Electron flow from this source implies that the current to the probe is no longer simply an ion current, and thus cannot be analysed to yield ion concentrations. The effect therefore rules out the use of probes in particulate flames.

The spikes are of interest in their own right, since they yield information on the thermionic properties of the emitting material. In the course of the work the spikes produced by a number of materials were examined, and although absolute values for work functions were not obtained, the expected trends were observed. These results are particularly interesting since they suggest that the technique if further developed may allow the determination of electronic work functions in gaseous environments.

Fig. 1 The gas supply system

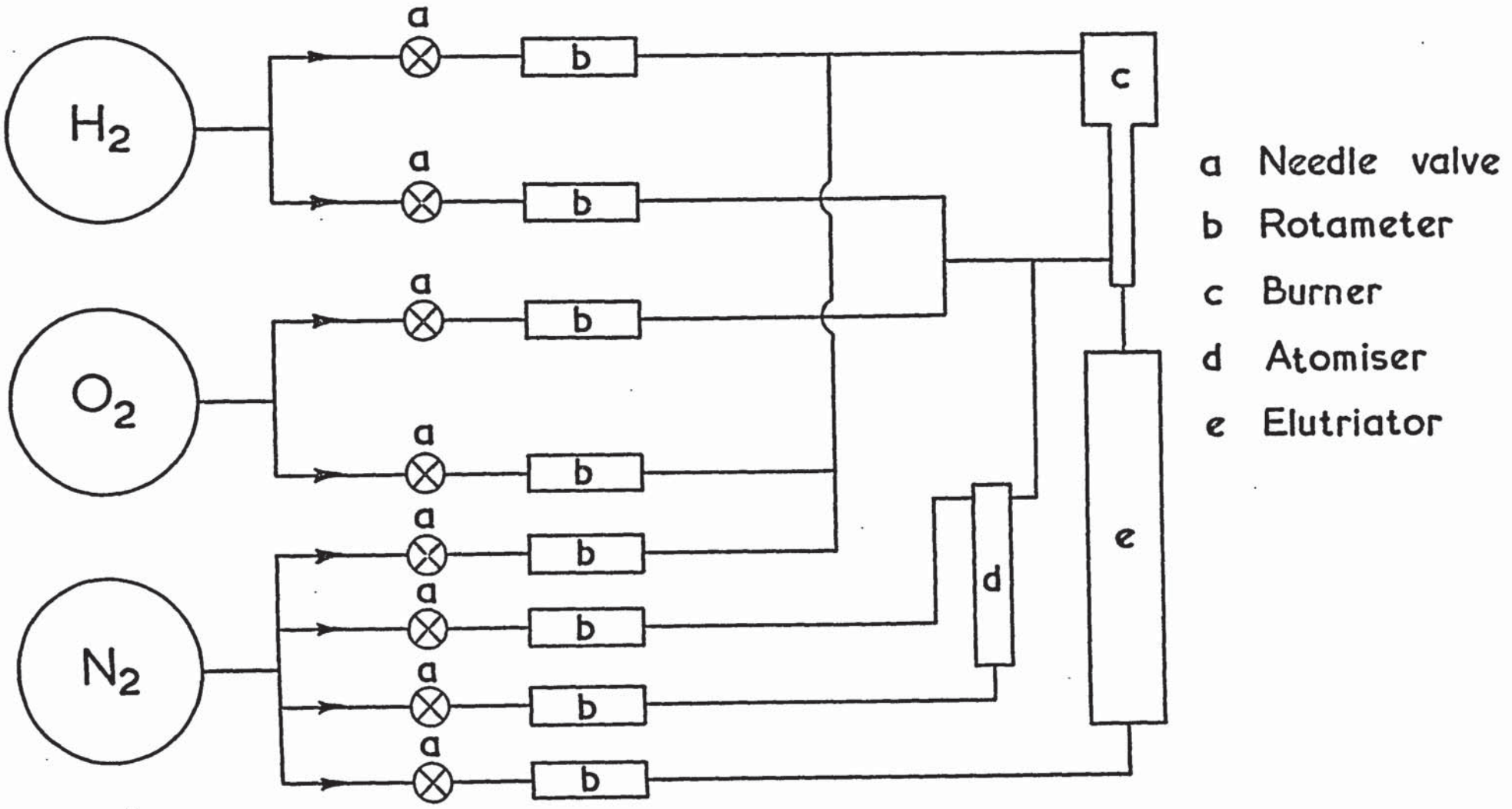

2. THE APPARATUS

2.1 THE FLAMES.

Hydrogen flames were chosen for the work to be described, since they possess a very low level of "natural" ionisation, which makes them eminently suitable as media in which to study the ionisation of compounds of interest. The flames used were premixed, laminar hydrogen-oxygen flames, containing nitrogen as diluent. All gases were obtained from commercial cylinders, their flow rates regulated by Clockhouse needle valves and separately metered by rotameters. For flow rates greater than 1.5 litres/min the rotameters were calibrated using a wet-gas meter, and for smaller flows with a bubble flowmeter.

In practice two flames were burned, an inner test flame on which measurements were made, surrounded by a sheath flame of similar composition which minimised effects of air entrainment. Flame compositions used in the investigations, together with their measured temperatures, are shown in Table I, and Figure I is a diagram of the layout of the gas supplies.

TABLE I

FLAME COMPOSITIONS AND MEASURED TEMPERATURES

No.	Pre-burned flame mixture $H_2 : O_2 : N_2$	Temperature ^oK
1	41 : 9 : 50	1806
2	41 : 10 : 49	1912
3	41 : 12 : 47	2135
4	41 : 13 : 46	2247
5	41 : 14 : 45	2336
6	41 : 15 : 44	2427
7	41 : 16 : 43	2487
8	48 : 16 : 36	2507
9	50.9 : 17 : 32.1	2570
10	55 : 18.4 : 26.6	2610
11	54.5 : 19.1 : 26.4	2630

Fig. 2

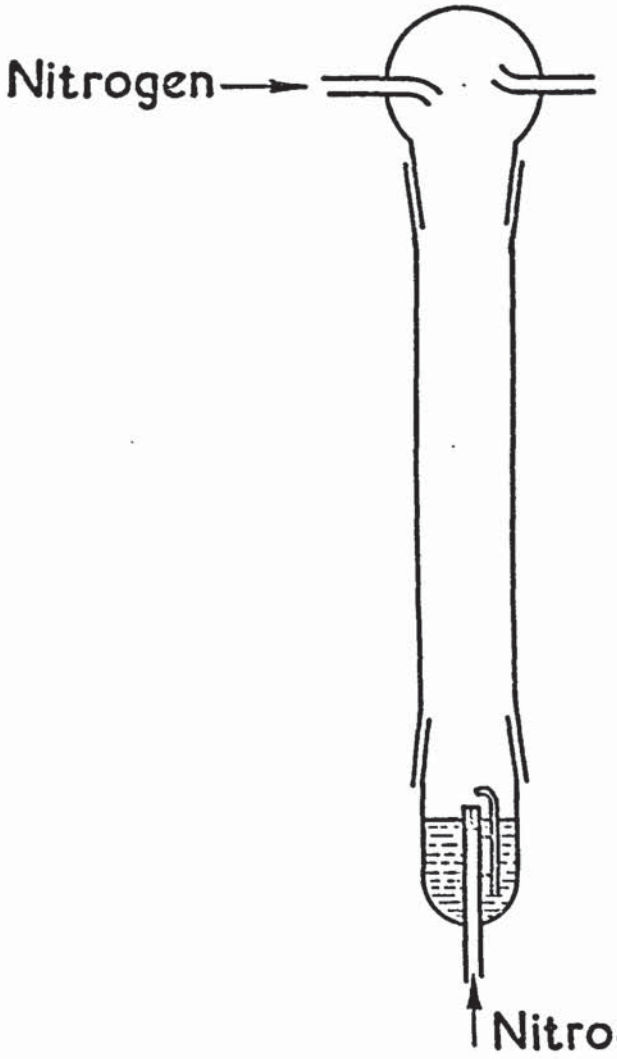

a) The atomiser

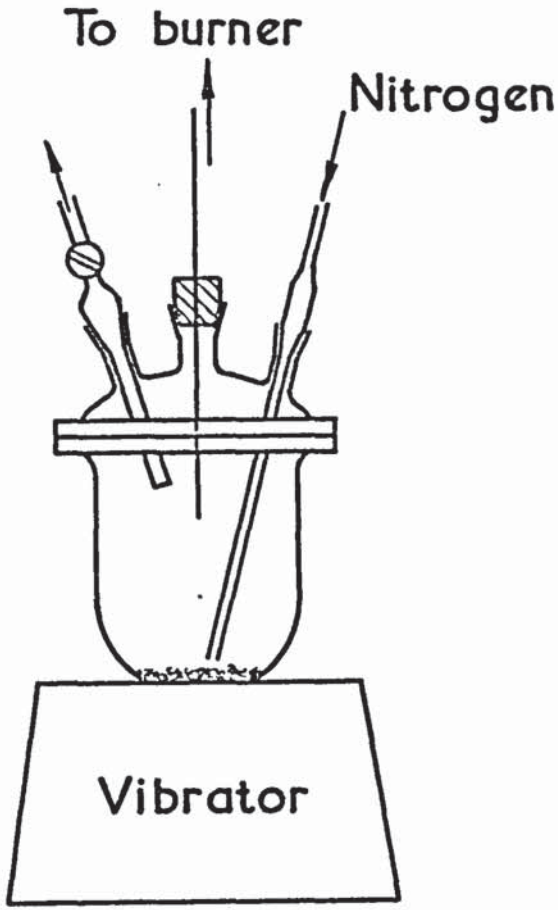

b) Dust cloud generator

2.2 SUPPLY OF LIQUIDS TO THE FLAME

Metal salt solutions were introduced into the flame as fine mists from a pneumatic atomiser (Figure 2a) operated by a part of the nitrogen supply to the inner flame. The gas flow across the tip of the jet created a reduced pressure at this point, and solution from the bulb was drawn up to be disintegrated by the high velocity gas stream. A settling column interposed between the atomiser and the burner ensured that only the finest droplets reached the flame. This type of atomiser has been used by many previous workers[15,16] and has been shown to be linear in operation over a wide range, the partial pressure of metal atoms in the flame being proportional to the molarity of salt solution in the atomiser for all concentrations below about 0.25 molar. Nitrogen flow for the atomiser was monitored by a mercury manometer and the apparatus was operated at a fixed pressure head of 21.6 cm of mercury throughout the work.

Calibration of the atomiser delivery was achieved along with the calibration of the probe, by matching experimental dilution plots for caesium with theoretical curves obtained using the Saha equation. The calibration procedure is described in Section 4.1.

2.3 THE SUPPLY OF SOLID PARTICLES TO THE FLAME.

2.3.1 GENERAL

Methods of introducing solid particles into flames fall into two classes, firstly the addition to the flame of solutions or liquids which will form particles on decomposition, and secondly the direct addition of powdered solids. It is well known to analytical chemists that some elements when sprayed into a flame as salt solutions will form oxides, so reducing the intensity of the atomic emission. A number of these elements, e.g. uranium, chromium, vanadium, produce refractory oxides of so low a vapour pressure that the oxide is present as unvapourised solid particles. The production of solid particles from aqueous sprays has been used by Kelly and Padley[17] in studies of particle formation in flames.

Liquid additives, conveniently conveyed to the flame by saturating a part of the gas supplies with vapour, have also been used by a number of workers. Egerton and Rudrakanchana,[18] investigating the combustion of zinc dimethyl observed the formation of copious quantities of oxide smoke. This approach was also used by Woolley[19] in studies on iron and nickel carbonyls. However, the use of either volatile liquids or aqueous sprays for particle formation, although enabling delivery to the flame to be controlled within narrow limits, suffers from two disadvantages. The first of these is the obvious requirement that it must be possible to form the material to be studied by addition of a suitable compound to the flame. There are many cases in which this criterion cannot be satisfied, one of particular relevance to this work being that of alumina. When aluminium compounds were added to the slightly reducing flames used in these studies it was found that the major species present in the flame was the gaseous suboxide AlO. In consequence the behaviour of alumina can only be examined by addition of the oxide

itself to the flame. A second problem is the small particle size obtained when particles are formed from sprays or vapours. Particle diameters are usually below 1000Å and often below 200Å,[17] and for materials of high evaporation rate, particles of this size will be completely volatilised early in the flame. This occurrence is effectively a further restriction on the type of material which can be investigated by formation from sprays of vapours. In view of these considerations it was decided to adopt the alternative technique of conveying powdered solids to the flame.

The use of solid additives has been employed very litte in flame work because of the problem of maintaining a steady supply to the flame. Gilbert[20] has shown that this difficulty can be alleviated by the use of powder suspensions in liquids of moderate viscosity, which can be atomised into the flame. However, a different liquid mixture is required for each material studied, and the volatilisation of the last traces of liquid can cause premature disintegration of the particles, noted under similar circumstances by Kelly and Padley. It was thought that these difficulties could well be more troublesome than fluctuations in powder supply to the flame, and so the principle of using a dry dust suspension in nitrogen was adopted.

2.3. 2. THE DUST CLOUD GENERATOR.

The apparatus used in the initial work is shown in Figure 2b. Nitrogen, entering the vessel through the jet as shown, dispersed the powder lying at the bottom of the vessel. A slight positive pressure was maintained in the system, so that some small fraction of the contents of the vessel was caused to pass up the capillary tube communicating with the burner column, thus carrying particles to the flame. Powder was kept in constant motion under the jet by a vibrator, which also caused powder

Fig. 3 The Elutriator

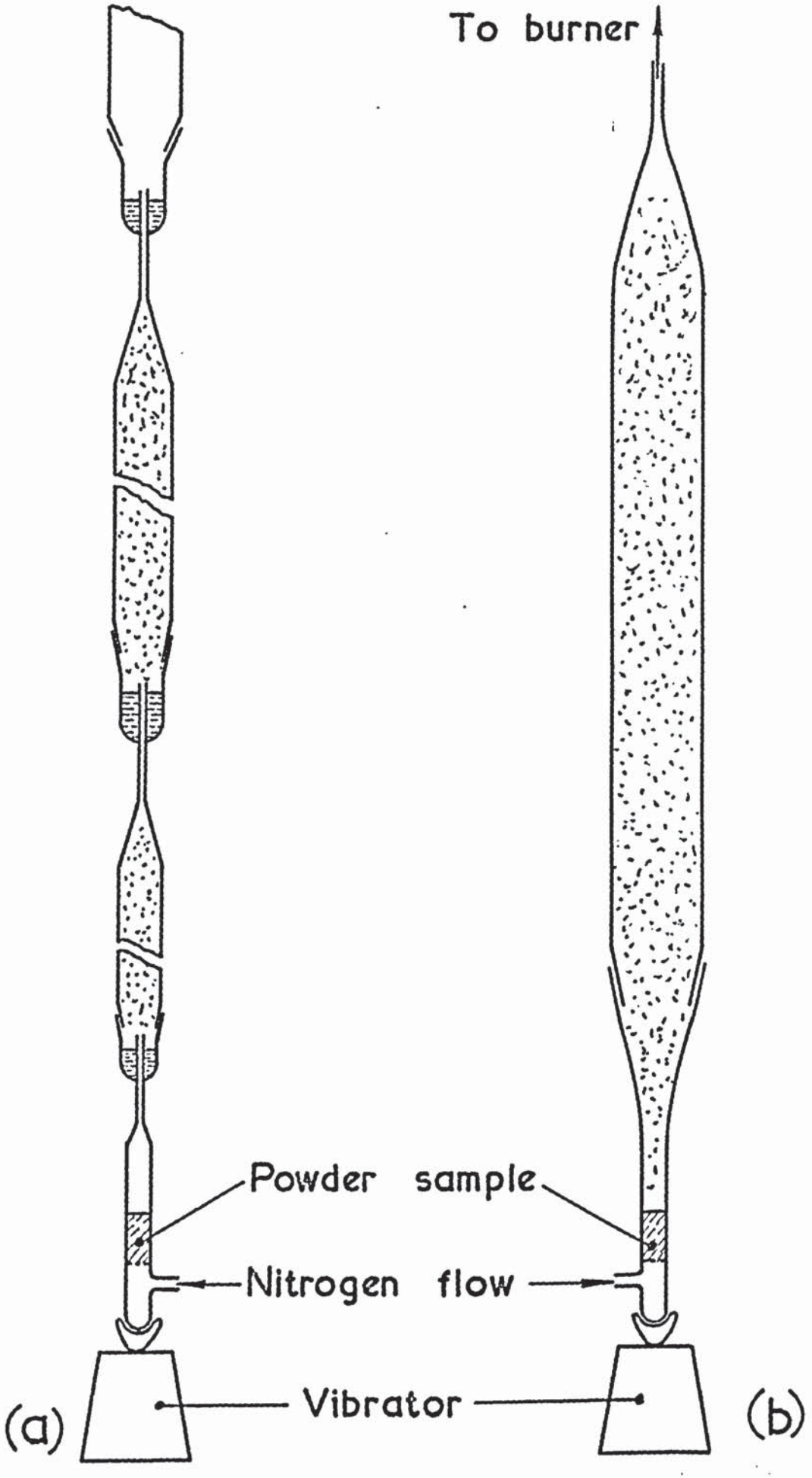

on the walls to return to the bottom of the flask. The most effective vibrator was found in practice to be a domestic orbital sander, which was mounted underneath the vessel. The apparatus was well suited to the requirements of low particle density in the flame, and operated reliably over long periods.

When investigations had reached the stage that quantitative analysis was required, the particle size distribution (53 μ to dust)of the aluminium powder in use was too wide to allow interpretation of flame phenomena. It was therefore necessary to fractionate the powder, and the method chosen was nitrogen elutriation. The elutriation apparatus is described below.

2.3. 3. THE ELUTRIATOR.

Elutriators are based on the principle that for a particle to be able to be suspended in a flowing fluid the velocity of the fluid must be greater than the terminal falling velocity of the particle. The terminal falling velocity, u_t, is given for small spherical particles of diameter d by Stokes Law, in the form.

$$u_t = \frac{a_e\, d^2\, (\rho_\rho - \rho)}{18\eta} \qquad 2.1$$

where a_e is the acceleration due to gravity, ρ_ρ and ρ are the particle and gas densities, and η is the gas viscosity. If, therefore, a powder is dispersed in a rising column of gas, and the velocity of the gas is reduced in steps, particles will settle out in order of decreasing particle size. In the apparatus used in this work (Figure 3a) the required stepwise reduction in gas velocity was achieved by passing the dispersion through a series of vertical glass tubes of increasing

diameter. The tubes were linked by lengths of narrow-bore tubing, which passed through the centre of the powder collecting cups. The powder dispersion was generated at the bottom of the column in a small vessel, where unclassified powder resting on a sinter was entrained by an upward flow of nitrogen. The vessel was vibrated very effectively by a "Whirlimixer" laboratory mixer.

Classification of aluminium powder was carried out using the elutriator. However, when fractions were examined under the microscope it was apparent that the distribution of particle sizes in each fraction was still unacceptably wide. This was at first attributed to the inherent limitation of all elutriators, which arises because the velocity distribution across any tube is not uniform, but tends to be parabolic. Hence a spread of particle sizes is usually obtained. In this apparatus the problem was aggravated by a further phenomenon. Inspection of the apparatus in operation showed that a great deal of turbulent mixing took place as the dispersion emerged into each tube, and particles were thrown down irrespective of their size. Mixing problems are overcome in commercial elutriators by painstaking design and precision engineering, and it became evident that improvement in the performance of the elutriator would demand an excessive (and unavailable) amount of time. The approach to particle sizing was accordingly modified.

Whereas the initial intention had been to classify powders by elutriation, and to supply sized fractions to the flame using the dust cloud generator, a single tube elutriator was now used to fulfil both of these functions. This apparatus is drawn in Figure 3b, and differed from the multitube elutriator only in that it consisted of a single tube, 8 cm in diameter, which was connected to the burner by a short length of flexible tubing. Part of the nitrogen supply to the inner

flame was used to operate the elutriator, and particles taken into suspension were carried at a steady rate to the burner. It is obvious with this system that the flow-rate through the elutriator governs both the quantity and the particle size of the powder conveyed to the flame. In practice the flow-rate was chosen to give the required particle concentration in the flame, and independent measurements of particle size were carried out.

2.3. 4 PARTICLE MEASUREMENTS.

The rate of powder supply to the flame was determined by passing the flow from the elutriator through a small weighed tube containing a sinter. The downstream side of the sinter was continuously pumped to give a pressure drop of 12 cm of water across the sinter, this being the normal pressure drop across the burner. Periodic weighing of the tube enabled an estimate to be made of particle concentration in the flame.

Particle sizing was accomplished by allowing the dust suspension leaving the elutriator to impinge on a microscope slide. Random fields of the powder film obtained were photographed using a Zeiss Universal photomicroscope, and the photomicrographs were analysed with a flying spot particle sizer.

Fig. 4 The burner

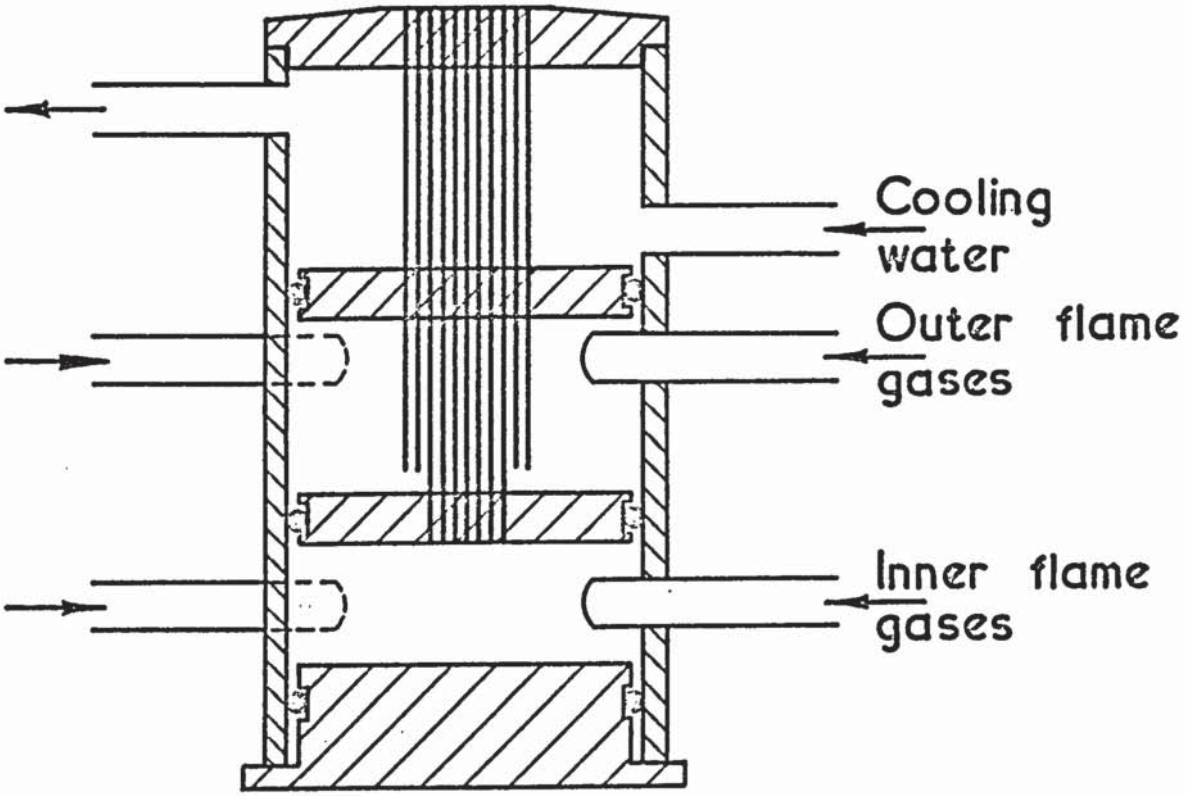

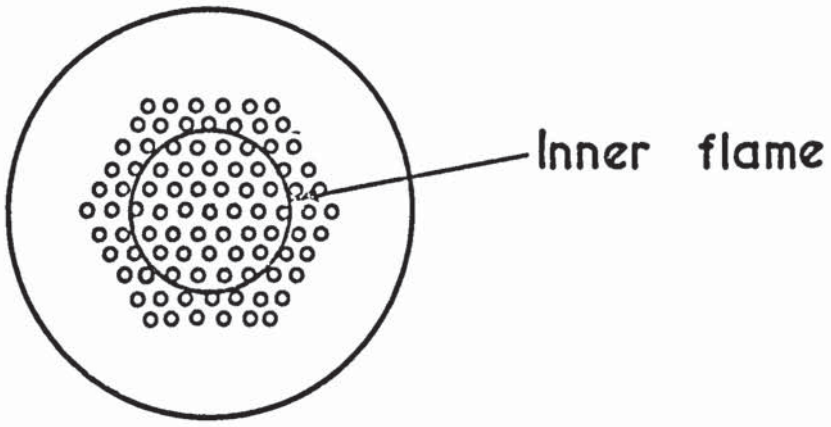

Top view

2.4. THE BURNERS.

2.4. 1 THE BASIC BURNER DESIGN.

The basic burner, shown in Figure 4, was of the water-cooled Meker type, the flame burning on a grid formed from the ends of stainless-steel hypodermic tubes, of internal diameter 0.032 inches. Burners of this type are frequently used in flame studies, and are often made from a bundle of hypodermic tubes tightly soldered together. These produce flames having a pronounced bulge immediately above the reaction zone, due to insufficient space between the tubes to allow for lateral expansion of the flame gases. This disadvantage was eliminated in the burner under discussion. For a gas expanding from ambient temperature to about 2000^{o}K at constant pressure, an approximate seven-fold increase in volume occurs, so that expansion in a horizontal plane is by a factor of $7\frac{3}{4}$. The capillary tubes of the burner were accordingly spaced apart such that the flame area was greater than the total area of the tubes by this factor.

In the construction of the burner, each tube was individually located in pre-drilled brass discs, with 0.063 in. between tube centres, before the whole assembly was soldered. These discs served to separate the three compartments of the burner when the tube assembly was fitted into the burner barrel. The top compartment was used for water cooling, while the centre and bottom compartments served as mixing chambers for the gases to the outer and inner flames.

This burner produced a laminar, parallel-sided flame from the burner top onwards. The primary combustion cones above each tube were 1 - 2 mm high, resulting in a very flat reaction zone, of prime importance in temporal studies of flame reactions. The outer sheath

Fig. 5 The burner for dust laden flames

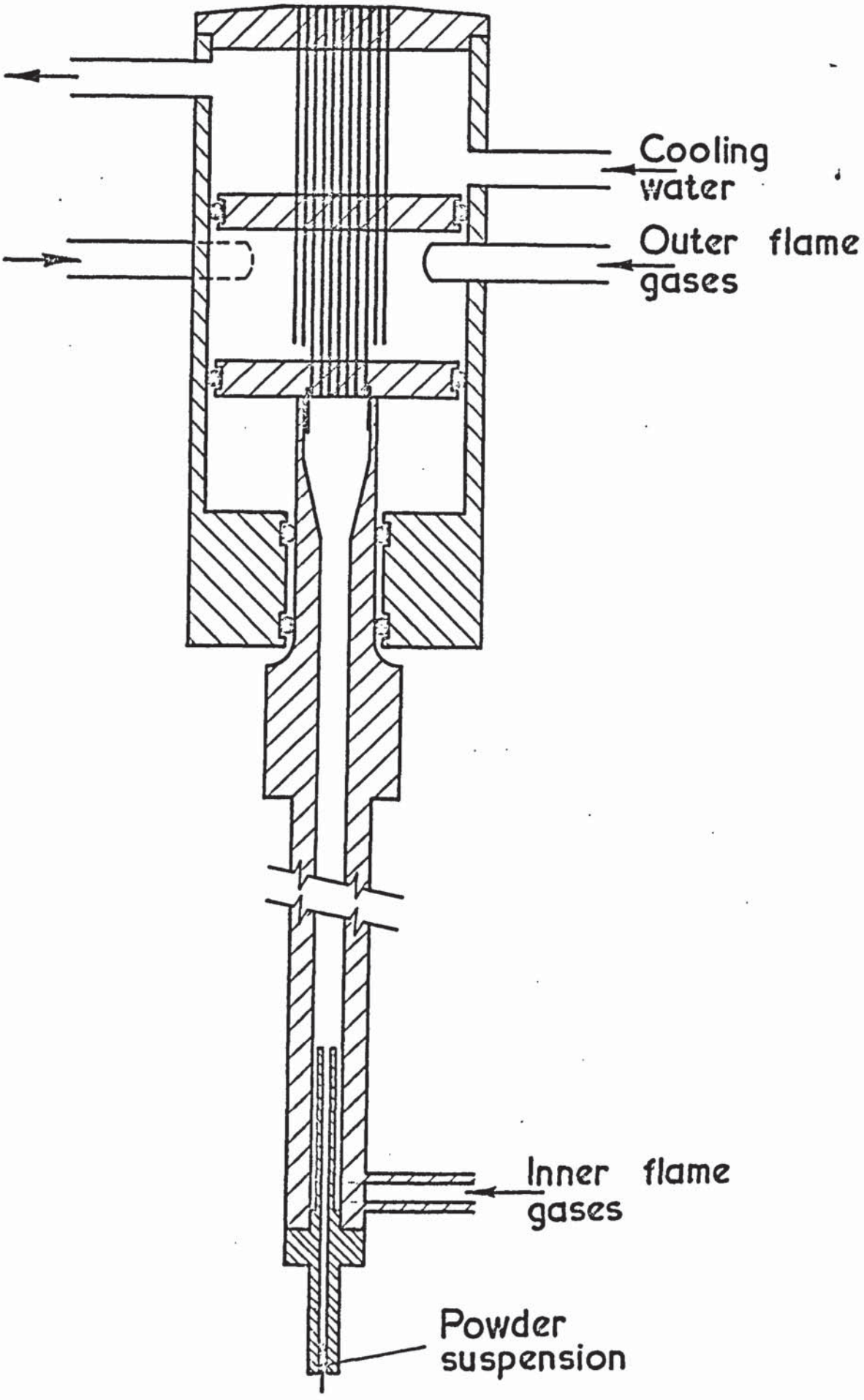

flame minimised effects of air entrainment up to a height of about 10 cm. The importance of this protection was readily demonstrated using the probe, which when swept through shielded flames containing alkali metals, produced a flat-topped pulse on the oscilloscope. If the outer flame was turned off, an 'M'-shaped profile was obtained for the same inner flame. The peaks in the ionisation at the edges of the flame are a consequence of secondary combustion.

2.4. 2 THE BURNER FOR DUST-LADEN FLAMES.

When powders were dispersed in the gases to the inner flame of the burner just described, it was found that the amount of material reaching the flame was very variable, and that the bottom mixing chamber of the burner frequently clogged up. This necessitated dismantling of the burner for cleaning. The clogging was caused by the swirling motion of the gases while mixing, which caused much of the powder to be deposited on the wall of the burner barrel. Periodically lumps of the deposit would fall into the gases and be carried into the flame, producing the observed irregularities. To alleviate this problem, the burner was modified as shown in Figure 5. In this design the dust suspension was conveyed to the burner through a brass tube, 30 cm. in length, terminating at the bottom of the capillary tubes. The length of this column ensured adequate mixing of the suspensions with the remainder of the flame gases. This burner was subject to much smaller variations in powder delivery, and was free from the problem of clogging. When cleaning was necessary this was readily accomplished by passing a very high flow of nitrogen through the delivery column while lightly tapping the burner.

2.5. MEASUREMENT OF FLAME TEMPERATURES.

Flame temperatures were measured by the sodium D-line reversal technique, which has been described in detail by several authors.[21,22] The method gives a value for the electronic excitation temperature of sodium, and can only be extended to describe the true thermodynamic flame temperature if there is thermal equilibrium between unexcited atoms of sodium and atoms in their first excited states. That equilibrium does prevail has been established by a number of workers,[23] who have shown that temperatures measured by the reversal technique are consistent with values obtained by other methods.

The background source employed in the measurements was a tungsten strip-filament lamp. Radiation from this lamp was focussed by a lens on to the centre of the inner flame, which was supplied with 0.25 molar sodium chloride solution from the atomiser. A second lens focussed light from the flame and from the lamp image on to the slit of a Hilger constant deviation spectrometer, and an iris diaphragm placed in between this lens and the flame ensured that light reaching the spectrometer from both lamp and flame was confined within the same solid angle. For each flame composition, the sodium D - lines were observed visually with the spectrometer, and the current through the lamp was varied until the lines were neither in emission nor absorption, but just merged into the background continuum. At the reversal point the colour temperature of the lamp filament and flame were equal. A number of observations were made on each flame, the reversal point being approached from both the emission and absorption directions, and it was found that the reversal point was reproducible to $\pm$ 10^{o}K.

A current - temperature calibration curve for the lamp was obtained by measuring the filament temperature with a Leeds and Northrup optical pyrometer, situated in the position occupied by the burner during the

Fig. 6 Temperature variation with height in flame

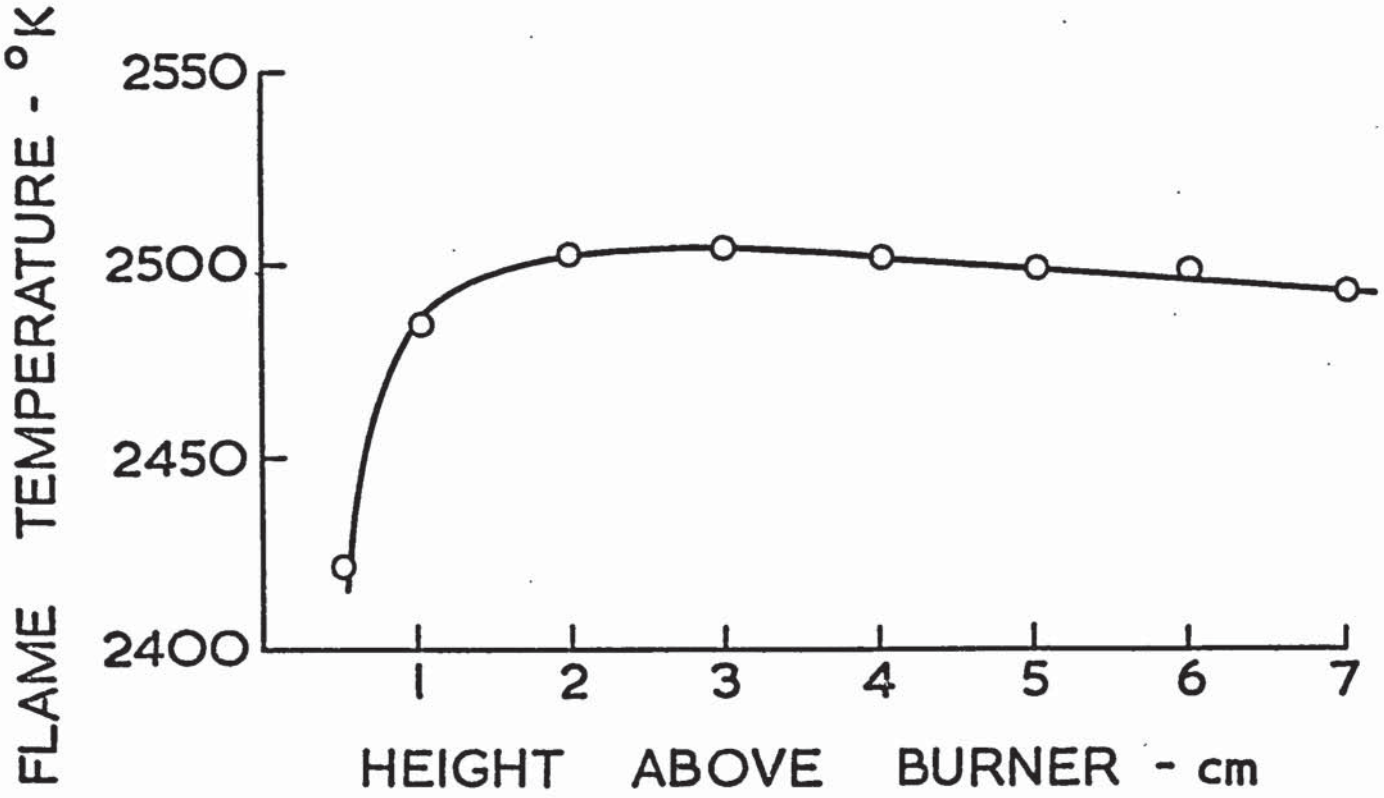

flame measurements. As the filament was observed through the lens used in the flame temperature measurements, no correction for reflection losses at this lens was required. However, the measured flame temperatures were corrected for the change in emissivity of tungsten with wavelength, since the pyrometer gave a value corresponding to the brightness temperature of the filament at 6550 $\mathring{A}$.

Measurements were made at a height of 5 cm for all flames, and in addition the variation of temperatuure with height above the reaction zone was studied for a number of the flames. A typical plot of temperature versus height is shown in Figure 6 for a flame at 2507^{o}K, used extensively in the subsequent work.

Fig. 7 The probe assembly

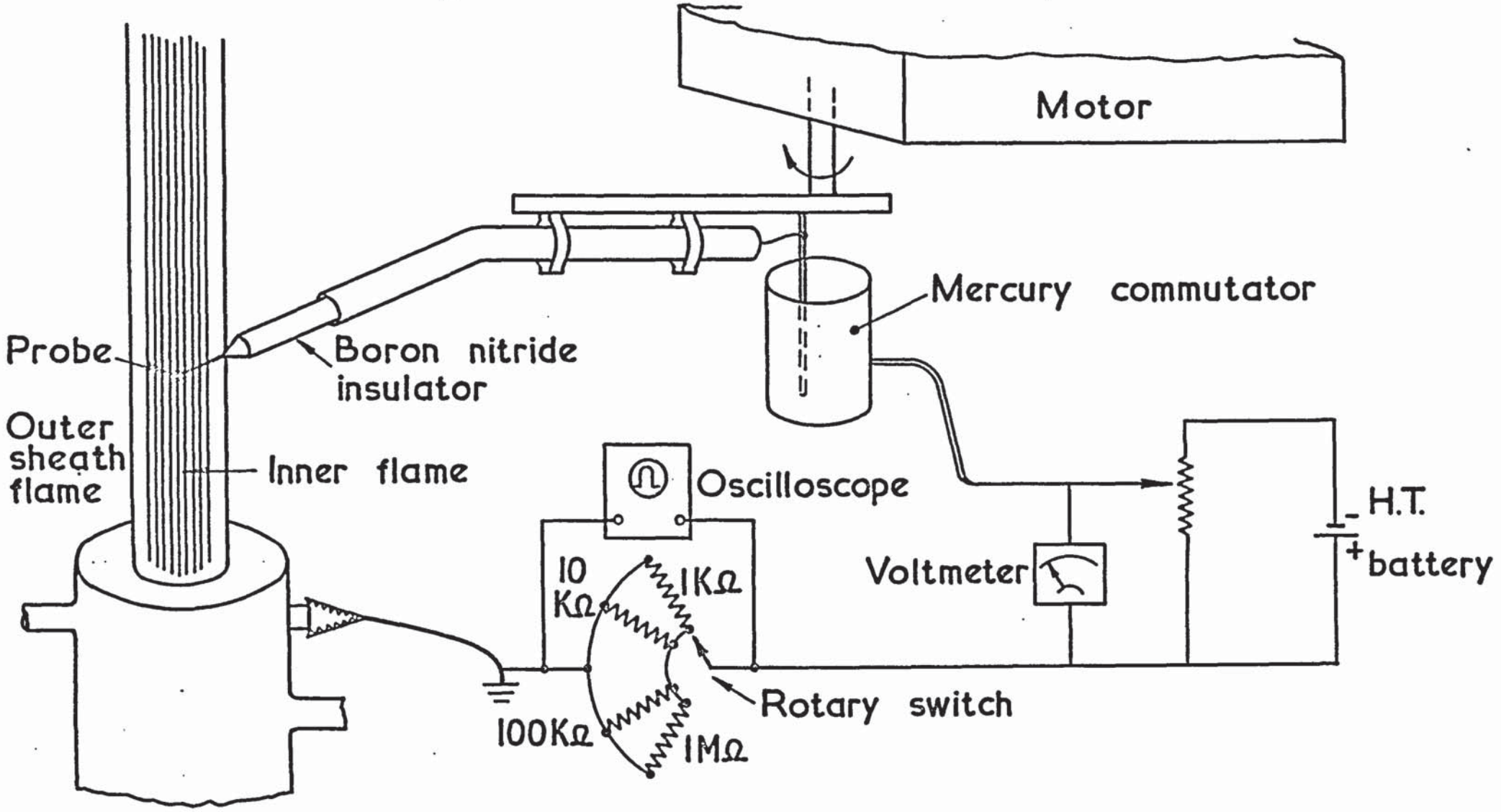

2.6. THE ELECTROSTATIC PROBE

A severe materials problem is encountered when probes are to be used in high temperature flames, in that there are no materials of sufficiently high melting point and non-violable nature which may be immersed in a flame without protection. A further limitation arises from the essential requirement that thermionic emission from the probe surface must be negligible. There are two principle methods of overcoming these problems, water-cooling of the probe and the use of a rotating probe which is allowed time to cool down in between each pass through the flame. Water-cooled probes have been reported,[29] but have the disadvantage that the presence of a cooling tube extending nearly to the probe tip may distort the ion sheath on the probe. In the work to be described, therefore, the probe was rotated by a synchronous motor and swept through the flame once a second, the residence time in the flame being about 20 milliseconds.

The probe itself, shown in Figure 7 together with its ancillary equipment, was a platinum sphere, 1.75 mm in diameter, formed at the end of 33 s.w.g. platinum wire. Thermal and electrical insulation of the probe wire, except for the spherical collecting area of the probe, was achieved by supporting the wire in a rod of boron nitride. This material retains its excellent insulating properties at high temperatures. A short length of wire between the spherical probe and the boron nitride insulator ensured that disturbance of the probe sheath was minimised. The probe was biased 100 volts negative to the burner top, which was held at ground potential. The current collected by the probe was measured on a Tektronix 515A oscilloscope, the time base of which was externally triggered as the probe entered the flame. For gaseous ions the oscilloscope response was a smooth pulse, the height of which was

related to the positive ion concentration. Pulse heights were normally measured visually against the graticule, but for detailed studies on flames containing solid particles oscillograms were taken with a Shackman oscilloscope camera.

For many of the measurements, particularly those on solid particles in low temperature flames, the oscilloscope was used at maximum sensitivity. Mains pick-up was found to be a problem in these measurements, and to eliminate this screened cable was used for all of the electrical leads, and the battery and other circuit components were placed in grounded metal boxes. Also when the probe was used for prolonged runs in flames containing either alkali metals or powders, the probe current tended to fall off because of contamination of the probe surface. Periodically therefore, the probe was cleaned by heating after treatment with hydrochloric acid, and by this means the sensitivity of the probe could be restored.

Fig. 8 Apparatus used in large scale model studies

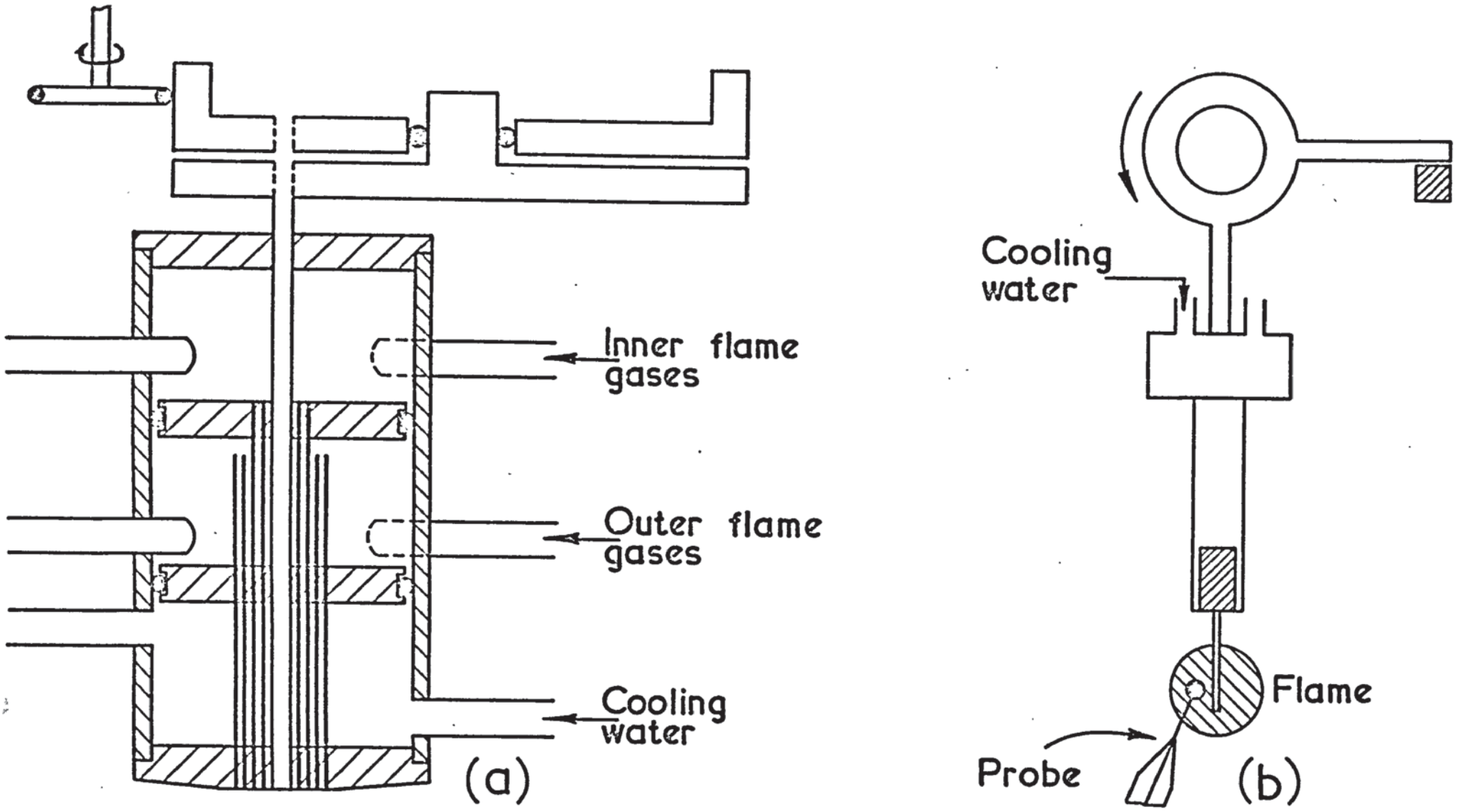

2.7. APPARATUS USED IN LARGE - SCALE MODEL STUDIES

The initial observation of the response of the probe to solid particles discussed in Section 4.2 was followed by two attempts to scale up the effect using very large particles, one method involving ball-bearings and the other a wire held in the flame. In this way the behaviour of a single particle of known size could be examined. It was hoped by this means to establish which of the possible theories was applicable to the effect.

2.7. 1 THE INVERTED BURNER

In order to cause ball - bearings to collide with the probe a burner was constructed with a hollow tube running axially along its length and extending beyond its base. Experiments were performed with the burner inverted, enabling the ball - bearings to fall through a downward burning flame. With the hot flames used this unusual operating position had very little effect on flame shape.

The probe itself was rather more substantial than the one normally used, consisting of a 3 mm sphere formed on a 1 mm diameter platinum wire. It was rotated at 20 r.p.m. for these studies. Control of the ball - bearings was achieved with the attachment to the burner shown in Figure 8a. On rotation of the top disc a ball - bearing was released down the tube when the position of the holes in the discs coincided. The top disc was rotated from a set position by an electric motor, started by a signal from the probe, and critical adjustment of the motor speed enabled collisions of the ball - bearings with the probe to be achieved with regularity.

2.7. 2 THE INSULATED WIRE

The other macro system consisted of a wire of 1 mm diameter inserted

through the centre of the flame in the path of the large probe used in the experiments with ball - bearings. The wire was fixed with ceramic cement into a cylindrical block of boron nitride, cemented in turn into a water - cooled copper holder, (Fig. 8b). Provided the cement was hardened sufficiently, and the end of the boron nitride was kept free of moisture, complete electrical insulation between the wire and copper holder was achieved. The holder was pivoted to allow the wire to swing out of the flame on collision with the probe, while tension from a spring maintained firm contact between the wire and the probe during the collision. The probe was rotated at 5 r.p.m. to minimise the impact when it made contact with the wire. To ensure that observations were made on equivalent lengths of wire, the end of each wire used was positioned in the flame at a fixed distance from a reference pillar on the burner.

This apparatus made it possible to simulate collision of the probe with a hot or cold particle, by controlling the length of time the wire was in the flame before collision occurred. The procedure followed was to measure the pulse height produced by the probe in the absence of the wire, and then by allowing the wire to enter the flame a few milliseconds before the probe, to observe the effect of a cool wire. When the temperature of the wire had become constant the effect of a hot wire could be determined.

The only three metals which were considered to be suitable for the wire were platinum (m.pt 2042^{o}K), iridium (m.pt 2716^{o}K) and tungsten (m.pt 3653^{o}K). Platinum tended to soften in the hotter flames and when this occurred the wire adhered to the probe and became locked in position in the flame. Most of the measurements were therefore made on tungsten and iridium.

3. THE THEORY OF ELECTROSTATIC PROBES.

3.1 FLAME PLASMAS.

An ionised flame is an example of a plasma, which is usually defined as a partially or fully ionised gas containing ions and electrons in approximately equal numbers, the whole assembly possessing overall electrical neutrality. Plasmas demonstrate characteristic behaviour arising from the simple fact that charged particles interact with each other by long-range forces. A charged particle will tend to be surrounded on average by particles of opposite charge, and will interact with many particles simultaneously. This interaction gives rise to collective modes of plasma behaviour which do not exist in ordinary gases, where the molecules interact by short-range forces only. A fundamental property of any plasma is the Debye length λ_D, which marks the division between single-particle behaviour and collective processes. The significance of this parameter may be obtained from a consideration of a spherical volume of plasma, from which nearly all of the electrons have been removed within a radius a. There will be produced an electrostatic potential $2\pi n e a^2$, where n is the number of electrons per cm^3 and e their charge, and a potential difference now exists between the centre and the neutral plasma boundary. Additional electrons will only be able to escape if their kinetic energy per degree of freedom kT/2 is given by

$$\frac{kT}{2} = 2\pi n e a^2 e \qquad 3.1$$

$$\text{or} \quad a = \left(\frac{kT}{4\pi n e^2} \right)^{\frac{1}{2}} \equiv \lambda_D \qquad 3.2$$

λ_D thus represents the largest distance over which a coulombic disturbance can extend in a plasma, and the plasma cannot of itself produce any significant charge separations exceeding the Debye length since the kinetic energies are insufficient. If the distance between two passing particles is appreciably less than λ_D, normal coulombic attraction or repulsion will occur and one can define the encounter as a simple collision, to which the ordinary laws of particle dynamics apply. However, if the minimum distance of approach of two particles is greater than λ_D, the collective motions of the surrounding plasma electrons induced by the passage of the particle will be such as to screen the test particle from feeling the influence of the other particle, or any others beyond the distance λ_D. In the vicinity of a boundary to the plasma such as an electrode, local fields will exist, and a sheath region will be produced containing predominantly particles of one sign. This sheath, which is of the order of a Debye length in thickness, serves to shield the bulk of the plasma from the influence of the perturbing field. A consequence of this sheath formation at plasma boundaries, is that a region of ionised gas must be many Debye lengths thick in order to deserve the name plasma. It is interesting to consider under what conditions the term plasma may justifiably be applied to laboratory flames, which have typical dimensions of a few centimetres. When numerical values are inserted into equation 3.2, this becomes

$$\lambda_D = 6.9 \left(\frac{T_3}{n'_e} \right)^{\frac{1}{2}} \qquad 3.3$$

For a flame at $2000^{\circ}K$ containing 10^8 electrons per cm^3 this equation gives a Debye length of 0.03 cm, while an electron density of 10^7 per cm^3 raises the Debye length to about 0.1 cm. It is apparent therefore that true plasma properties can only be expected in flames at this temperature which contain a minimum of 10^8 electrons per cm^3.

3.2 ELECTROSTATIC PROBES.

The electrostatic probe technique was originally developed as a means of measuring the potential distribution along the positive column of low pressure gas discharges. A probe in the form of a small insulated wire was inserted through the wall of the discharge and allowed to 'float', or assume its own potential relative to the plasma. The potential taken up by the probe was measured with an electrometer. However, the pioneering work of Irving Langmuir showed that very much more information could be obtained about the conditions in the plasma if the probe was not allowed to float, but was subjected to an externally applied potential. When operated in this manner a probe enables values to be obtained for the electron and positive ion concentrations, and the electron temperature.

A Langmuir probe usually consists of a small metallic sphere or wire which is inserted into the plasma at the location of interest. It is attached to a power supply capable of biasing it at various voltages positive and negative with respect to the plasma. Measurement of the current drawn by the probe enables a current-voltage characteristic to be constructed, from which the desired plasma parameters may be derived. For probe measurements to provide meaningful information about the plasma, it is an essential requirement that the perturbation of the plasma should be limited to a small region around the probe. The value of electrostatic probes lies in their ability to meet this specification over a wide range of conditions, because of the shielding properties of plasmas which are able to localise the disturbance created by the probe.

The first theoretical treatment of probe measurements was made by Langmuir[24,25], who concerned himself with low-pressure plasmas ($\sim$ 0·01 mm Hg) where mean free paths are large and collisions may be neglected. For high pressure plasmas some of his assumptions are no

longer valid, and in consequence modifications are required. In this discussion the original Langmuir theory will be reviewed first, as it introduces the basic concepts and terminology of probes. It will be followed by a consideration of the refinements necessary for collision dominated plasmas.

Fig. 9 Current - voltage characteristic for Langmuir probe

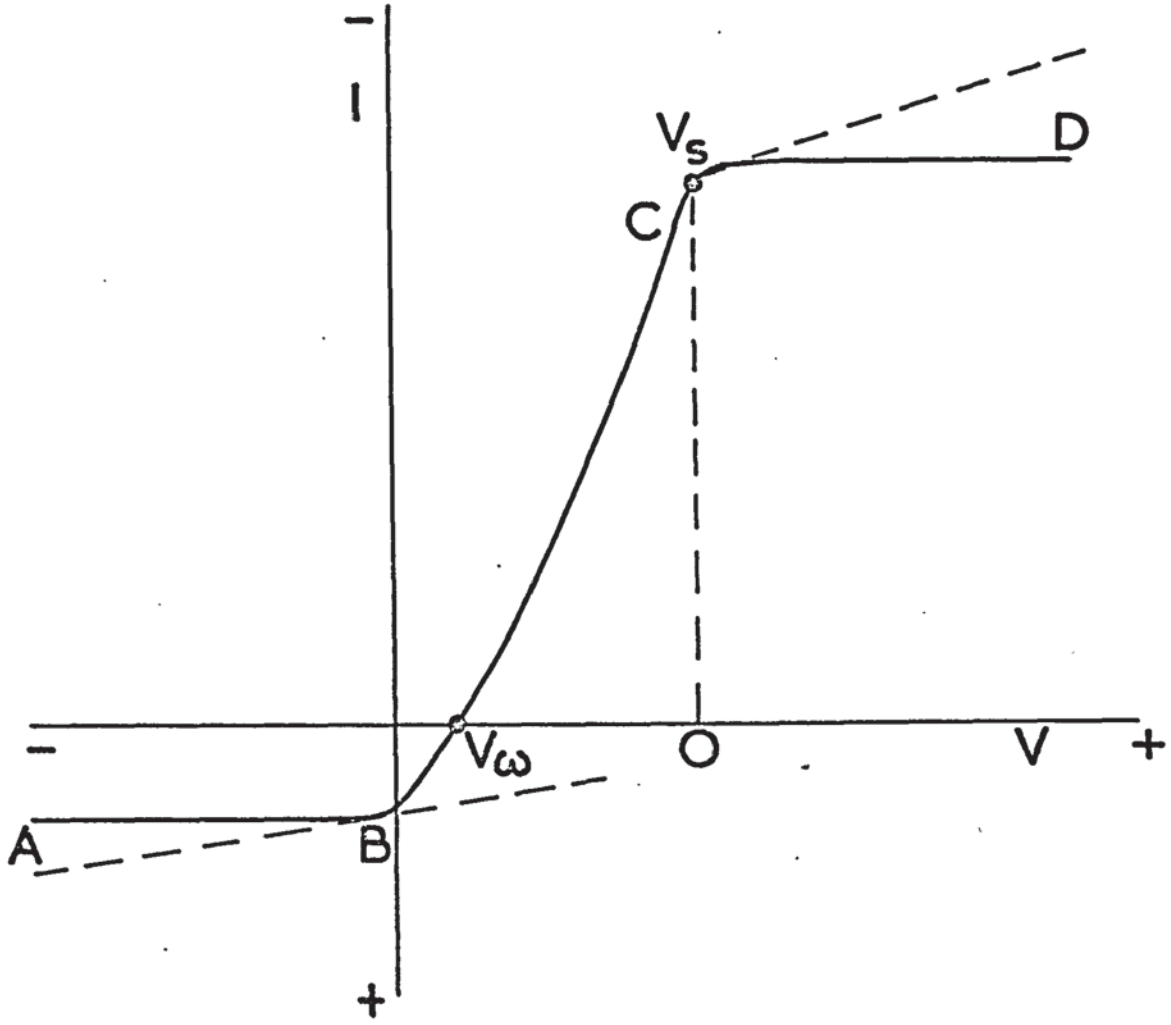

3.3 SIMPLE LANGMUIR PROBE THEORY.

The qualitative details of probe behaviour may be understood from Figure 9, which illustrates a probe current-voltage characteristic. Three regions of the characteristic are readily distinguished, corresponding to the saturation ion current (AB), the retarding field region (BC) and the saturation electron current (CD). The point at which the probe has the same potential as the surrounding plasma is marked on the curve as V_s, while V_w denotes the wall or floating potential where the probe draws no nett current from the plasma. V_w is the potential assumed by any insulated body immersed in the plasma.

When the probe is strongly negative relative to the plasma, electrons will be repelled and the current received will be entirely due to positive ions. These will form a space charge sheath over the probe surface, effectively screening the plasma from the field of the probe. Ions which strike the sheath will do so by virtue of their random thermal velocities, so that the probe will receive the random ion current of the plasma. Under these circumstances a decrease in probe potential will not enable any more ions to be collected, and a saturated ion current is drawn by the probe.

If the probe is made less negative, there comes a point (B) where a few of the high energy electrons can penetrate the positive ion sheath against the retarding potential. This causes a reduction in the nett probe current, which continues to decrease after B until it falls to zero at the point marked V_w, where the number of electrons reaching the probe is just equal to the random positive ion current. Potentials more positive than V_w cause a current of opposite sense to be registered, for the electron current to the probe will now exceed that from the positive ions.

Further reduction in the negative potential of the probe brings it to the plasma or space potential V_s. Here there are no electric fields present to disturb the plasma, which consequently extends right up to the probe surface, the remaining positive ion sheath being destroyed. Both ions and electrons now reach the probe by virtue of their random thermal velocities, so that the probe collects the carriers which would pass through the volume it occupies if it were not present. Because of the much higher velocity of electrons than ions very many more electrons are collected per second, and the current is mainly electron current.

If the probe is made increasingly positive relative to V_s, the small positive ion current rapidly disappears and an electron space charge sheath builds up around the probe. Since the probe is already receiving the full random electron current of the plasma an increase in its potential will not be reflected in a corresponding increase in electron current, i.e. the probe current is now saturated.

Quantitative interpretation of the characteristic just described enables values to be deduced for N_e and N_i, the electron and positive ion concentrations, and the electron temperature T_e.

3. 3. 1 THE DETERMINATION OF ELECTRON CONCENTRATIONS.

Electron concentrations are estimated from the saturated electron current. For a gas with N particles /cm^3 which are undergoing their random thermal motions with an average velocity $\bar{c}$, kinetic theory shows that the number of these striking unit area per second from all directions is

$$n = \frac{1}{4} N\bar{c} \qquad 3.4.$$

When these particles are electrons of charge e, they will constitute a current density per cm^2 per second of

$$J = \frac{1}{4} eN_e \bar{c} \qquad 3.5$$

Assuming that a Maxwellian distribution of velocities exists among the electrons, then the average velocity $\bar{c}$ is given by

$$\bar{c} = \left(\frac{8\,kT_e}{\pi m_e} \right)^{\frac{1}{2}} \qquad 3.6$$

where k is Boltzmann's constant, and T_e and m_e are the electron temperature and mass.

Combining 3.6 and 3.5 gives for the current density

$$J = \frac{1}{4} eN_e \left(\frac{8\,kT_e}{\pi m_e} \right)^{\frac{1}{2}} = eN_e \left(\frac{kT_e}{2\pi m_e} \right)^{\frac{1}{2}} \qquad 3.7$$

This current density is by definition the result of the random thermal motions of the elctrons, and it was shown earlier thatalong the region CD of the characteristic, that is the saturated electron current region, the probe current I_{es} is attributable to just this agency. The desoription of I_{es} is therefore

$$I_{es} = JA = eN_a A \left(\frac{kT_e}{2\pi m_e} \right)^{\frac{1}{2}} \qquad 3.8.$$

The measured value of I_{es}, together with a knowledge of the electron temperature as determined below, enable the value of N_e to be established.

3.3. 2 THE DETERMINATION OF POSITIVE ION CONCENTRATIONS.

The random ion current I_{is}, from which N_i is determined, may be expressed by an equation similar in form to 3.8 on replacement of N_e, T_e, and m_e by N_i, T_i, and m_i, so giving

$$I_{is} = J_{is}A = eN_i A \left(\frac{kT_i}{2\pi m_i} \right)^{\frac{1}{2}} \qquad 3.9$$

Unfortunately T_i is unknown and cannot be obtained from a retarding potential experiment as used for the electron temperature, because when the probe is positive with respect to the plasma, the ion current is masked by the very much greater electron current. However, it is often possible to assume a value for T_i, for reasons which are not applicable to the electron temperature T_e. The electrons in low pressure discharges are continuously supplied with energy from the electric field. In an elastic collision between an electron and a molecule, the electron because of its small mass is able to lose only a very small fraction of its kinetic energy, and as a result it is quite normal for electrons in the discharge to have energies much greater than those of the ions or neutral molecules. A collision between an ion and a molecule is quantitatively very different from the electron-molecule case, because an ion and a molecule have almost exactly the same mass. Consequently an ion may lose much of its kinetic energy when it strikes a molecule, and ions and molecules in a plasma exchange their kinetic energies in the same way as do the molecules in an unionised gas. Because the energies of ions and molecules are equilibrated in this way, the value of the gas temperature may be used for T_i, allowing N_i to be found from equation 3.9

3.3 3 THE DETERMINATION OF THE ELECTRON TEMPERATURE.

Over the region BC of the probe characteristic, electrons reaching the probe, do so only because their kinetic energy $\frac{1}{2} mv^2 = \frac{3}{2} kT$ is greater than the retarding potential on the probe. The shape of BC is thus a function of the electron energy distribution, which Langmuir assumed to be Maxwellian. Assuming the probe to be a perfect reflector, all electrons which strike it will rebound and the distribution will be undisturbed. Under these conditions the ratio of the electron concentration n' right at the surface of the probe to that outside the sheath is given by the Boltzmann

equation

$$\frac{n'}{n} = \exp\left(-\frac{eV}{kT_e}\right) \qquad 3.10$$

where n is the electron concentration just outside the sheath.

Now the currents at the probe surface and at the edge of the sheath are given by

$$J' = \frac{1}{4} n' e v \quad \text{and} \quad J = \frac{1}{4} n e v \qquad 3.11$$

so that $$\frac{n'}{n} = \frac{J'}{J} = \exp\left(-\frac{eV}{kT_e}\right) \qquad 3.12$$

J, the electron current at the sheath edge is the random electron current J_{es}, enabling 3.12 to be written logarithmically as

$$\ln I' = \ln JA = \ln J_{es} A - \frac{eV}{kT_e} \qquad 3.13$$

Thus if the electron current to the probe is measured as a function of V over the region BC of the characteristic, a plot of log I' against V should be linear with slope, $-e/kT_e$, determined by the mean energy of the electrons in the plasma. These plots are the normal method of estimating the electron temperature, and the linear form is usually obtained serves to confirm the assumption of a Maxwellian distribution of electron energies.

It is important to note that the use of Boltzmann's equation in 3.10 is strictly only valid for a reflecting probe, whereas in practice the probe draws a current. The above treatment can, however, be applied when small probes are used in low pressure plasmas, so that the mean free paths of the electrons are large compared with the probe diamater. Under these conditions the electrons come from regions so far removed from the probe that the Maxwellian distribution is unaffected.

Fig. 10 The double floating probe

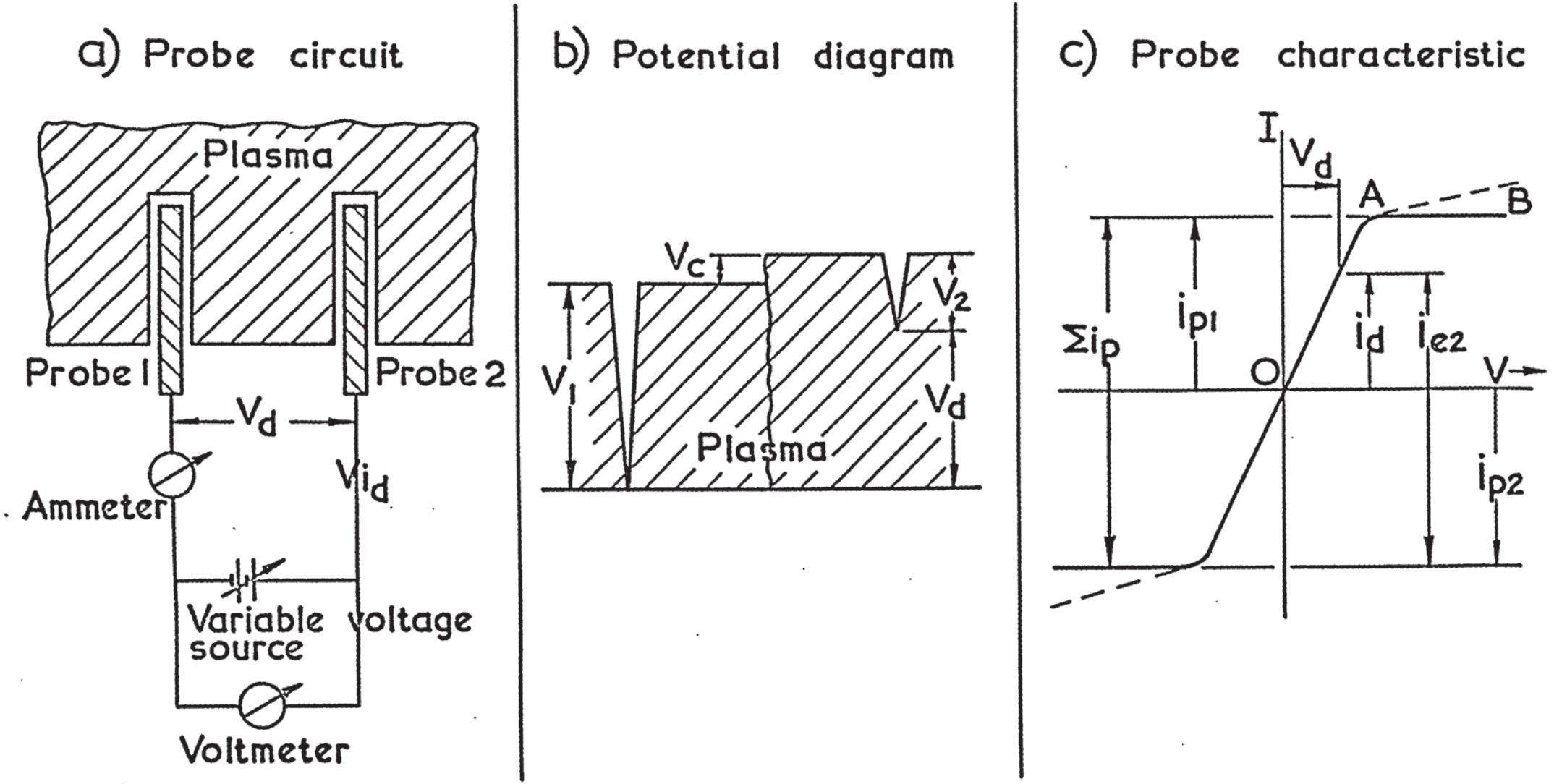

3. 4 THE DOUBLE-PROBE TECHNIQUE.

It was stated earlier that a criterion of probe operation is that the probe should not disturb the surrounding plasma. With negative probes no problem arises, because the presence of a positive ion sheath shields the plasma from the field of the probe. As a probe approaches plasma potential, however, the electron current drawn from the plasma may become so large that a serious depletion of electrons occurs in the region adjacent to the probe. The plasma potential seen by the probe then becomes a function of probe current. This problem may be overcome by the use of a double probe (Figure 10a), which was first developed by Johnson and Malter[26] for decaying plasmas, where the problem of depletion is particularly serious since carriers removed by the probe cannot be replaced.

The behaviour of a double probe is governed by the fact that the system as a whole is electrically floating, so that no nett current is drawn from the plasma. With no voltage applied ($V_d = 0$) both probes are at the same floating potential. If a potential difference is applied between the probes they will act in concert to fulfil the requirement of zero current. This can be seen from the potential diagram of Figure 10b, where, as a consequence of the applied negative potential, probe 1 has moved away from plasma potential and probe 2 has moved up towards plasma potential. The increased electron current into probe 2 flows round the circuit to compensate for the deficiency at probe 1. Thus i_d is the excess of electron current over positive ion current for probe 2. Further increase in V_d enables the portion of the characteristic CAB in figure 10c to be obtained, and reversal of the whole procedure traces out the lower limb of the characteristic.

The important point to be recognised is that the saturation of the

current to probe 2 is not a true electron current saturation, but is a limitation imposed by the saturation of positive ion current to probe 1. Herein lies the great value of the double probe technique, that the total current to the system can never exceed the saturation ion current, since any electron current to the probes must be balanced by an equal ion current. Thus the disturbance of the plasma is minimised. The characteristic provides values for the saturation ion current to each probe, and the electron temperature may be obtained from the transition region of the characteristic by the analysis set out below.

The equality of current to the probes sets

$$i_{p_1} + i_{p_2} = \sum i_p = i_{e_1} + i_{e_2} \qquad 3.14$$

The values of i_{e1} and i_{e_2} are given by the Boltzmann relations

$$i_{e_1} + i_{e_2} = \sum i_p = A_1 j_{01} \exp^{-\phi V_1} + A_2 j_{02} \exp^{-\phi V_2} \qquad 3.15$$

where $\phi = e/kT_e$ and j_{01} and j_{02} are the random electron currents in the plasma.

The diagram of potentials shows

$$V_1 = V_2 + V_d - V_c$$

Where V_c allows for any small difference in plasma potential between the regions surrounding the probes, plus the total contact potentials acting on the system.

Substitution of 3.16 into 3.15 yields on re-arrangement

$$\ln \left(\frac{\sum i_p}{i_{e2}} - 1 \right) = -\phi V_d + \phi V_c + \ln \left(\frac{A_1 j_{01}}{A_2 j_{02}} \right) \qquad 3.17$$

A plot of $\ln(\sum i_p/i_{e2}-1)$ against the applied voltage V_d will thus have a slope of ϕ, since V_c is a constant, which provides a value

for the electron temperature T_e. Equation 3.17 shows that the slope of the log plot is independent of errors in probe areas, electron random current densities, differences in local plasma potentials between the two probes, and contact potentials. The values of i_p used for the plot are obtained from the points at which the curve in Figure 10c breaks away from the saturated regions. Johnson and Malter[26] have shown that any uncertainty in the choice of these break points has very little effect on the slope of the log plot, since any change in the selected values of the i_p's introduces a change (in the same direction) in the estimated values of i_{e2}. However the real merit of the double probe is the one already emphasised, that excessive disturbance of the plasma is avoided because of the limit on electron current set by the positive ion current. This principle of double probe operation means that only the high energy tail of the electron energy distribution is samples, and the technique has been criticised on this account. This criticism can hardly be regarded as justification for the single probe method, in which the benefit of sampling the whole electron energy distribution is lost because of the errors caused by plasma depletion.

The characteristic in Figure 10c is applicable to a symmetrical floating probe for which the area A_1 and A_2 are equal. When $A_1 > A_2$, the smaller probe 2 will be able to receive a larger electron current before probe 1 is saturated with respect to positive ions. In the limit, when $A_1 \gg A_2$, probe 2 will be able to reach plasma potential and draw a saturation electron current, and an unsymmetrical probe characteristic will be obtained having the same form as the single probe characteristic discussed earlier. A single probe may in fact be considered as the limiting case of a double probe when the latter consists of two probes of greatly differing areas.

3. 5 ELECTROSTATIC PROBES AS DIAGNOSTIC TOOLS IN FLAME PLASMAS.

3. 5. 1. RELIABILITY OF PROBE MEASUREMENTS IN FLAMES.

Single electrostatic probes have been used at various times for the determination of electron concentrations, ion concentrations, and electron temperatures in flames, but it is now recognised that the range of applicability of the probe technique is more restricted in flames than is the case in glow discharges. The probe in flames differs from its counterpart in discharges in three principal respects.

First, the probe is exposed to a much higher gas temperature in flames, which raises practical problems of electrical and thermal insulation of the probe, and so affects the operation of the probe in that the use of small probes is rendered very difficult.

Secondly, the probe operates at pressures up to atmospheric, so that ions or electrons on their way to the probe will make collisions with neutral gas molecules. Under these circumstances the application of the simple Langmuir low-pressure theory to the measurements is not possible. The theoretical treatments applicable to positive ion collection in a collision-dominated plasma are considered in section 3.5.2.

Thirdly, there is no fixed reference of potential in the system, and it follows that the probe must be floating. In flame studies it is customary to place a large wire grid in the flame gases to define a reference of potential, and probe measurements are made relative to this grid. It is apparent that the arrangement is essentially a double probe, and that electron concentrations can only be measured by the single probe method when the area of the grid is sufficiently large to prevent its saturation

by positive ions. Furthermore, reliable values for electron temperature will only be obtained if no depletion effects occur as the probe nears plasma potential.

In spite of these difficulties, a number of flame studies employing single probes have been reported. Ion and electron concentrations and electron temperatures were measured by Calcote [27, 28, 29], in detailed investigations of the ionisation in hydrocarbon flames. Experiments were carried out at a range of pressures, and a number of different probe designs were employed with the object of achieving the necessary asymmetry conditions for single-probe action, and of minimising errors from leakage currents. Two surprising observations were made in the course of this work, first, that positive ion concentrations exceeded electron concentrations, in some cases by a factor as high as 30, and second, that very high electron temperatures existed in flames. In some hydrocarbon flames Calcote recorded electron temperatures exceeding the adiabatic gas temperature by $8000^{o}K$[29]. These observations are difficult to interpret. Calcote attributed the deficiency of electrons in the flame to the presence of negative ions. However, this is in conflict with mass spectrometric evidence. The OH^{-} ion, which by virtue of the abundence and high electron affinity of the OH radical is the most likely negative ion to be present, has been shown to occur in very small concentrations, and then only in the cool outer regions of the flame[30]. Moreover Padley [31], considering equilibrium attachment of electrons to OH radicals using the Saha equation, has pointed out that for OH^{-} to explain the discrepancy between positive ion concentration and electron concentration at low pressures, an unreasonably high concentration of OH radicals in the flame would be required. The persistence of enhanced electron temperatures beyond the reaction zone is also open to question, since the redistribution of excess energies of electrons produced in the reaction zone would be expected to be

quite rapid.

The difficulties of using single probes in flames have been discussed at length in an incisive article by Travers and Williams[32]. These workers examined the effect of an alteration in probe length on the saturation ion and electron currents to a single probe, at increasing distances along the flame. It was found that, for positive ion collection anywhere in the flame, an increase in probe length produced an increase in ion current in accordance with the increased collecting area of the probe. On the other hand, the saturation electron current to a positive probe situated in a region of high ionisation was independent of probe length, a clear indication that saturation of the reference electrode was occurring. Variation in probe length gives a much more sensitive indication of current limitation than does the variation in grid size used previously[28], and it must be concluded that earlier measurements of electron concentration were low.

It is very difficult to overcome the limitations of the single probe technique. The problem stems from the very nature of an ionised flame, which in the absence of additives is a plasma decaying rapidly with distance above the reaction zone. A grid situated high in the burned gases thus requires an enormous collecting area if current limitation at this electrode is to be avoided. The use of very small probes, which would assist in the achievement of the necessary assymetry in eletrode sizes, is hindered by the difficulties of thermally and electrically insulating such probes in high temperature flame gases. In general therefore, single probes are not applicable to the determination of electron concentration in flames.

Returning to the question of electron temperature in flames, Travers and Williams determined this parameter in low pressure ethylene and

acetylene flames using a symmetrical double probe. They found in all cases that the electron temperature was essentially the same as the gas temperature. Because of its safeguards against plasma depletion, a double probe is inherently more suitable for the determination of electron temperatures than is the single probe. The anomalously high values of electron temperature obtained in the early work are therefore probably in error, and it would appear that the use of the single probe for the determination of electron temperature is best avoided. The only area in which a single probe can be employed with confidence is in the estimation of positive ion concentrations. This fact, together with the high degree of spatial resolution which the probe technique possesses, led to its adoption in the work being described, in which the quantity of interest was the concentration of positive ions. It is now necessary to consider the means by which the ion concentrations are deduced from the measurements of ion current to a negative probe.

3.5. 2 THE COLLECTION OF POSITIVE IONS IN A COLLISION-DOMINATED PLASMA.

In the determination of positive ion densities by the Langmuir method, the ion saturation current I_{is} is obtained from the probe characteristic. If the positive ion saturation region is extrapolated to the plasma potential, I_{is} is obtained at a point where the sheath thickness is zero, and the area of the probe may be used as the collecting area. Alternatively the theoretical treatment may allow calculation of the area of the sheath, which with I_{is} gives the value of J_{is}, the random ion current in the plasma. There now remains the task of obtaining the number density of positive ions, N_i, from the experimental value of J_{is}. Equation 3.9,

$$I_{is} = eN_iA \left(\frac{kT_i}{2\pi m_i} \right)^{\frac{1}{2}} \qquad 3.9$$

was derived on the assumption that the mean free paths of all particles

in the plasma were large compared with the probe dimensions. When this assumptionis valid, the probe is screened from the plasma by a space charge sheath and does not affect the plasma beyond the sheath edge. Plasma parameters determined from the probe characteristic are then those of the undisturbed plasma. When this condition is violated, as it must be at high pressures, density gradients are created, which cause ions to diffuse from the plasma to the sheath region and allow the probe's electric field to penetrate the plasma beyond the sheath edge. The presence of the probe therefore causes a perturbation of both the plasma density and potential in its vicinity. In this case the plasma parameters determinod from the probe characteristic are not the same as those of the undisturbed plasma, and the straightforward application of equation 3.9 cannot now be made.

There have been many treatments of positive ion collection in a high pressure ($>$ 1 mm Hg) gas. Bohm, Burhop and Massey[33] treated the case of a probe at plasma potential, assuming that under these conditions no electric fields exist. For a spherical probe in a high pressure plasma whose ions have a mean free path λ, ions reaching the probe originate from collisions occurring at an average distance λ from the probe, i.e. within the spherical volume of radius λ no collisions will occur. The disturbance caused by the probe at a point P, distance λ from the surface, will be due to the obstruction offered by the probe to ions which would normally pass through the volume occupied by the probe to reach P. The probe will increase the density of ions at P in the ratio of thefraction of all the solid angle subtended by the probe at P, which is $r_p^2/4\lambda^2$ where r_p is the radius of the probe. When r_p/λ is small, the simple Langmuir equation 3.9 will be valid, and when r_p/λ is appreciable this factor may be used to correct the experimental value of N_i. The relationship between positive ion saturation current and ion density for a spherical probe is thus given by

$$I_{is} = eN_iA \left(\frac{kT_i}{2\pi m_i}\right) \frac{r_p}{\lambda} \qquad 3.18$$

Calcote and King[27,34], who found experimental values of N_i obtained by means of equation 3.9 for flames containing alkali metals to be below the theoretically predicted values by a factor of 200-400, adopted the work of the above authors. Using equation 3.10 they obtained ion densities which were essentially independent of probe size and in good agreement with theory. This procedure has been employed subsequently in other investigations, but the correction factor is rather large and is obtained from the incorrect assumption that no fields disturb the plasma when the probe is at the plasma potential.

A number of theoretical treatments specific to the positive ion saturation region in high pressure plasmas have been produced. Boyd[35] considered the problem of a spherical probe at pressures greater than 1 mm Hg. He divided the plasma around the probe into four regions, commencing at the probe surface with a space charge sheath in which high fields were sustained, and moving outwards through regions of weaker field to the undisturbed quasi-neutral region. By considering these regions in turn and matching the solutions at each boundary, he was able to derive a relationship for the ion currents to the probe. Apart from the rather ad hoc approach to the problem, a major drawback to this treatment is the necessity for an independent determination of the thickness of the probe sheath. This may be measured with difficulty in a glow discharge, but is impossible to obtain in flames, a result which precludes the application of the theory to these systems.

Schultz and Brown[36] evaluated the positive ion currents to a cylindrical probe for a range of gas pressures. They considered cases in which varying numbers of collisions occur in the passage of ions through the sheath, and derived expressions for the resulting ion currents. Microwave measurements

Fig. II Ion density n and electron density n_e in the vicinity of the probe

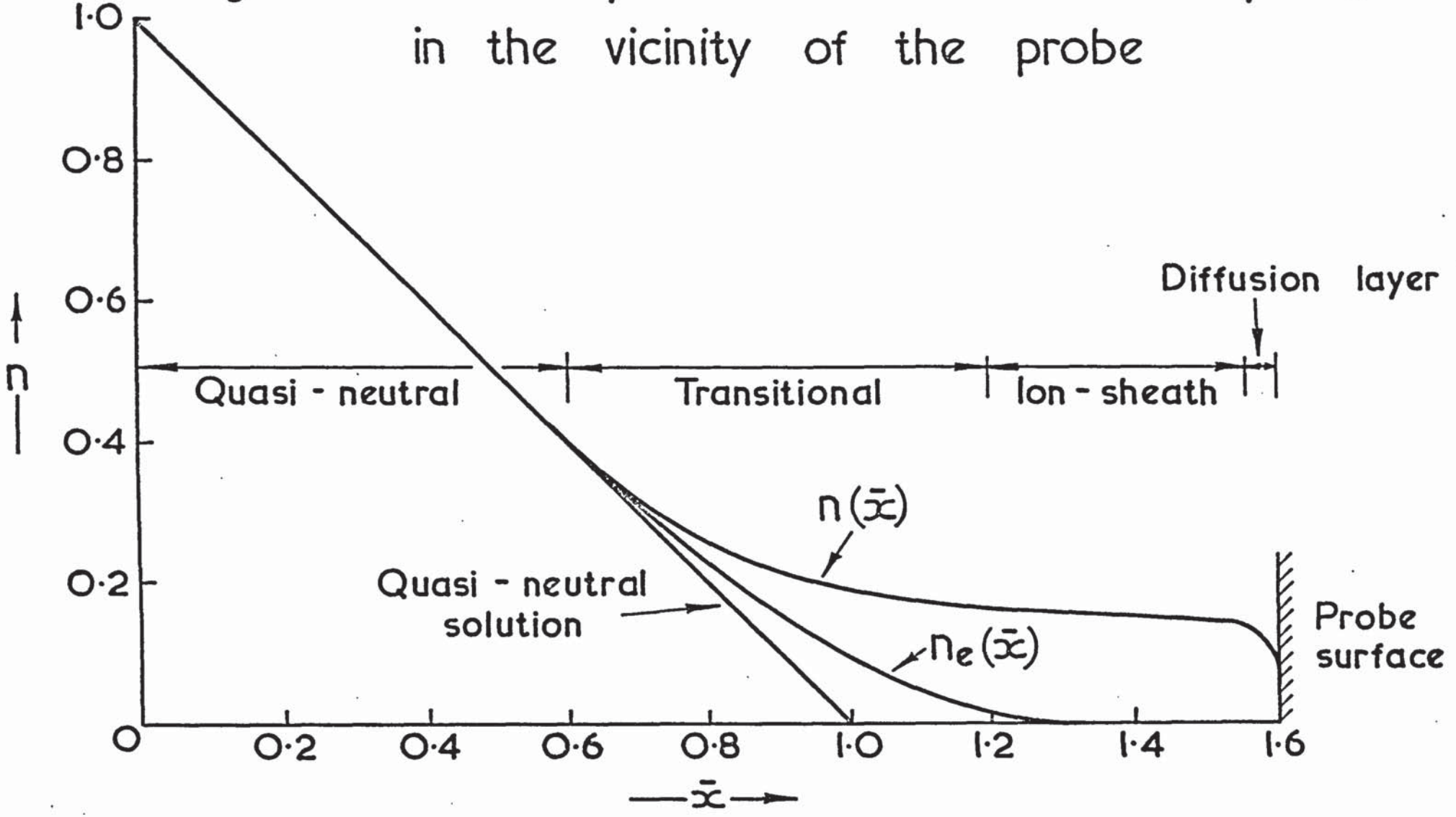

of electron concentrations showed extremely good agreement with their theoretical predictions. The theory has been applied to flames by Travers and Williams[32], and again very good correlation with experiment was reported.

The most rigorous treatment of positive ion collection by a negative probe is the continuum theory of Su and Lam[14], in which no a priori assumptions are made. The potential distribution around a charged body in a plasma is determined by Poisson's equation, together with the continuity equations for ions and electrons. Su and Lam start from these fundamentals and develop from them the relation between probe current and potential. In the course of the analysis a model is constructed of the plasma surrounding the probe, and it is shown that in general this is divided into four distinct regions. Far removed from the probe the plasma is undisturbed, and ions and electrons are present in approximately equal numbers in the quasi-neutral region. A transition region is interposed between the quasi-neutral region and the ion sheath region in which positive ions predominate, while immediately adjacent to the probe is an ion diffusion layer. This model of the plasma around the probe is shown diagrammatically in Figure 11, after Su and Lam. Here the ion and electron densities are shown at various values of $\bar{x}$, a dimensionless parameter inversely related to the radial distance from the probe surface.

This theory has been applied to flames by Soundy and Williams[37] who showed that for the particular case of a large probe biased to a high negative potential the analysis gives for the relationship between ion density N_i and probe current I,

$$N_i = \frac{1}{4\pi kT} \left(\frac{1}{4 r_p \mu_i}\right)^{\frac{2}{3}} \left(\frac{I^2}{\phi_p}\right)^{\frac{2}{3}} \qquad 3.19$$

where r_p is the probe radius, μ_i the ion mobility, and ϕ_p the probe potential. The other symbols have their usual meanings. The essential

assumptions in the derivation of this expression are:

(i) Only single ionised species are present.

(ii) The free electron temperature is equal to the gas temperature.

(iii) The probe radius is large compared to a Debye length.

(iv) The probe potential ϕ_p is so large as to make the current collected very much greater than that collected when the probe is at the plasma potential.

These assumptions are readily justified. The limited energy available in flames makes the presence of multiply charged ions very unlikely, and, as shown in the previous section, present evidence indicates the electron temperature and gas temperature to be equal. The third point can be satisfied by suitable choice of probe size. For the hottest flames used in the present work, around 2600°K, the lowest ion densities employed were 10^9 cm^{-3}. Equation 3.3 gives 10^{-1} mm for the Debye length in such flames. The probe used in the work was 1.75 mm in diameter, and this would therefore be expected to satisfy the third condition so long as the ion density did not fall below 10^9 cm^{-3}. The fourth condition is fulfilled if the probe is operated at a sufficiently high negative potential, which for the present work was - 100 volts.

Soundy and Williams demonstrated that the dependence of N_i on I was as predicted by equation 3.19, and subsequently confirmed[38] the dependence of N_i on $r_p^{-\frac{2}{3}}$ and $\phi_p^{-\frac{2}{3}}$. However they found the expression to be in error on absolute magnitude. The current predicted for a flame of known temperature and ion density was lower by two orders of magnitude than the experimental value. Since the only unknown in their calculation was the ion mobility, μ_i, which was assumed to be 1 cm^2 volt^{-1} sec^{-1}, the result casts some doubt on the accuracy of the commonly accepted value for the mobility of ions in flames. However, although mobility measurements date back to very early work in flames[58], and were often made using crude

experimental techniques, it is difficult to accept that the values could be in error to the extent suggested by the Su and Lam equation. The problem of the discrepancy between experimental and theoretical ion currents thus remains to be resolved. Leaving aside this difficulty, the favourable operating characteristics of negative probes in flames are now supported by a rigorous theoretical treatment, which closely correlates with experimental observations.

Fig. 12 Comparison of a normal probe characteristic and that for an emitting probe.

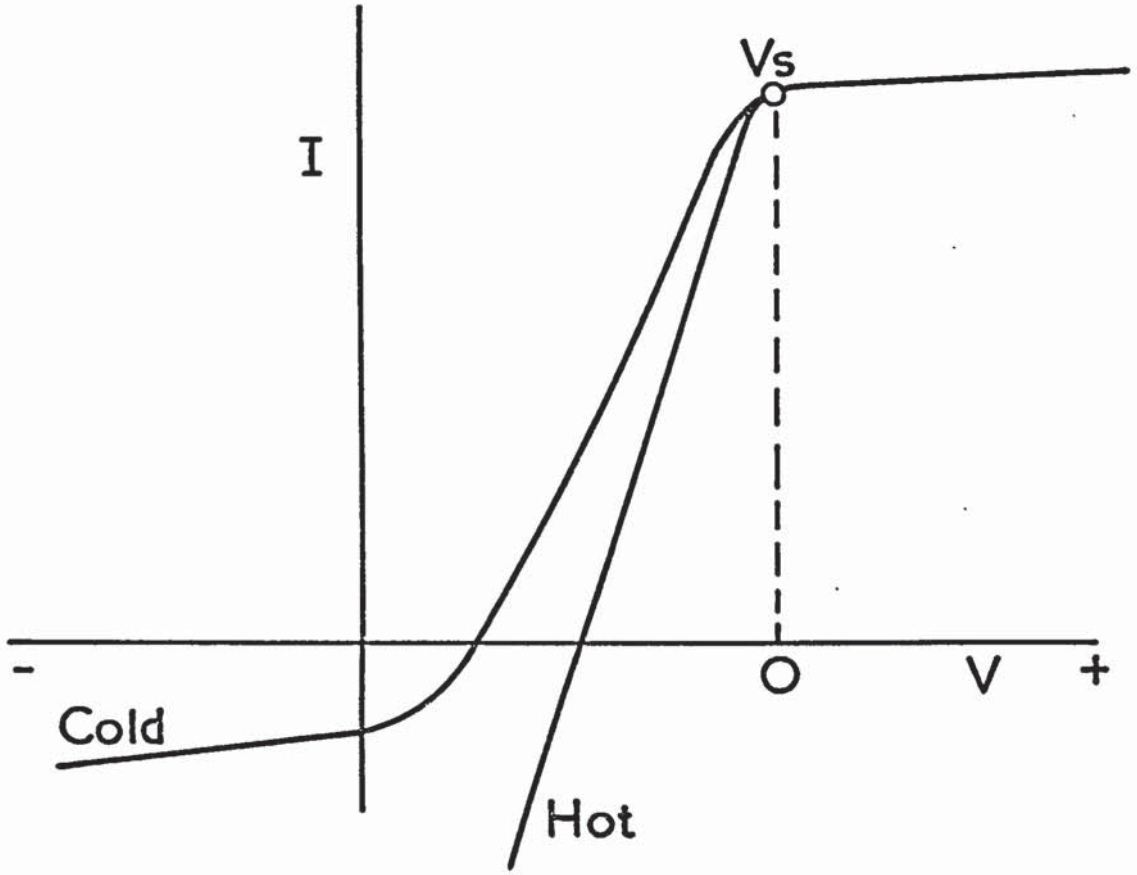

3. 6 EMITTING PROBES.

One of the difficulties of using probes in hot plasmas such as flames or arcs arises from the need to prevent thermionic emission from the probe surface, for emitted electrons will disturb the charge distribution around the probe. Normally probes which are water-cooled or which swing through the plasma are used, and it is general practice to employ metals of high work function, e.g. platinum and tungsten, in the construction of the probe. However, there are circumstances in which the probe is designed to emit thermionically, and Langmuir[39] has shown that probes of this type may be used to locate the plasma potential. Emitting probes usually consist of a small wire loop which can be heated by the passage of an electric current. When the probe is sufficiently positive, emitted electrons will be returned to the probe, and the probe will collect the normal electron current from the plasma. On the other hand, when the probe is negative relative to the plasma potential, emitted electrons will be able to escape and contribute an apparent ion current to the probe. The potential at which the hot-probe and cold-probe characteristics begin to diverge therefore locates the plasma potential, as shown in Figure 12. For negative potentials the difference between corresponding ordinates measures the electron current from the probe. A probe of this type will never draw a positive ion saturation current, and hence is not applicable to the determination of positive ion concentrations. At sufficiently negative potentials the saturation emission current corresponding to the probe temperature will be registered. The technique is thus restricted to the determination of plasma potentials.

4. THE USE OF THE ELECTROSTATIC PROBE IN FLAMES CONTAINING SOLID PARTICLES.

In section 3.5.2 mention was made of the success of the Su and Lam theory in predicting the observed dependence of N_i on $r_p^{-\frac{2}{3}}$, $\phi_p^{-\frac{2}{3}}$ and $I^{4/3}$, but of its failure with regard to the absolute magnitude of ion current. This weakness prevented the treatment of probe currents as absolute values from which ion concentrations can be calculated, and it was therefore necessary to calibrate the probe. In flames at atmospheric pressure where known concentrations of alkali metal can be readily supplied to the flame at a constant rate, calibration may be achieved by relating experimental measurements to the theoretical Saha ionisations for the alkali metal at the temperature in question. This procedure has the advantage that calibration of the atomiser delivery is achieved at the same time. The rotating probe was calibrated by this method, as described below.

4.1 CALIBRATION OF THE PROBE AND ATOMISER.

4.1.1 THE IONISATION OF ALKALI METALS.

The equilibrium ionisation of an alkali metal atom A to its positive ion A^+ and a free electron e^- is analogous to a diatomic dissociation process, and is governed by the equation.

$$A \rightleftharpoons A^+ + e^- \qquad 4.1$$

for which the corresponding equilibrium constant K is

$$K = \frac{[A^+]\,[e^-]}{[A]} \qquad 4.2$$

When the only ions present are A^+ and e^-, the condition of charge balance allows 4.2 to be written as

$$K = \frac{[A^+]^2}{[A]} \qquad 4.3$$

The value of K at any temperature is given by the Saha equation[40]

$$\log_{10} K = \frac{-5050V}{T} + \frac{5}{2} \log_{10} T - 6.49 + \log_{10} \frac{g_{A^+} g_{e^-}}{g_A} \qquad 4.4$$

Where V is the ionisation potential in electron volts, T is in ^oK, K in atmospheres and the g terms are the statistical weights of the ionised atom, the electron and the neutral atom. For alkali metals the final term is zero.

If $[A]_o$ represents the total alkali metal added, i.e. $[A]_o = [A] + [A^+]$, equation 4.3 gives

$$[A^+]^2 + K_1 [A^+] - K_1 [A]_o = 0 \qquad 4.5$$

This equation describing the ionisation of the alkali metals is over-simplified, since it neglects the effect on the level of ionisation of side reactions occurring between the metal and free radicals of the flame gases. For positive ions, the only occurrence which needs to be considered is hydroxide formation, which will reduce the number of neutral atoms and hence the ion concentration in the flame. Hydroxides are formed to varying degrees by the alkali metals, the effect being negligible for sodium and most marked for lithium. Caesium, which was used in the calibration of the probe, has recently been shown by Jensen and Padley[41] to form hydroxide in significant amounts even at temperatures as high as 2600^oK. Accordingly its effect on the ionisation equilibrium needs to be taken into account.

Under conditions when part of the alkali metal added to the flame takes part in the reaction

$$A + H_2O \rightleftharpoons AOH + H \qquad 4.6$$

then the mass-balance equation becomes

$$[A]_o = [A^+] + [A] + [AOH] \qquad 4.7$$

Defining $\phi = \frac{[AOH]}{[A]}$ this may be written

$$[A] = \frac{[A]_o - [A^+]}{1 + \phi} \qquad 4.8$$

which on substitution into 4.3 yields

$$K = \frac{[A^+]^2 (1 + \phi)}{[A]_o - [A^+]} \qquad 4.9$$

$$\text{or} \quad [A^+]^2 + \frac{K}{1+\phi}[A^+] - \frac{K}{1+\phi}[A]_o = 0 \qquad 4.10$$

This may be written

$$[A^+]^2 + K_1 [A^+] - K_1 [A]_o = 0 \qquad 4.11$$

where $K_1 = K (1 + \phi)^{-1}$ is the equilibrium constant for the ionisation reaction corrected for hydroxide formation.

Equation 4.11 gives $A^+ = (K_1 [A]_o)^{\frac{1}{2}}$ for $A_o \gg K_1$ and $[A^+] = [A]_o$

for $A_o \ll K_1$. A plot of log $[A^+]$ against log $[A]_o$ should therefore be a straight line of slope 0.5 at large $[A]_o$, turning over to a slope of unity at small $[A]_o$. The construction of this curve requires a knowledge of ϕ, which was obtained from the work of Jensen and Padley. If K_ϕ is the equilibrium constant for 4.6,

$$K_\phi = \frac{[AOH]\ [H]}{[A]\ [H_2O]} = \phi \frac{[H]}{[H_2O]} \qquad 4.12$$

Fig. 13 Calibration of the probe and the atomiser.

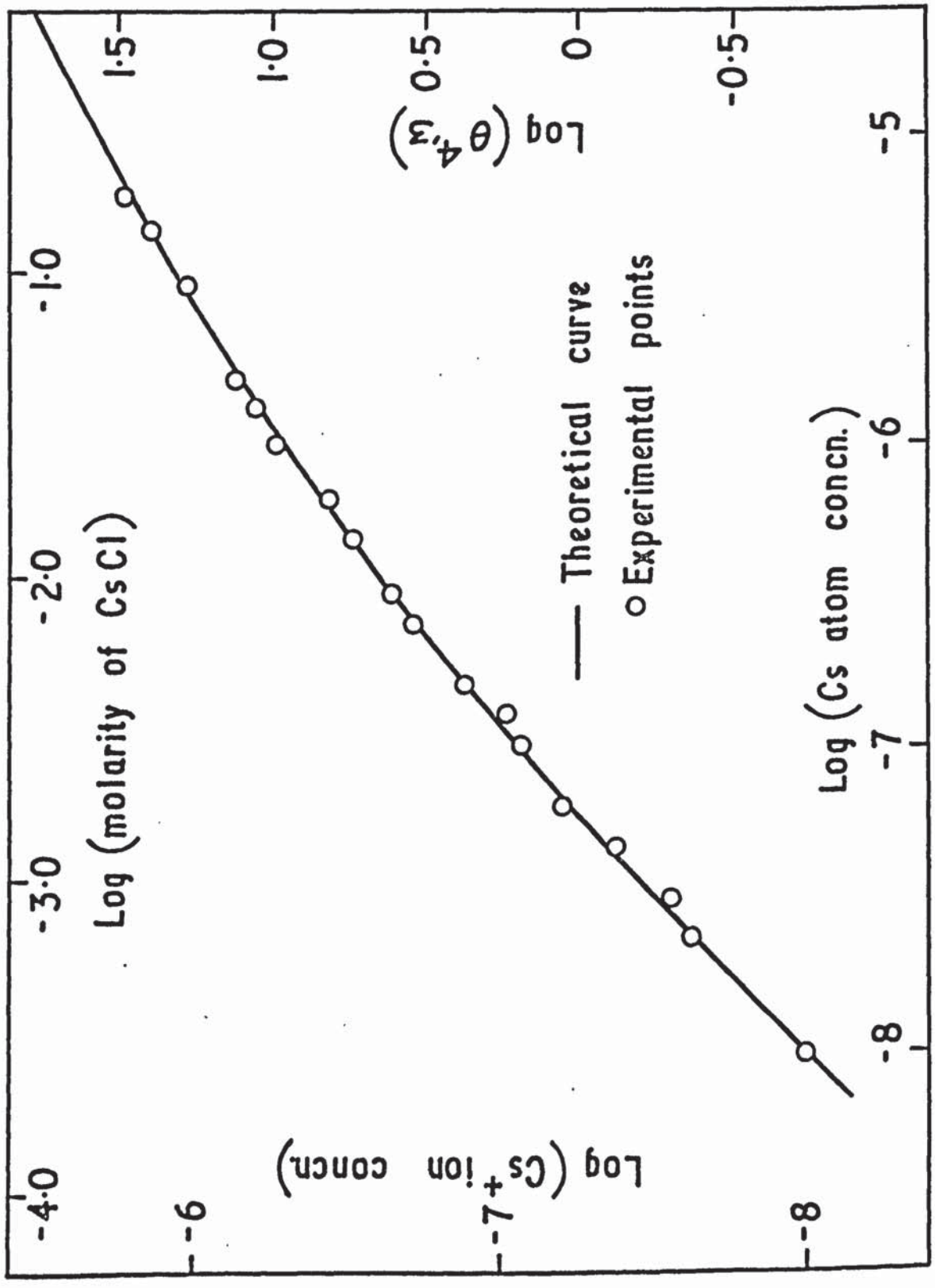

ϕ was calculated from this equation using the reported value of K_ϕ for caesium. It was assumed that a few cm above the reaction zone the concentrations of H and H_2O would be equilibrated, and theoretical values for these concentrations were used in the calculation. Substitution of the value for ϕ into equation 4.10 enabled a plot of log $[A^+]$ against log $[A]_o$ to be made for caesium at 2507^oK. The resulting curve, for the theoretical ionisation of caesium at this temperature, is shown in Figure 13.

4.1. 2 CALIBRATION PROCEDURE.

The rotating probe was used to measure the ion concentrations of a flame at 2507^oK supplied in turn with a range of caesium chloride solutions from 10^{-1} to 10^{-4} molar. By this means the pulse height (θ) on the oscilloscope was determined as a function of solution molarity (M). Since for the probe, ion concentration is proportional to $\theta^{4/3}$, and the caesium concentration in theflame is proportional to the caesium chloride molarity in the atomiser, a plot of log $\theta^{4/3}$ against lof (M) exhibits the same form as the theoretical one of log (Cs^+) against log $(Cs)_o$. By plotting the experimental log $\theta^{4/3}$ - log (M) curve on transculent graph paper it was possible to fit this curve to the theoretical curve, so locating the two vertical axes and the two horizontal axes with respect to one another. In Figure 13 the experimental points are shown fitted to the theoretical curve. This procedure simultaneously calibrates $\theta^{4/3}$ in terms of (Cs^+) and (M) in terms of $(Cs)_o$. The calibration factors so obtained were

1 unit of $\theta^{4/3} = 1.59 \times 10^{11}$ Cs^+ cm^{-3}

1 unit of (M) = = 1.06×10^{14} Cs_o cm^{-3}

The relationship between N_i and $\theta^{4/3}$ given by the Su and Lamb equation 3.19, is dependent on ion mobility, and this precludes the general application of the caesium calibration to any ion. It is therefore necessary to include a mobility correction factor in order to enable the

calibration to be transferred to other ions. It is well known, that for ions in the same gas, the term controlling the mobility is $(1 + M_g/M_i)^{\frac{1}{2}}$ [42], where M_g is the mass of the neutral gas molecules and M_i is the mass of the ion. From inspection of equation 3.19,

$$N_i = \frac{1}{4\pi KT} \cdot \frac{1}{(4r_p u_i^2)^{2/3}} \cdot \left(\frac{I^2}{\phi_p}\right)^{2/3} \qquad 3.19$$

it can be seen that the mobility correction factor will be of the form

$$\left(\frac{1 + M_g/M_{Cs^+}}{1 + M_g/M_i}\right)^{\frac{2}{3}} \qquad 4.13$$

where M_{Cs^+} is the mass of the caesium ion (133). The general equation for ion collection by the probe, in the flame in question, thus becomes,

$$N_i = 1.59 \times 10^{n} \left(\frac{1 + M_g/M_{Cs^+}}{1 + M_g/M_i}\right)^{\frac{2}{3}} \theta^{4/3} \qquad 4.14$$

It can be seen from equation 4.14 that the mobility correction factor will be most important for light ions ($M_i < M_g$), while for heavy ions, ($M_i > M_g$), the deviation from the caesium calibration will be quite small. For a hydrogen - oxygen - nitrogen flame, M_g for these purposes may be taken as 23, the mean of the masses of H_2O (18) and N_2 (28), since these are the predominant neutral gas molecules in the flame.

Fig. 14 Oscillograms of the response of the probe

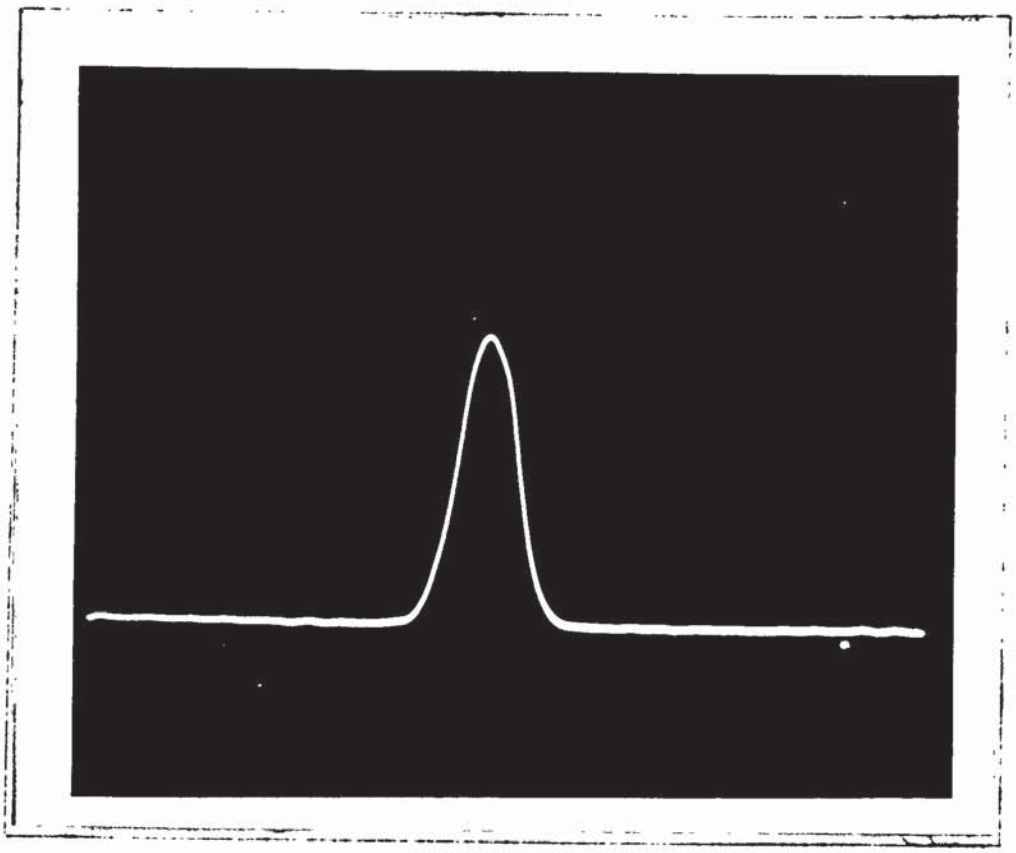

Gaseous ions

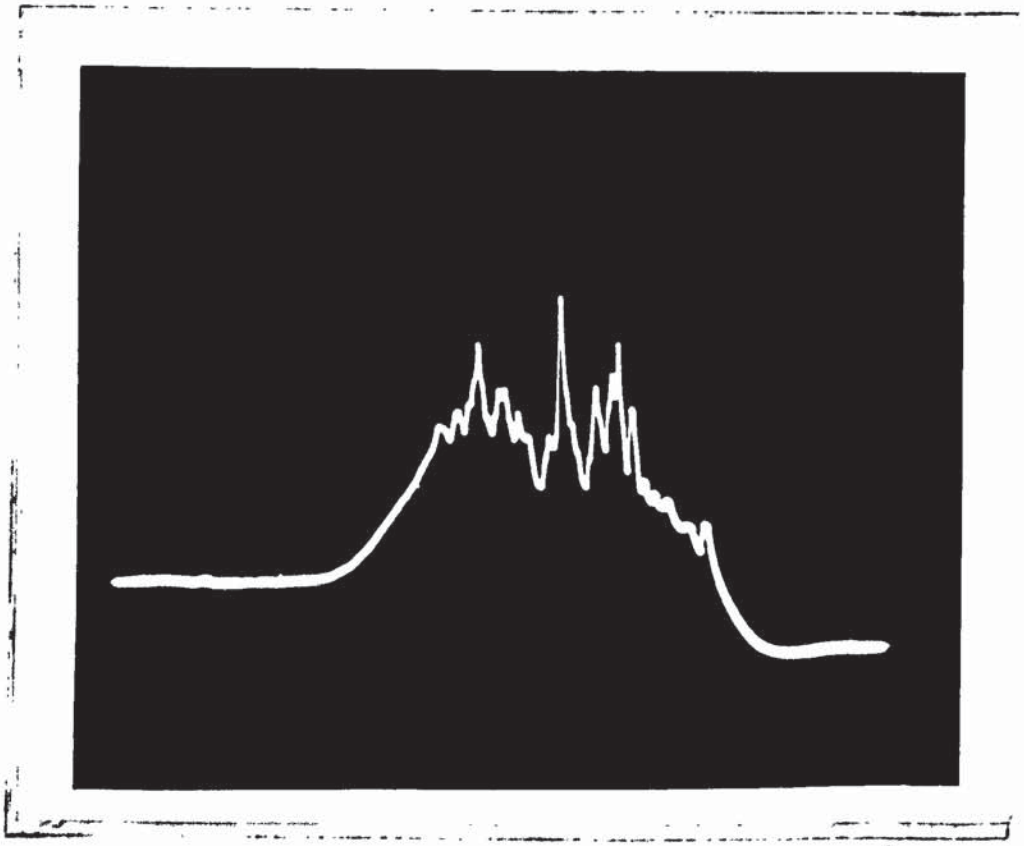

Solid particles

4.2. THE RESPONSE OF THE PROBE IN FLAMES CONTAINING SOLID PARTICLES.

4.2.1 INITIAL OBSERVATIONS.

Following the calibration of the probe, exploratory investigations of the positive ion concentration in flames containing aluminium particles were commenced. Atomised aluminium powder, of particle size 53 microns to dust, was supplied to the flame using the dust cloud generator. When the probe was swept through the flame it was immediately obvious that the probe was exhibiting novel behaviour. Whereas a flame containing gaseous additives produced a smooth-topped pulse on the oscilloscope, the presence of solid particles caused the top of the pulse to be broken up into a large number of spikes. Oscillograms for flames with and without solid particles are shown in Figure 14. This interference with the operation of the probe was ascribed to interaction of individual solid particles with the probe, and in view of the valuable information which might be gained from an interpretation of the effect, an investigation of the spikes was commenced.

To determine whether the effect was specific to aluminium, or was a general one occurring with particles of any material, a number of different powders possessing a range of properties were supplied in turn to a flame at 2336^{o}K and examined with the probe. The results are shown in Table 2. The survey showed that the production of spikes was a general effect, and that there was a degree of dependence on particle size, in that particles formed in situ in the flame did not give rise to spikes which were detectable with the measuring system at maximum sensitivity. In this connection the result for carbon was misleading, for particle size measurements carried out subsequently showed that although the carbon black used was nominally in the sub-micron

region, the particles reaching the burner consisted of very large aggregates. Most of the materials examined produced spikes of approximately the same size, the notable exception being lanthanum hexaboride, which was characterised by appreciably larger spikes. In view of the low work function of lanthanum hexaboride (2.66eV), this occurrence indicated that the spikes could be associated with the thermionic emission.

TABLE 2

THE EFFECT OF POWDER TYPE ON THE RESPONSE OF THE PROBE.

Material	Nominal Particle Size	Remarks
Aluminium	53μ to dust	Spikes observed
Alumina	Unspecified	" "
Carbon	$< 1\mu$	" "
Tungstic oxide	Unspecified	" "
Vanadium pentoxide	Unspecified	" "
Tungsten carbide	5μ	" "
Chromium	5μ	" "
Iron	7μ	" "
Lanthanum hexaboride	5μ	Large spikes
Vanadyl sulphate	Added as solutions	No spikes observed
uranyl nitrate	from atomiser.	" " "
ammonium dichromate	Particle size of oxide $< 1\mu$	" " "

It was observed that, for aluminium, the majority of the spikes possessed peaks corresponding to current flow of about 10^{-7} amps, the spikes having a duration of about 0.1 m.sec. The area under a typical spike was thus roughly equivalent to 5×10^{-12} coulombs, or 3×10^{7} electron charges. On the assumption that a spike is produced by the collision of a single particle with the probe, it appeared to the author that there are three processes which could accompany the collision and give rise to charge transfer of the type observed. The first of these is concerned with the potential adjustment which must occur if at collision the particle is at a different potential to the probe. The potential of a particle in a flame will not differ substantially from plasma potential. Collision with highly negative probe must therefore result in charge flow until the particle falls to the potential of the probe.

The second effect is an extension of the above process which must be considered if the particle has lost electrons by thermionic emission, for in this case the particle will possess a nett positive charge. In consequence the potential of the particle will be raised above plasma potential, and additional charge will be required to bring the particle to the probe potential. The magnitude of this additional charge will be equivalent to the number of electrons lost by the particle in its passage through the flame.

When the particle has been brought to the probe potential, a third process may occur, namely, thermionic emission from the incandescent particle in contact with the probe. The extent to which this takes place will depend on a number of factors, perhaps the most obvious being the work function and temperature of the particle.

A theoretical assessment of each of the three processes was made, to establish which of them would involve charge transfer of sufficient

magnitude to account for the spikes. It was considered that a particle diameter and temperature of 20 microns and 2300°K would approximate to the experimental conditions, and these values were used in the calculations.

4.2. 2 THERMAL ELECTRIFICATION OF SOLID PARTICLES

Taking the processes accompanying a collision in the order in which they occur, it is necessary to determine the extent to which a solid particle can be charged by thermionic emission of electrons. Now the equation governing thermionic emission by an infinite solid at temperature T°K was first derived by Richardson[43] and may be written

$$N_e = \frac{2\,(2\pi mk\,T)^{3/2}}{h^3} \exp\left(\frac{-\phi}{kT}\right) \qquad 4.15$$

where N_e is the number of free electrons per cm^3 above the solid, m is the mass of the electron, k is Boltzmann's constant, h is Planck's constant, and ϕ is the work function of the material.

In the case of small solid particles immersed in a hot gas, electrostatic forces make it increasingly difficult to remove electrons as the particles build up a positive charge, and equation 4.15 consequently requires modification. The first theoretical treatment allowing for the effect of electrostatic attraction was that of Sugden and Thrush[5], who proposed the equation

$$N_e = \frac{2\,(2\pi\, m\, k\, T)^{3/2}}{h^3} \exp\left(-\phi + \frac{N_e}{N_p}\,\frac{e^2}{r}\,\frac{1}{kT}\right) \qquad 4.16$$

where N_p is the number density of solid particles of radius r. This equation is true only if all of the particles are ionised to the same degree, and more elaborate treatments were made by Einbinder[6]

and Smith[7], in which the statistical distribution of particles in different states of ionisation were taken into account. These treatments produced an equation of the form

$$N_e = \frac{2\left(\frac{2\pi m kT}{}\right)^{3/2}}{h^3} \exp\left(-\phi + \left\{\frac{N_e}{N_p} + \frac{1}{2}\right\}\frac{e^2}{r}\cdot\frac{1}{kT}\right) \quad 4.17$$

However, it can be seen that for $\frac{N_e}{N_p} > 10$ the correction factor of $\frac{1}{2}$ which allows for the distribution of particle charge may be neglected, and the above equation reduces to that of Sugden and Thrush, equation 4.16. A solid particle is thus visualised as carrying a positive charge Ne and surrounded by an electron sheath. Emitted electrons which possess energy exceeding the potential $\frac{Ne}{r}$ at the surface of the particle are able to escape from the field of the particle into the gas. Soo[8,44] has applied the term "thermal electrification" to the process whereby positively charged particles are produced in a gas by thermionic emission and dispersal of the electron cloud.

Against this background, it is instructive to consider under what circumstances a value of $\frac{N_e}{N_p}$ of 3×10^7 would be attained, since this is the degree of charging necessary for an explanation of the spikes. Substitution of numerical values into equation 4.16 gives

$$N_e = 4.84 \times 10^{15}\, T^{3/2} \exp\left(-\frac{11{,}600}{T}\left\{\phi + \frac{14.4}{r(\text{Å})}\frac{N_e}{N_p}\right\}\right) \quad 4.18$$

Taking ϕ for aluminium to be 3.57 eV, and assuming r and T to be 10 μ and 2300°K respectively, a value of $\frac{N_e}{N_p}$ of 10^4 is found to give $N_e = 5.6 \times 10^9$ cm^{-3}, and hence $N_p = 5.6 \times 10^5$ cm^{-3}. An increase in the assumed value of N_e/N_p decreases the allowable number density of solid particles; for example if N_e/N_p is increased to 2×10^4 N_p becomes 2×10^2 cm^{-3}, and for $N_e/N_p = 3 \times 10^4$, N_p becomes 10^{-1} cm^{-3}.

It is apparent that any significant increase over 10^4 for N_p/N_g, since this term appears within the exponential, produces impossible answers for N_p. It was estimated from weighings of the powder delivery that the number density of solid particles in the flame was of the order of 50 cm^{-3}, which is consistent with a value of around 10^4 charges per particle. These results indicate that under the particular flame conditions employed thermal electrification is incapable of making a significant contribution to the spikes, and this part of the overall process may therefore be neglected.

It is interesting at this stage to consider the effect of electrostatic charge on the stability of a liquid aluminium droplet. When a spherical droplet carries an electric charge, this resides in the surface and the electrostatic repulsion creates a force tending to explode the drop. This tendency is opposed by surface tension forces. The maximum charge Q e.s.u. that an isolated spherical droplet may carry without disintegration is given by Rayleigh's instability theory[45],

$$Q = (16 \pi^2 r^3 \gamma)^{\frac{1}{2}} \qquad 4.19$$

where γ is the surface tension and r the radius of the droplet.

In the determination of Q for present purposes, the absence of data on γ at high temperatures made it necessary to calculate the value at 2300°K using the Ramsay - Shields - Eötvös correlation[46],

$$\left(\frac{M}{d}\right)^{\frac{2}{3}} = k_E (T_c - T - 6) \qquad 4.20$$

where M is the molecular weight, d the liquid density, T the temperature of interest and T_c the critical temperature. k_E is the Eötvös constant, which for non-polar-liquids is 2.12. For aluminium, M = 27, and d was estimated from the coefficient of expansion to be 2.12. A value of

T_c of 4744°K was obtained from the work of Gates and Thodes.[47] Substitution of these values into equation 4.20 enabled γ to be calculated, the value of obtained being 447 dyne cm^{-1}.

Equation 4.19 was then used to determine the maximum charge a particle of radius 10 μ is able to support, using the calculated value for γ. A value of Q of 4.74×10^{-3} e.s.u. was obtained, equivalent to just under 10^7 electron charges. It therefore appears that on stability grounds, aluminium particles are highly unlikely to possess 3×10^7 charges.

4.2. 3. CAPACITANCE CHARGING.

Irrespective of the number of electrons required to neutralise the charge on an emitting particle, any particle will undergo potential adjustment on striking the probe. The magnitude of the attendant charge flow may be calculated if the potential of the particle at collision is known. Since the particle is insulated, it must draw zero current from the plasma, and hence its potential relative to the plasma will be governed by the nature of the charge distribution in the regions around the probe, which are shown in Figure 11.

Well-removed from the probe, in the quasi-neutral region, the particle will be at floating potential, slightly negative to plasma potential, and will remain at this potential until it enters the transition region. Here, at shown in Figure 11 the local electron density falls below the positive ion density and the particle accordingly moves closer to plasma potential in order to reduce the ion current collected.

Further adjustment of the particle potential must occur on entering the ion sheath region, in which no electrons are present. At the point of entry ($N_e = 0$), the particle must have risen in potential above the plasma potential by an amount sufficient to reduce the positive ion

current to zero, since the eletron current is zero. The particle potential is unaffected by further penetration into the sheath, and no charged carriers of either sign will flow between it and the plasma. The particle thus remains at a constant potential during its travel through the ion sheath, until on collision with the probe it is abruptly charged to a potential of -100 volts. It can be seen that the number of electrons required to adjust the particle potential is dependent, therefore, on the particle potential when at the outer edge of the ion sheath, which may be estimated in the following manner.

The plasma potential will fall steadily in passing through the quasi-neutral region and transition region, and at the edge of the ion sheath region will have reached a level such that inward electron flow is just prevented. For a mean electron energy of $\frac{3}{2}$ kT, the upper limit on electron energies that need be considered is twice this value, or 3kT. The potential ϕ at the outer edge of the sheath, assuming the zero of potential to be at infinity, is therefore given by

$$3kT \doteqdot -e\phi \quad \text{or} \quad \phi = \frac{-3kT}{e} \qquad 4.21$$

For T = 2300^{o}K, the plasma potential at the sheath edge is given by 4.21 to be -0.6 volts. Now a particle at this point must repel all possible ions. Assuming that the ions are of equal energy to the electrons, the particle must rise in potential above the local plasma potential by + 3kT/e or + 0.6 volts. Thus at the sheath edge the particle, o.6 volts above a plasma potential of - 0.6 volts, is at a potential corresponding to that at infinity, i.e. zero. The full potential on the probe of - 100 volts is therefore available to charge the particle on striking the probe. The charge q transferred to the particle on collision with the probe is given by

$$q = C\,V \qquad \text{e.s.u} \qquad 4.22$$

where the capacitance C is numerically equal to the particle radius in cm and V is the potential on the probe = 0.33 statvolts. For $r = 10\,\mu$,

$$q = 0.33 \times 10^{-3} \text{ e.s.u} \qquad 4.23$$

and since one electronic charge is equivalent to 4.8×10^{-10} e.s.u, the number of charges transferred is given as 0.7×10^{6}.

When the above value of 0.7×10^{6} is compared with the experimental one of 3×10^{7} charges for the charge transfer involved in one spike, it is seen to be somewhat low. However, the theoretical value was considered to be sufficiently close to warrant further examination, particularly in view of the uncertainties in the early experimental results.

4.2. 4 THERMIONIC EMISSION FROM AN INCANDESCENT PARTICLE ON THE SURFACE OF THE PROBE.

It can be seen from the previous section that the final outcome of the collision of a particle with the probe is effectively the application of a high negative potential to the particle, which may, therefore, depending on its temperature and work function, emit electrons into the gas. In this situation the particle is analogous to the cathode of a diode with the heater current on, collision with the probe corresponding to a sudden application of the H.T. supply. However, in the latter case the current through the valve will remain constant after the initial rapid rise, assuming that the temperature and plate potential are not altered. For the particle, one of two factors will curtail the emission current. If the particle adheres to the probe, it will immediately begin to cool and eventually cease to emit, while if a transient collision takes place the emission will be limited by the particle-probe contact time. In either event one would expect the result to be a pulse of some description.

For this mechanism to be significant in the production of the spikes, thermionic emission from particles of the size order used must be capable of producing a current of around 10^{-7} amps. Now the saturation electron current density J amps cm^{-2}, obtainable from an emitting surface is given by the Richardson - Dushman equation[48],

$$J = AT^2 \exp\left(\frac{-e\phi}{kT}\right) \qquad 4.24$$

where A is a semi-empirical constant and other symbols are as in equation 4.15. For a particle of radius r this becomes

$$I = 4\pi r^2 AT^2 \exp\left(\frac{-e\phi}{kT}\right) \qquad 4.25$$

where I is the saturation electron current in amps. This equation may be used to estimate the emission current obtainable from an aluminium particle, assuming once more that $r = 10\mu$ $T = 2300^{o}K$ and taking $\phi = 3.57$ eV. In the absence of an empirical value of A for aluminium, the theoretical 120 amps $cm^{-2}\ {}^{o}K^{-2}$ must be used. Substitution of these numerical values into the above equation gives $I = 1.2 \times 10^{-4}$ amps, showing thermionic emission from an aluminium particle to be theoretically capable of producing a current greatly in excess of that equivalent to a spike.

The discrepancy between the experimental and theoretical currents is not unexpected, in that the saturation electron current calculated from equation 4.25 is the maximum current which can be drawn from the surface. It is well known that under vacuum conditions and moderate voltages, emission from a heated filament does not approach the saturation current predicted by the Richardson - Dushman equation, due to the presence of electron space charge. The current drawn obeys the Langmuir - Childs[49] equation, and is a function of voltage and electrode spacing. Now a particle on the surface of the probe is immersed in a sheath of positive ions, which will neutralise the electron space charge, and the high electric field at the probe should enable the full emission current to be obtained. However, it will be seen from the oscillograms in figure 14 that the current producing a single spike is equivalent to an appreciable fraction of the ion current collected over the total probe surface. Because of the low mobility of positive ions, a small ion current is able to neutralise the space charge of a large electron current. Nevertheless it is possible that for very high electron current densities, such as could be produced by a small emitting particle on the probe, the diffusion of ions to that local area of the probe may be insufficient to completely eliminate electron space charge. In these circumstances the height of the spikes

will be dependent on the ion density in the flame.

4.2. 5 COMPARISON OF THE CAPACITANCE AND THERMIONIC EMISSION MECHANISMS

The capacitance and thermionic emission mechanisms discussed in the last two sections both seem capable of making a significant contribution to the spikes. The mechanisms differ in a number of respects in their dependence on flame and material properties, and thus in the event of one effect being predominant, the information obtainable will depend on which this happens to be. It is clear that for a capacitance mechanism, the magnitude of the spikes will be directly proportional to the radius of the particle. The thermionic properties of the material would be expected to be of minor importance, since the positive potential on the particle when entering the ion sheath should be adequate to restrict electron emission. Increase in flame temperature, although lowering the floating potential because of higher electron energies, would not be expected to affect the overall process because of the potential cancellation effect occurring at the sheath edge. The process should therefore be temperature independent. It can be seen that if the spikes are produced by a capacitance mechanism, the effect will provide a means of determining particle sizes in combustion gases.

In contrast, spikes produced by thermionic emission should display exponential dependence on temperature and work function, and should also be proportional to the square of the particle radius. The confirmation of this mechanism should thus allow the determination of thermionic work functions in gaseous environments.

Despite the apparent major differences between the two proposed mechanisms, the experimental identification of the actual process occurring presented difficulties, which were primarily associated with the need to

relate the size of a given spike to the size of the particle producing it. The powders available at this time were coarsely classified, and the state of aggregation of the particles reaching the flame was unknown. Moreover, it was difficult to be certain that the probe was not colliding simultaneously with more than one particle. It was therefore decided to scale up the process to enable the collision between the probe and a single particle of known size to be studied.

4.3. EXPERIMENTS WITH BALL BEARINGS.

These experiments were carried out using inverted burner assembly described in section 2.7. 1. Degreased stainless steel balls were placed singly in the rotating disc and dropped into the flame to collide with the probe, which passed through the flame 5 cm below the reaction zone. Fast burning flames were found to be least subject to fluctuations when burned on the inverted burner, and a flame at 2507^{o}K was therefore used in the work. Independent measurements with the normal probe showed the positive ion density to be 8 x 10^{8} cm^{-3}.

It was found that the majority of the balls released into the flame did not give rise to spikes, although occasionally a spike would be observed. This problem was resolved by having one observer watch the collision of the ball with the probe, while another watch the oscilloscope. It then transpired that even with careful adjustment of the speed of the rotating disc not all ball bearings entering the flame collided with the probe, and that the few spikes which were observed were produced by balls which narrowly missed the probe. These spikes were attributed to the probe passing through high local concentrations of alkali metal vapour, since flashes of sodium could sometimes be seen arising from the ball bearings. This was confirmed by subjecting the balls to even more stringent cleaning and degreasing, when no spikes were observed under any conditions. It was concluded that no charge transfer by a capacitative mechanism was taking place.

Because of their large size and the short residence time in the flame the ball bearings were not heated to any extent before colliding with the probe, and no information on the thermionic emission mechanism could be obtained. This process was investigated in the experiments using a stationary wire.

Fig. 15 Collision of the probe with an insulated tungsten wire. Temperature dependence.

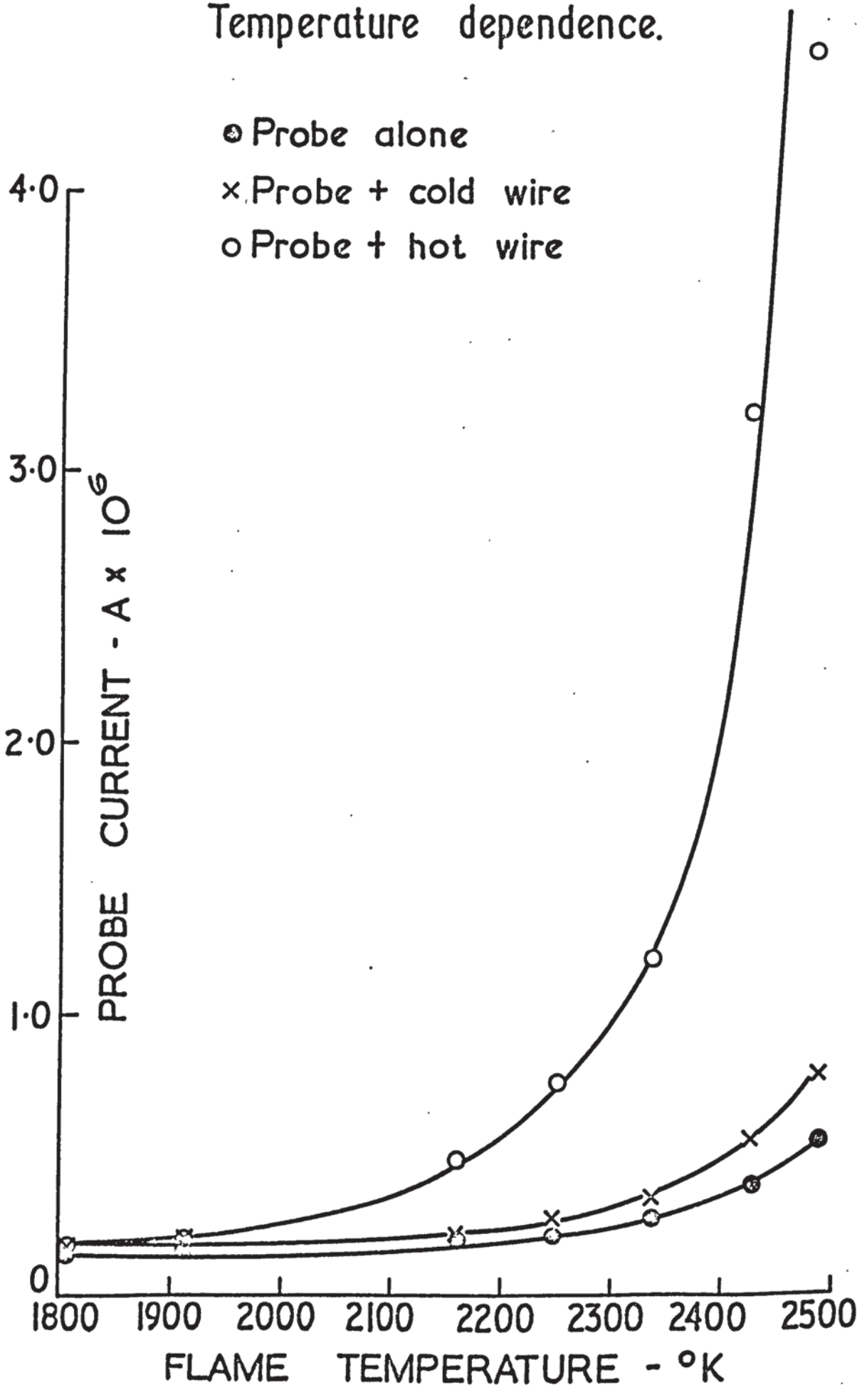

4.4. EXPERIMENTS WITH THE STATIONARY WIRE.

It was possible to examine probe - particle collisions in more detail in the experiments on the insulated wire (Fig. 8b), which although only yielding qualitative results confirmed the importance of thermionic emission in the production of the spikes. Measurements were made in 'clean' flames over the range 1806 - 2507°K, and a typical result for temperature dependence in the case of a tungsten wire in shown in Figure 15. It was found that the collision of the probe with a cold wire resulted in a slightly increased current. This increase was largely independent of temperature and corresponded with the increase expected by virtue of the enlarged collecting area of the probe. In cooler flames no difference between the effect of hot or cold wires was in evidence, but as the temperature was raised a markedly increased current was obtained from the hot wire, indicating the onset of thermionic emission. It was unfortunately not possible to establish whether the temperature dependence was in accord with the Richardson - Dushman equation, because of the temperature gradient along the wire. It will be noted that flame temperature is used as the abscissa in Figure 15. Pyrometric measurements showed that the hotter end of the wire lagged the flame temperature by 700 - 800°C, and that there was generally a temperature drop along the wire of the order of 400°C.

When similar experiments were carried out on iridium, an additional phenomenon was noted. An iridium wire when first introduced into a flame gave an exceptionally large current, which progressively decreased over a period of some minutes until a steady value was reached. If the wire was then allowed to stand at room temperature for a few hours the original condition was restored, and the effect could be repeated. In Figure 16 this decay of emission current is shown at two temperatures, and it can be seen that the rate of decay is accelerated by increase in

Fig. 16 Effect of adsorption on thermionic emission from iridium.

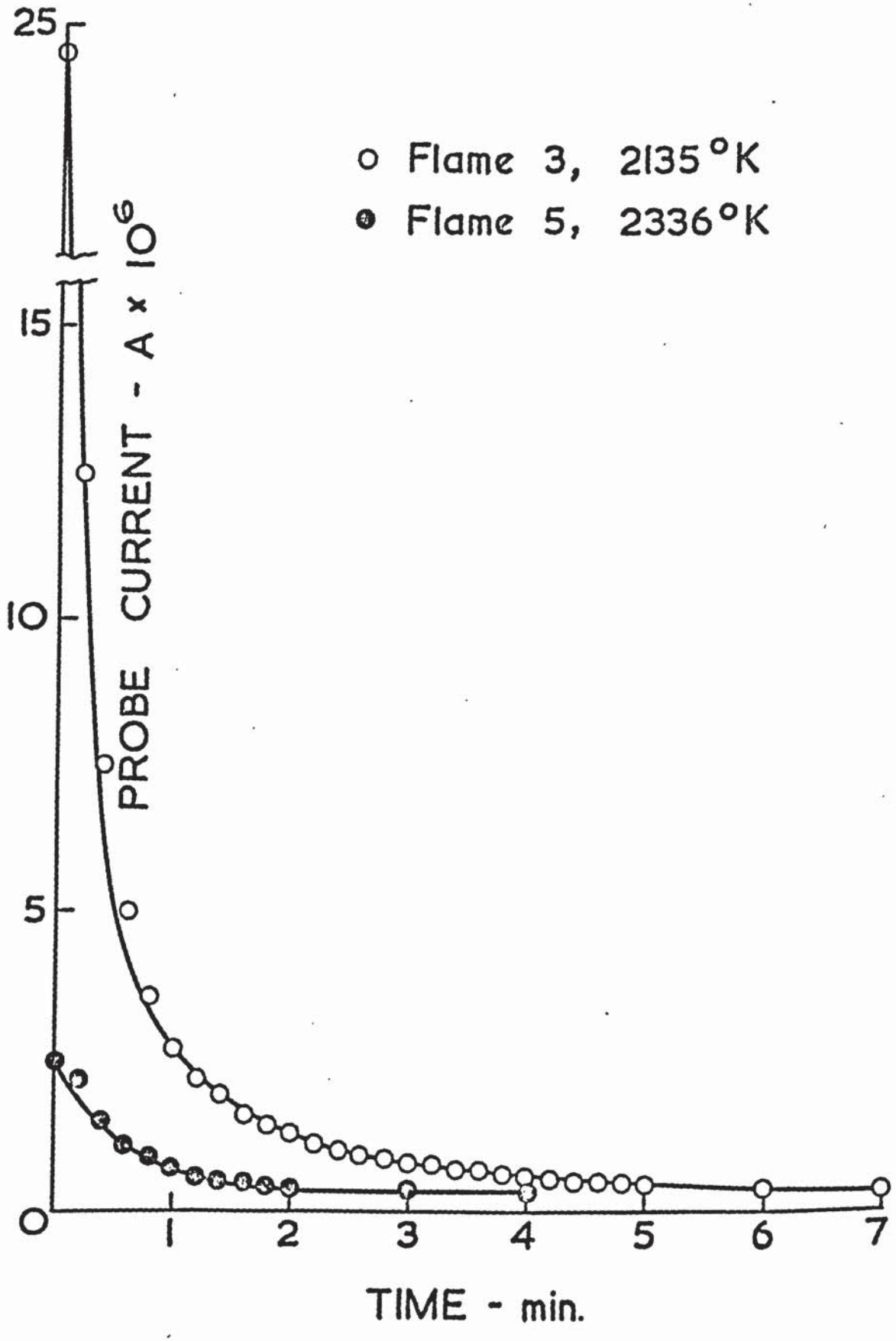

temperature. This phenomenon was ascribed to an increase in the work function of iridium accompanying the adsorption of an electronegative species, the most probable species being oxygen. Farragher[50] has reported that the effect of low pressures of oxygen on iridium at 1590°K is to raise the work function from 3.8 to 6.95 e V. An increase of this order would reduce the emission current at 1300°K by a factor of 10^{13}. Since for the wire in the flame the current was reduced by a factor of 10^{2}, and the duration of the process was much longer than would be expected, it may be safely concluded that only the tail end of the adsorption process was observed. This precluded the determination of the activation energy of the reaction, for which continuous recording of the emission current would be required.

Because of the adsorption effect, all iridium wires used were first conditioned until the emission reached a constant value. Probe measurements made in flames of increasing temperature then yielded similar curves to those obtained with tungsten, as shown in Figure 17. There are two obvious differences. First, the temperature at which the curves for the hot and cold wire diverge is several hundred degrees higher for iridium than tungsten, and secondly iridium produces a lower emission current than does tungsten in the same flame. Since the surface areas of both wires were equal, and the wire temperatures would not differ significantly, these differences must be attributed to the higher work function of iridium.

These experiments demonstrate that in the interaction between the probe and a solid particle, any increased current flow is produced by thermionic emission. For micron sized particles the increase in probe area on striking a particle will be negligible, and hence there will be no contribution to the current flow from an area effect. No attempt was made to extend the measurements to include the influence of probe voltage or flame conductivity on emission currents. For such investigations a

Fig. 17 Collision of the probe with an insulated iridium wire. Temperature dependence.

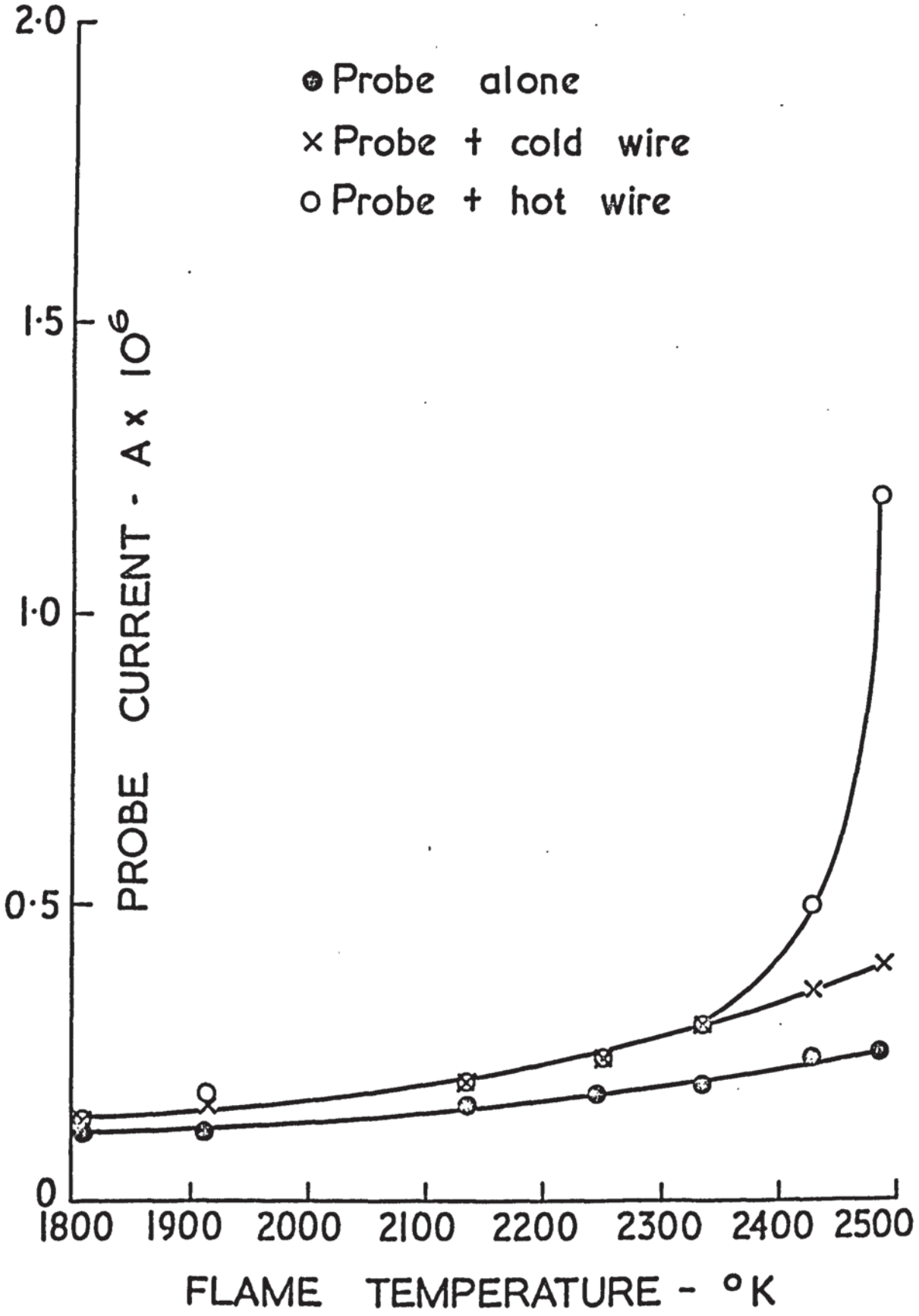

more symmetrical arrangement of electrodes is required, ideally in which the probe wire and anode form a concentric electrode system. This arrangement also allows the determination of a meaningful wire temperature. However, a system of this type becomes effectively a conductivity cell as used by Mullaney, Kydd and Dibelius[51] in measurements of the electrical conductivity of flames. It was thought unlikely that the dependence of emission current on probe voltage and ion density would be the same for large electrodes as for a particle on the probe, and this approach was not pursued.

4.5. DISCUSSION OF RESULTS.

The evidence from the experiments on the stationary wire points to thermionic emission as the major contributor to the spikes produced by solid particles, in agreement with the early indications from lanthanum hexaboride. The failure to detect any capacitance charging in the experiments with the ball - bearings is surprising, in that there seems no good reason why this process should not occur. It is possible that the method of introduction of the bearings into the flame allowed them to carry in their own atmosphere, so preventing any adjustment of potential in their passage through the flame. If this were so, the only means of detecting the effect would appear to be by measurements with a more sensitive measuring system on particles in low temperature flames. In the general problem of the analysis of the spikes from emitting particles, it may be safely assumed that the capacitance effect will not make a significant contribution to the spikes. As shown in section 4.2. 3, the level of charge transfer predicted for aluminium particles by a capacitance mechanism is about 2% of that observed. Subsequent work showed that for materials of lower work function this value was reduced by a further order of magnitude.

These results suggest that analysis of the spikes should yield information on the work functions of materials in gaseous environments. The importance of such information is emphasised by the effect of adsorption on the emission current from the iridium wire, an effect not confined to iridium alone. Klemperer[52] has reviewed the effect of oxygen adsorption on a large number of metals, and Huber and Kirk[53] have shown that the presence of water vapour can also produce marked effects. For aluminium, chemisorption of water was found to reduce the work function of both clean and oxidised surfaces by 1 e V. In flames, adsorption of alkali metals, present as additives or trace impurities, may also lead to anomalous work functions. In view of these considerations,

it is evident that calculations of electron concentrations in flames using "clean surface" work functions may be in considerable error. The subsequent programme on the spikes was carried out with the objective of obtaining direct information on work functions of compounds in flames.

5. EXPERIMENTAL MEASUREMENTS OF ELECTRON EMISSION FROM SOLID PARTICLES IN FLAMES.

5.1 INTRODUCTION.

The powders selected for detailed study with the probe are listed, along with their relevant properties, in Table 3 below.

TABLE 3

PHYSICAL PROPERTIES OF THE MATERIALS STUDIED

Material	Work function, øeV[54]	Melting Point, ^{o}K
Graphite	3.93	3923
Aluminium	4.25	933
Alumina	4.70	2318
Tungsten Carbide	3.60	3143
Lanthanum hexaboride	2.66	2503 ± 50
Barium oxide	1.66	2198

All of the powders were commercial grade materials, and would be expected to contain trace impurities, particularly alkali metals. This would certainly be the case for graphite, which was actually a carbon black sample, in the manufacture of which small amounts of sodium are deliberately added. The atomised aluminium powder used earlier was replaced for these investigations by a grade composed of flakes 2 - 3μ in thickness, and 8 - 14 μ in diameter. The particles seen by the probe would possess approximately half this diameter, since the flakes would be converted to spherical droplets on entering the flame. Alumina itself was not examined in the experiments, but is included in the Table since its properties are of great importance in the combustion of aluminium.

None of these materials are inert in high temperature flames. Carbon and aluminium will be subject to combustion. In the case of carbon, this will occur at the particle surface and adsorbed species participating the reaction are likely to affect the work function. Oxidation of aluminium, which will be slow in the cooler flames by virtue of the protective oxide coating, will dramatically increase at the melting point of alumina, when the particles ignite[55]. Both the existence of a metal - metal oxide system and the change of phase on melting would be expected to affect the thermionic properties of the material. Oxidation of tungsten carbide and lanthanum hexaboride is also known to occur, and is most severe for these materials above 1000^{o}K and 1500^{o}K respectively. This was borne out in the present work by the appearance of flames containing large amounts of lanthanum hexaboride. Such flames displayed the characteristic green emission of boron dioxide at heights in the flame greater than 5 cm. Barium oxide, like aluminium, is molten in the hotter flames used and is also of interest because of its high reactivity. It has been shown that the predominant species formed by barium compounds in hydrogen-oxygen flames are the gaseous mono- and di-hydroxides[56]. Low in the flame, where H and OH radical concentrations are well in excess of equilibrium values, the formation of the hydroxides from solid oxide particles will occur by reaction of these radicals at the surface.

The above comments indicate that the surface properties of the particles will be grossly altered when they are surrpunded by flame gases, because of the high temperature and reactivity of the environment. In consequence the "clean surface" work functions listed in Table 3 will not have direct application to flame conditions, and significant differences must be expected in the work functions measured in flames.

Fig. 18 The Powders

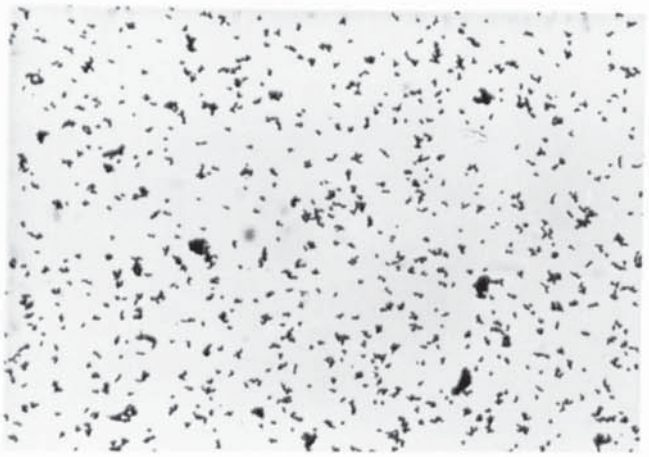

Tungsten carbide

Lanthanum hexaboride

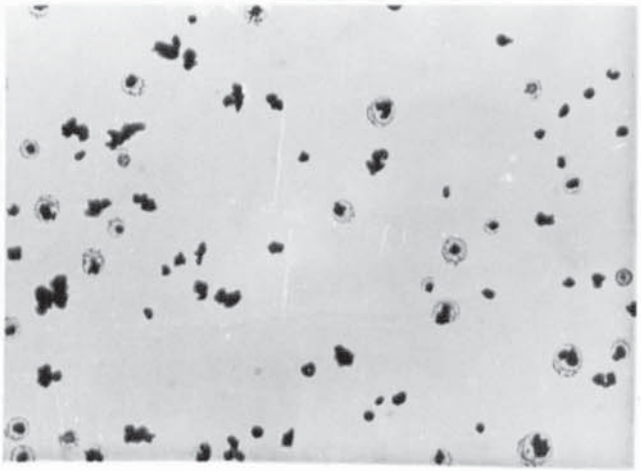

Barium oxide

Fig.19 The Powders

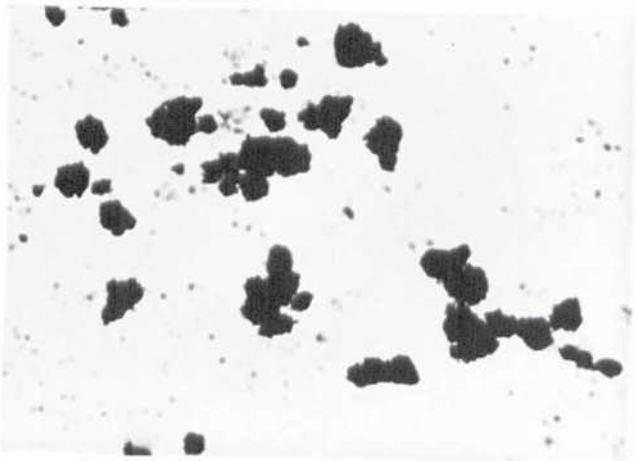

Carbon

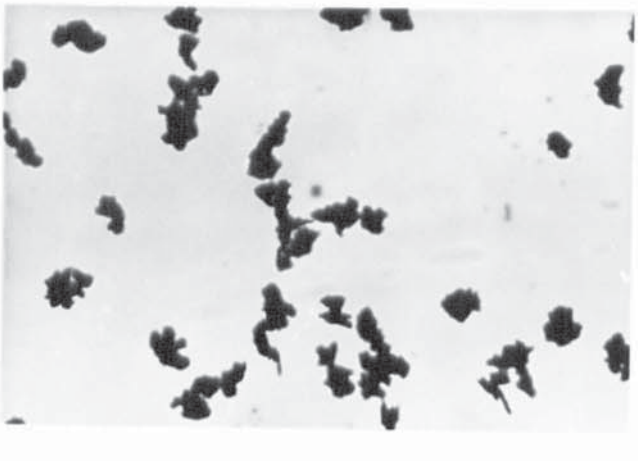

Aluminium

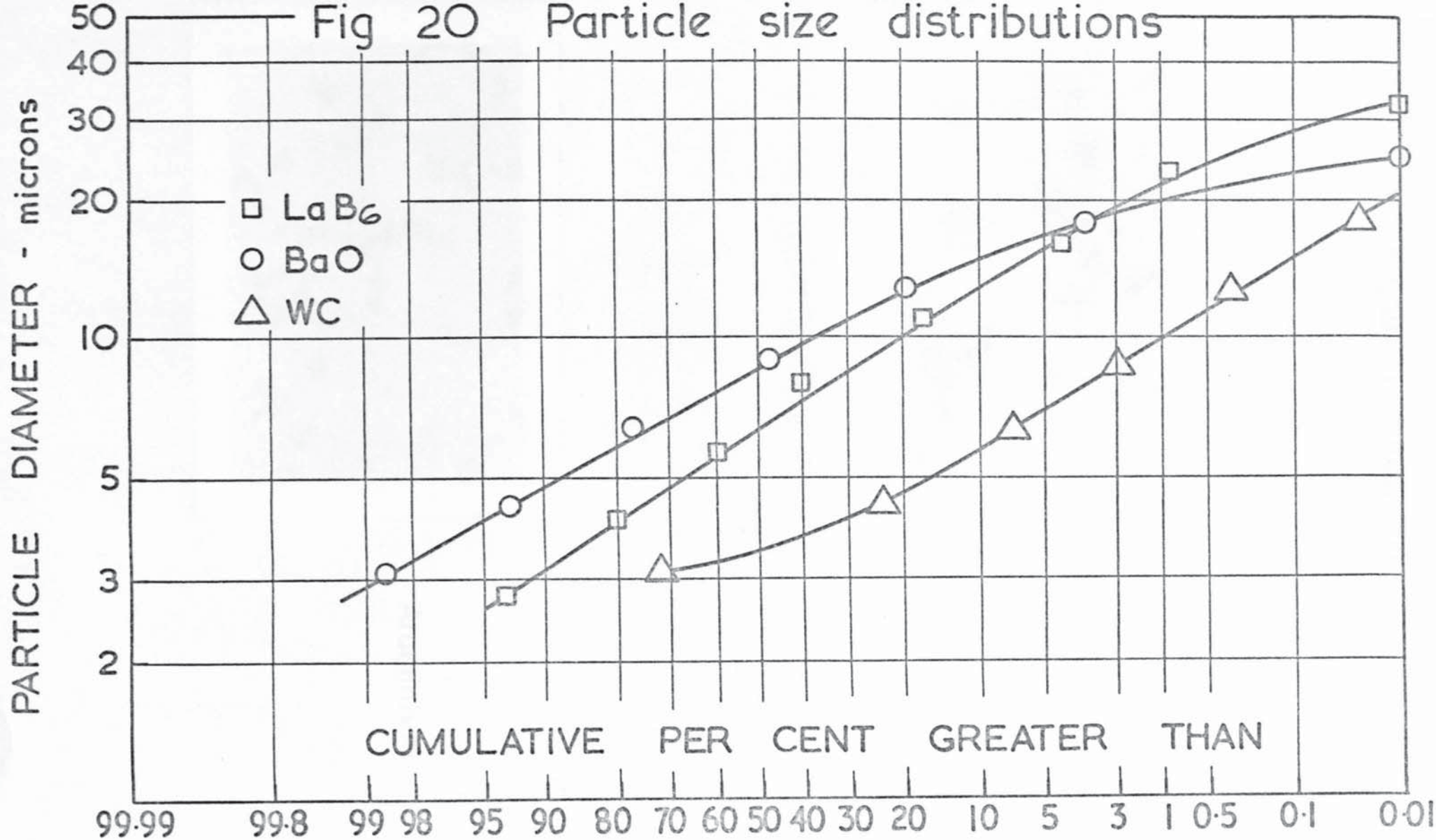
Fig 20 Particle size distributions
PARTICLE DIAMETER - microns
50
40
30
20
10
5
3
2
□ LaB6
○ BaO
△ WC
CUMULATIVE PER CENT GREATER THAN
99·99
99·8
99
98
95
90
80
70
60
50
40
30
20
10
5
3
1
0·5
0·1
0·01

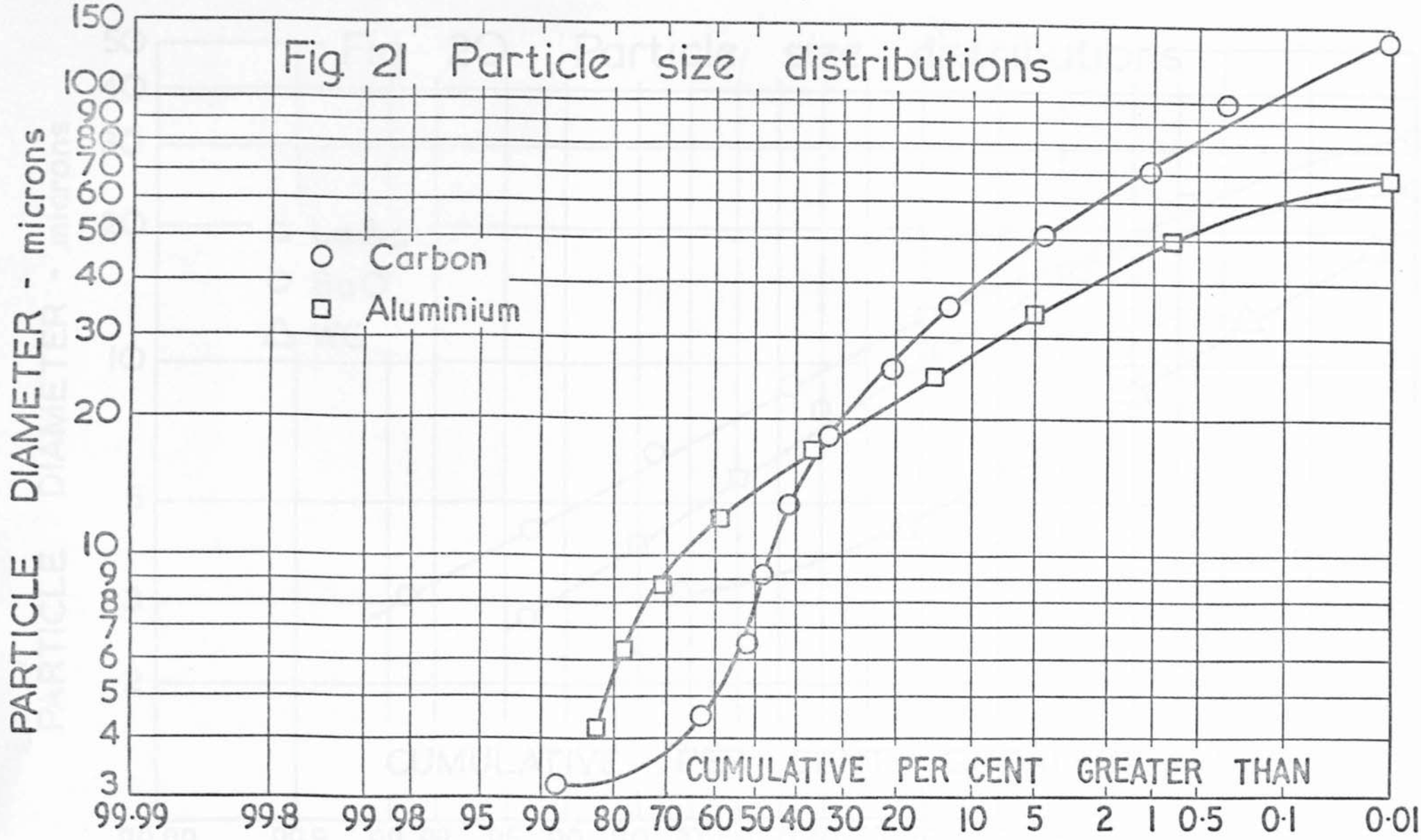
Fig. 21 Particle size distributions
PARTICLE DIAMETER - microns
150
100
90
80
70
60
50
40
30
20
10
9
8
7
6
5
4
3
Carbon
Aluminium
CUMULATIVE PER CENT GREATER THAN
99·99
99·8
99
98
95
90
80
70
60
50
40
30
20
10
5
2
1
0·5
0·1
0·01

5.2. PARTICLE SIZE MEASUREMENTS.

Typical photomicrographs of powder samples collected at the top of the elutriator are shown in Figures 18 and 19, for the five materials used. It can be seen that particles of tungsten carbide, lanthanum hexaboride are barium oxide lie in the same size range, and that much larger particles are present at the aluminium and carbon samples. For carbon, these large particles are plainly aggregates of much smaller particles. Although the flying spot particle analyser used in the determination of the distribution attempts to distinguish aggregates, it performs most satisfactorily with regularly shaped particles. The result for carbon must accordingly be treated with caution.

Cumulative particle size distribution plotted on log-normal probability paper are shown in Figures 20 and 21. While it is not unusual to find the experimental points at the upper and lower extremes of the distribution deviating considerably from a straight line, there is no semblance of linearity in the carbon plot (Figure 21), again a consequence of aggregation. The data obtained from the distributions is shown in Table 4.

TABLE 4

PARTICLE SIZES

Material	Geometric mean diameter (μ)	Standard Deviation	Predicted diameter (μ)
Carbon	8	-	7.2
Aluminium	14.1	1.8	5.5
Tungsten Carbide	3.3	1.5	2.5
Lanthanum hexaboride	6.6	1.6	3.4
Barium oxide	8.8	1.7	2.6

Fig. 22 The Spikes

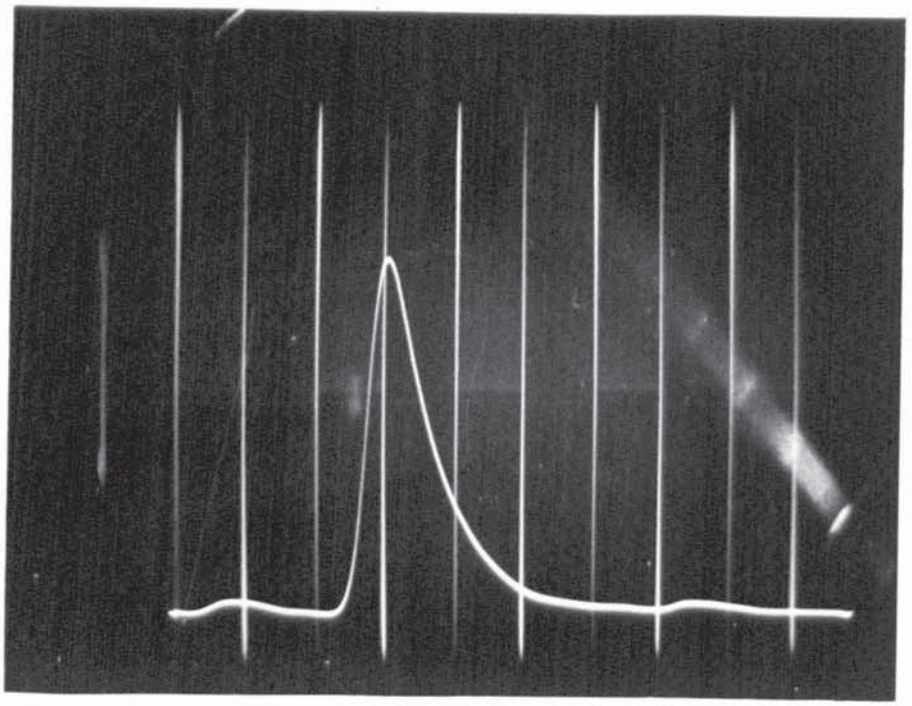

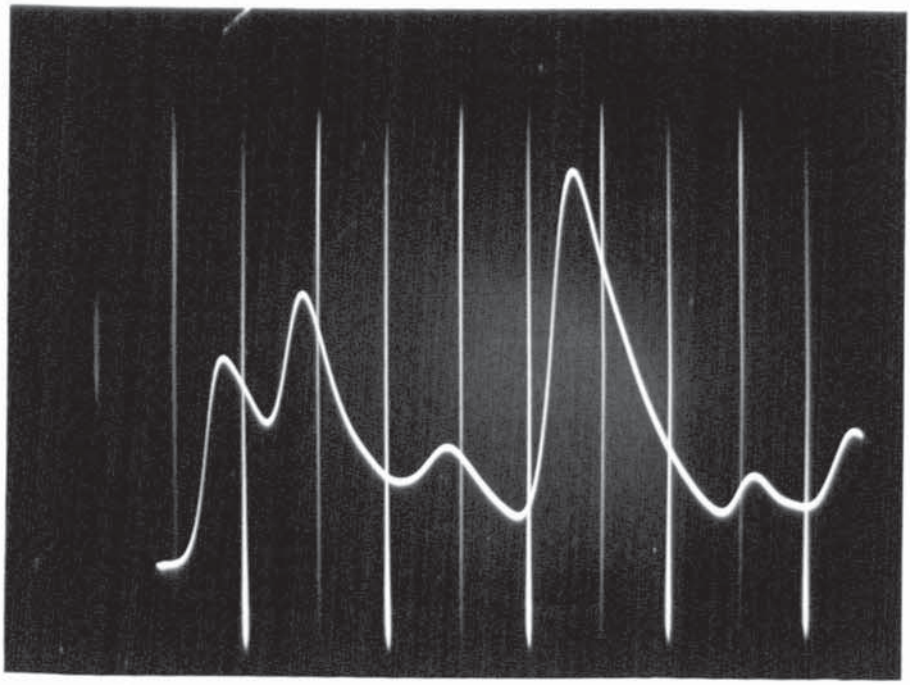

The results for barium oxide are disappointing. Visual microscopic observations on this material made using a stage micrometer at the time of the experiments showed that particle diameters were mostly around 1 μ, and certainly no particles were larger than 5 μ. This is in keeping with the vapour phase method of manufacture of the material. Barium oxide is extremely hygroscopic, and it is thought that the much larger particle size reported above was caused by moisture absorption in between sampling and taking the photographs. Indeed, on several of the photomicrographs a halo could be discerned around some particles, undoubtedly due to this effect. Again, with reference to the particle sizes listed in Table 4, it must be remembered that for the aluminium platelets an effective size reduction will occur when the particles enter the flame.

In Table 4, predicted diameter refers to the diameter of particles whose terminal falling velocity was equal to the gas velocity through the elutriator, i.e. the largest particles which should theoretically have been elutriated. The discrepancy between the predicted diameter and that at the upper limit of the particle size distributions is unavoidable, and may be attributed to the parabolic velocity profile across the elutriator tube.

5.3. THE SHAPE OF THE SPIKES.

In these investigations of the current spikes produced by particles striking the probe, data was obtained by taking a number of oscillograms at each set of experimental conditions, and subsequently printing each exposure at a fixed magnification. The spikes were than measured on these photographs with calipers.

The characteristic shape of the spikes is shown in the oscillograms of Figure 22, in this instance for lanthanum hexaboride. The vertical line crossing the oscillograms are a 1 Kc/s square wave superimposed for calibration purposes. It will be observed that the trailing edge of the

Fig. 23 The slope of the leading edge of the spikes

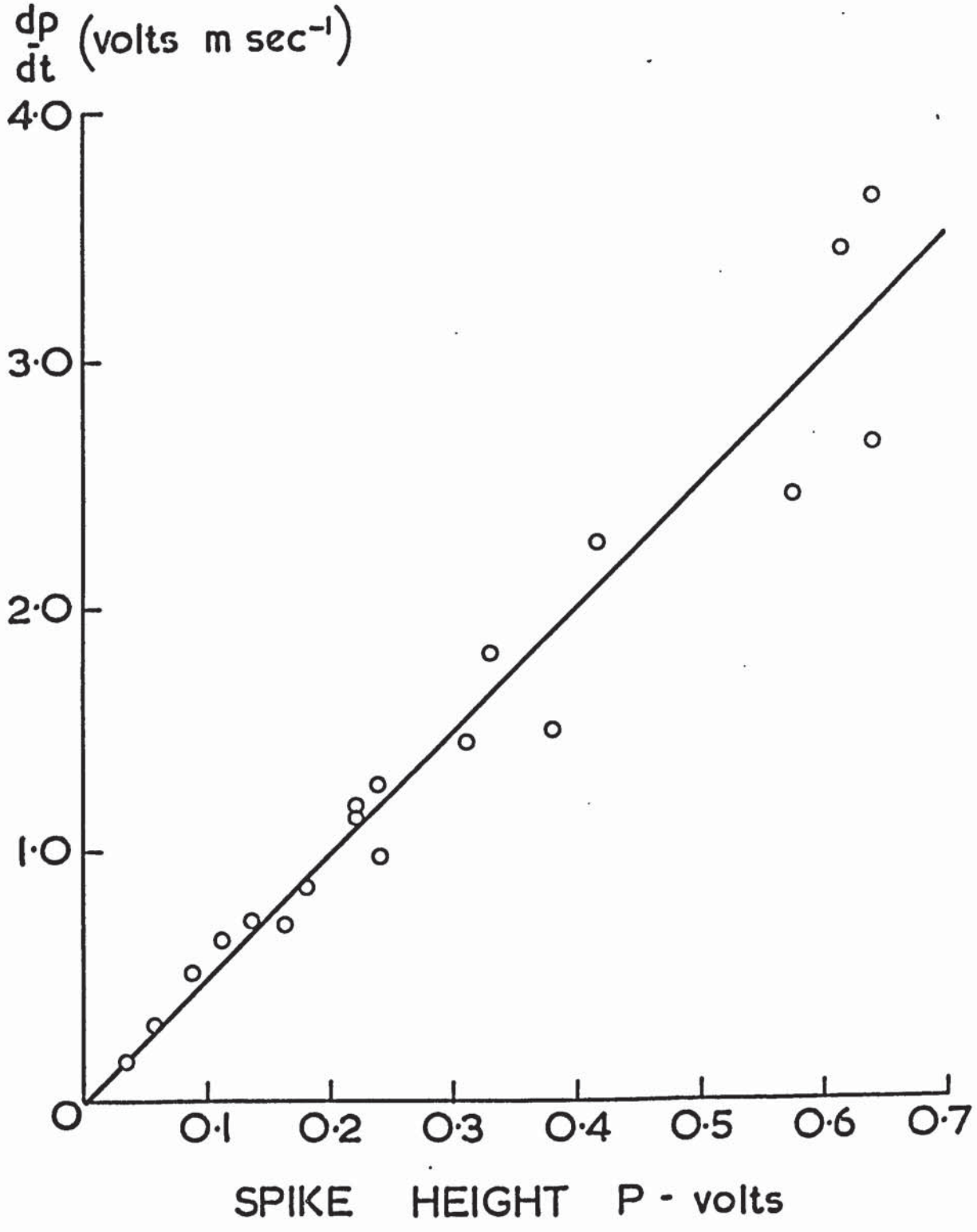

waveforms has an exponential appearance, suggestive of wave shaping. Since the rise time of the oscilloscope was 0.023 microseconds, compared with a pulse rise time approaching a millisecond, the shaping must be caused by other circuit elements. It would seem that the coaxial leads used in the apparatus would be the major contributor, for in total these would possess a capacitance of around 100pF. The complementary high resistance would undoubtedly be the flame itself. The current density J in the flame is given by

$$J = nev = ne\mu E \qquad 5.1$$

where v is the drift velocity in the direction of the field E, and n is the number density of electrons of charge e and mobility μ. The resistivity may therefore be written

$$\rho = \frac{E}{J} = \frac{1}{ne\mu} \qquad 5.2$$

For a clean flame, $n = 8 \times 10^{8}$ cm^{-3}, $e = 1.6 \times 10^{-19}$ coulombs and $\mu = 2500$ cm^{2} volt^{-1} sec^{-1}. Substitution of these values into equation 5.2 gives a value for $\rho = 5 \times 10^{6}$ ohm cm, so that for the particular flame size and probe height employed the resistance of the flame is given as 3.5×10^{7} ohms. The value of the time constant of the circuit T = RC is thus 3.5 milliseconds, which is of the correct order of magnitude for the observed wave shaping.

More important than shaping of the trailing edge of the spikes is any effect on the leading edge, since this will directly influence the spike height in a transient of this type. It can be seen from the oscillograms of Figure 22 that the slope dp/dt of the leading edge of the spikes is related to the height p of the spikes, and is greater the larger the spike. The graph in Figure 23 shows that there is a linear relationship between dp/dt and P. This in itself indicates

Fig 24 Shaping of pulses by a low pass RC circuit

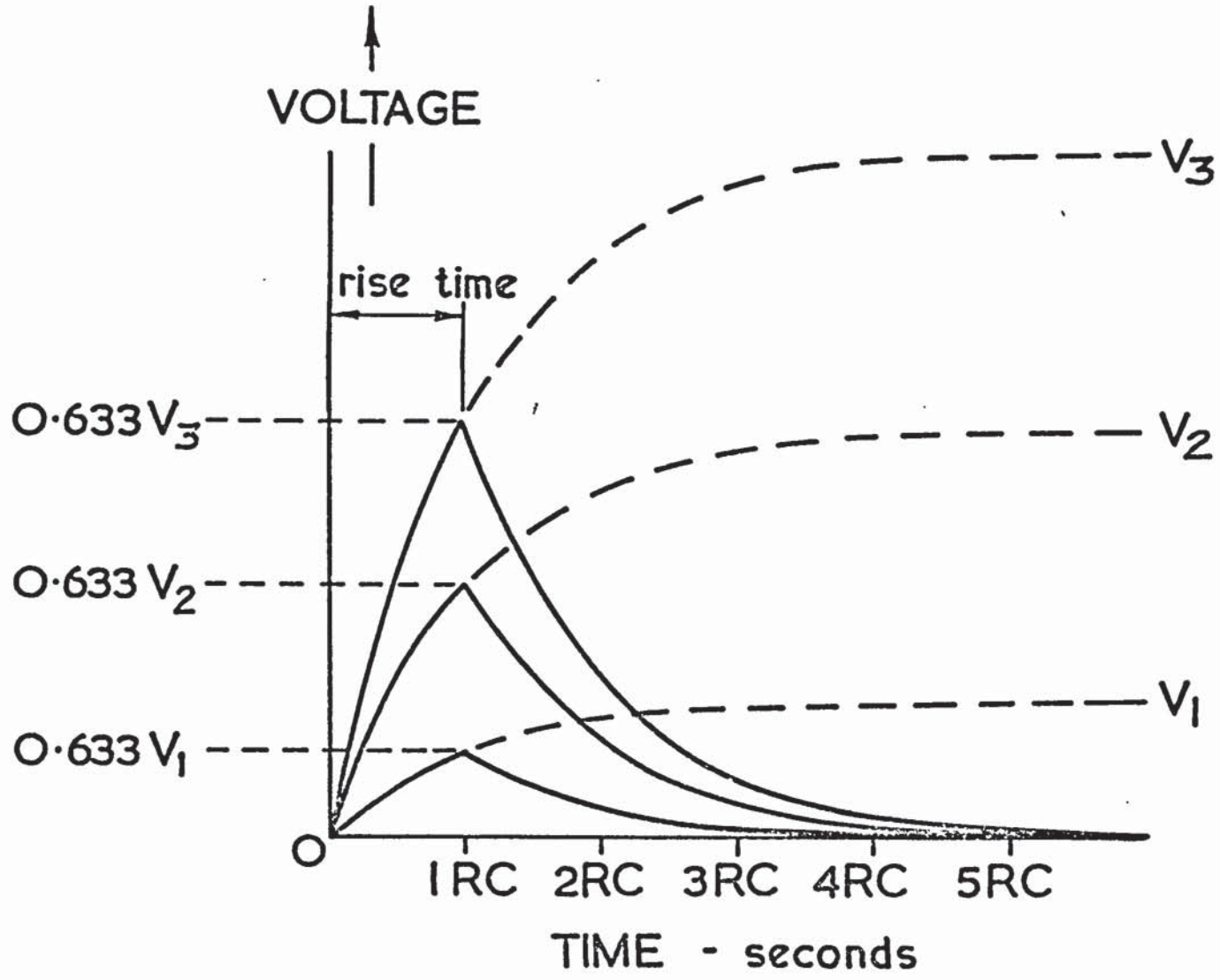

shaping of the spikes by a long time constant, and it might appear that the pulse heights are controlled by this factor. Howevever, it will be seen that the scatter in the experimental points in Figure 23 is quite small, indicating the rise time of the spikes to be independent of spike height, an occurrence which considerably simplifies the analysis of the spikes. The rise time is given by the slope of the plot as 0.2 m.sec. It will be shown later that particles striking the probe do not adhere to the probe surface, but undergo a transient collision. In this situation the rise time of the spikes may be equated with the contact time of the particle and the probe. The instant at which the particle leaves the probe then corresponds with the peak voltage, which is followed by exponential decay with a time constant RC. It can be seen from the foregoing that the quantity which limits the spike height is the probe-particle contact time, which is a constant. Now in a system in which a long time constant is shaping pulses of varying amplitude, the amplitude of all pulses after a fixed time lapse is a constant proportion of the steady state values which would be reached if sufficient time were available. This is shown diagramatically in Figure 24, where it is assumed that termination occurs after one time constant and that the time constants for the rise and decay portions of the pulse are equal. In the case of the spikes, where emission is terminated after a fixed interval by the particle leaving the probe, spike heights will be proportional to the saturation emission current from the particle. It is this proportionality which allows the temperature dependence of the spikes to be interpreted by a Richardson plot.

5.4. THE EFFECT OF A HOT PROBE ON THE SPIKES.

The conclusion that particles do not adhere to the probe, but rather undergo a transient collision, was arrived at following a number of experiments using a probe heated to 1000^{o}C before it entered the flame.

Fig 25 Effect of a hot probe on the spikes

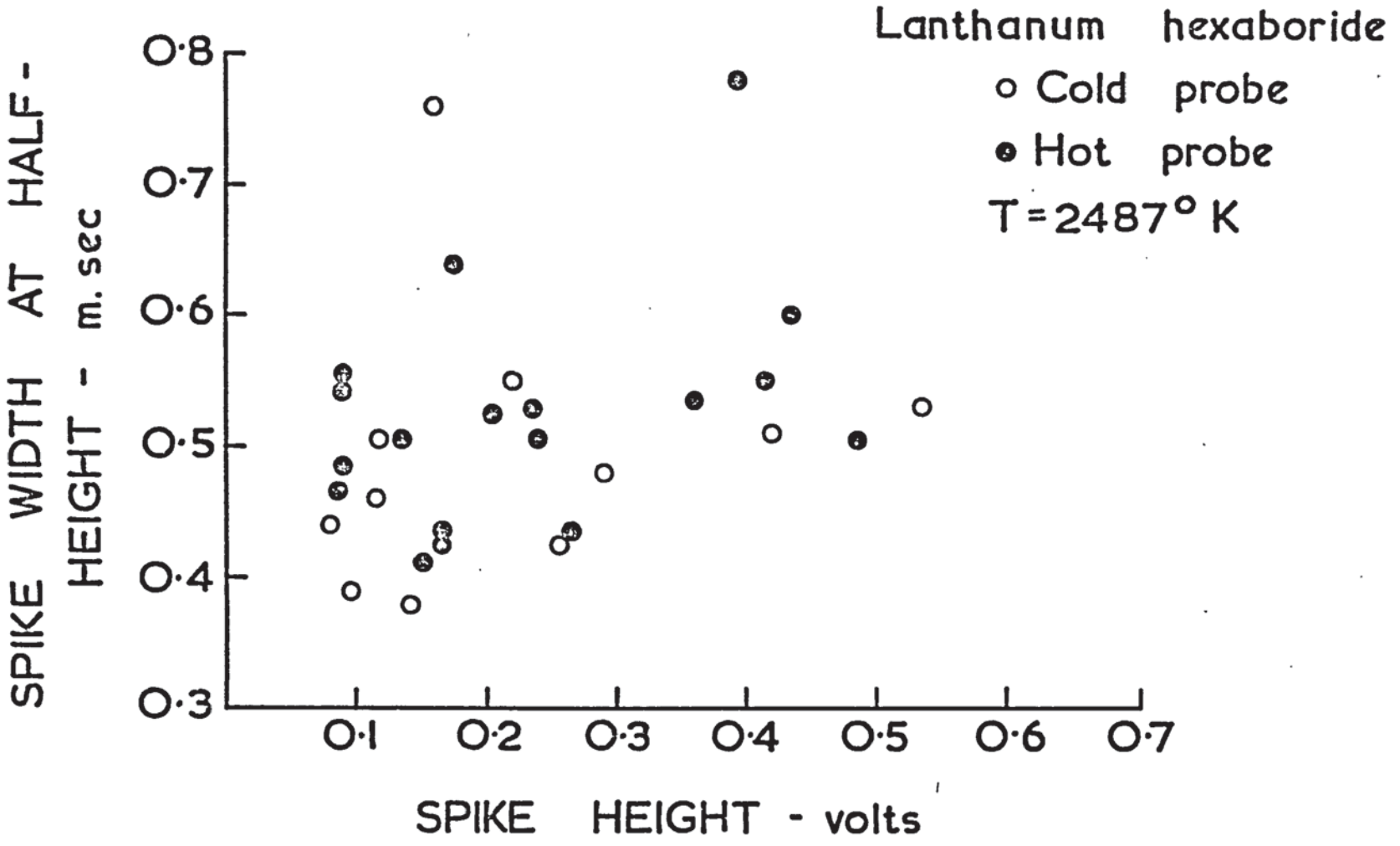

The pre-heating was achieved using a horizontally burning oxy-coal gas flame, which was positioned such that the probe passed along this flame for some 10 cm before it entered the experimental flame. It would be expected that, if cooling of the particles were limiting the spikes, spike heights would be significantly increased using a hot probe. On the other hand, little effect would be expected if the probe-particle contact time were the limiting factor.

A typical result in a flame at 2487^{o}K is shown for lanthanum hexaboride in Figure 25, in which spike height is plotted against spike width at half-height, for both the hot and the cold probe. It will be noted that no increase in spike height has resulted from the use of a hot probe. It might be argued that the extent by which the temperature of the hot probe exceeded that of the cold probe might not have been sufficient to have a significant effect on the cooling time of the particles, remembering that the rate of cooling of a particle is proportional to the difference in temperature between the particle and the probe. However, it was observed in the experiments that the use of the hot probe resulted in a baseline on the oscilloscope with a pronounced tendency to rise. This was not caused by thermionic emission from the hot probe itself, since a stable baseline was obtained in clean flames. The baseline drift did not occur at every pass through the flame, and it was concluded that the effect was caused by an occasional particle sticking to the probe, and emitting continuously on subsequent passes until it was dislodged from the probe surface. This behaviour indicated that at the temperature of the hot probe, emission from lanthanum hexaboride was appreciable, and if it were the normal occurrence for particles to stick to the probe, a marked effect on the rate of cooling, and hence on spike height, would have been evidenced.

The corresponding graph for barium oxide is shown in Figure 26,

Fig. 26 Effect of a hot probe on the spikes

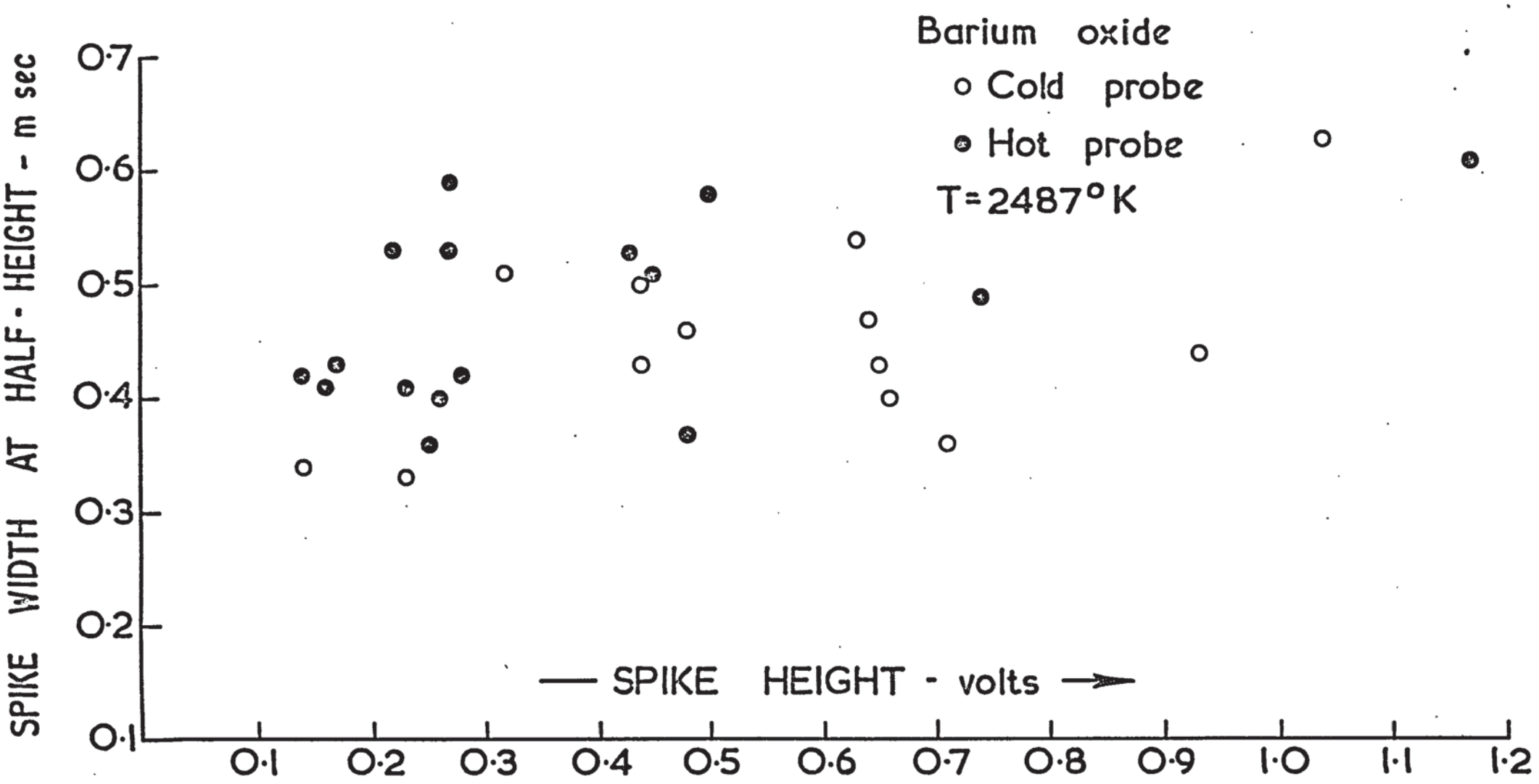

and again no enhancement of spike height is demonstrated, supporting the conclusion that the particles do not adhere to the probe. Two additional features may be noted on comparing this Figure with its predecessor. First, the range of spike widths is essentially the same in both cases, lying between 0.3 and 0.7 milliseconds, This constancy of spike widths is a further indication of the shaping of the spikes by the external circuit. Secondly, the upper limit of spike height is higher for barium oxide than for lanthamum hexaboride, in agreement with their respective work functions.

5.5. THE EFFECT OF FLAME CONDUCTIVITY ON THE SPIKES.

The majority of the work on the spikes was carried out in clean flames, i.e. flames to which no intentional addition of ionisable species was made. One run only was made in a seeded flame, and since fewer spikes than normal were observed, the results must be treated with reserve. In the experiments in question, 5×10^{-4} molar caesium chloride solution was atomised into a flame simultaneously supplied with lanthanum hexaboride. Measured spike heights and half-widths in the presence and absence of seeding are shown in Figure 27. It will be seen that there is no enhancement of spike height, but, significantly, a number of the half-widths for the spikes in the seeded flame are below 0.3 milliseconds. In Figure 25, 26 and 27 no spikes in clean flames possessed half-widths below thisfigure. In the discussion of thermionic emission from solid particles in Section 4,2,4, it was pointed out that space charge limitation could occur for very high electron currents, and that this would be reflected in a dependence of spike height on flame conductivity. It has since been established that the spikes are limited by the circuit response coupled with the contact time of the particle and the probe. Space charge effects may therefore be neglected, and the observed absence

Fig. 27 Effect of flame conductivity on the spikes

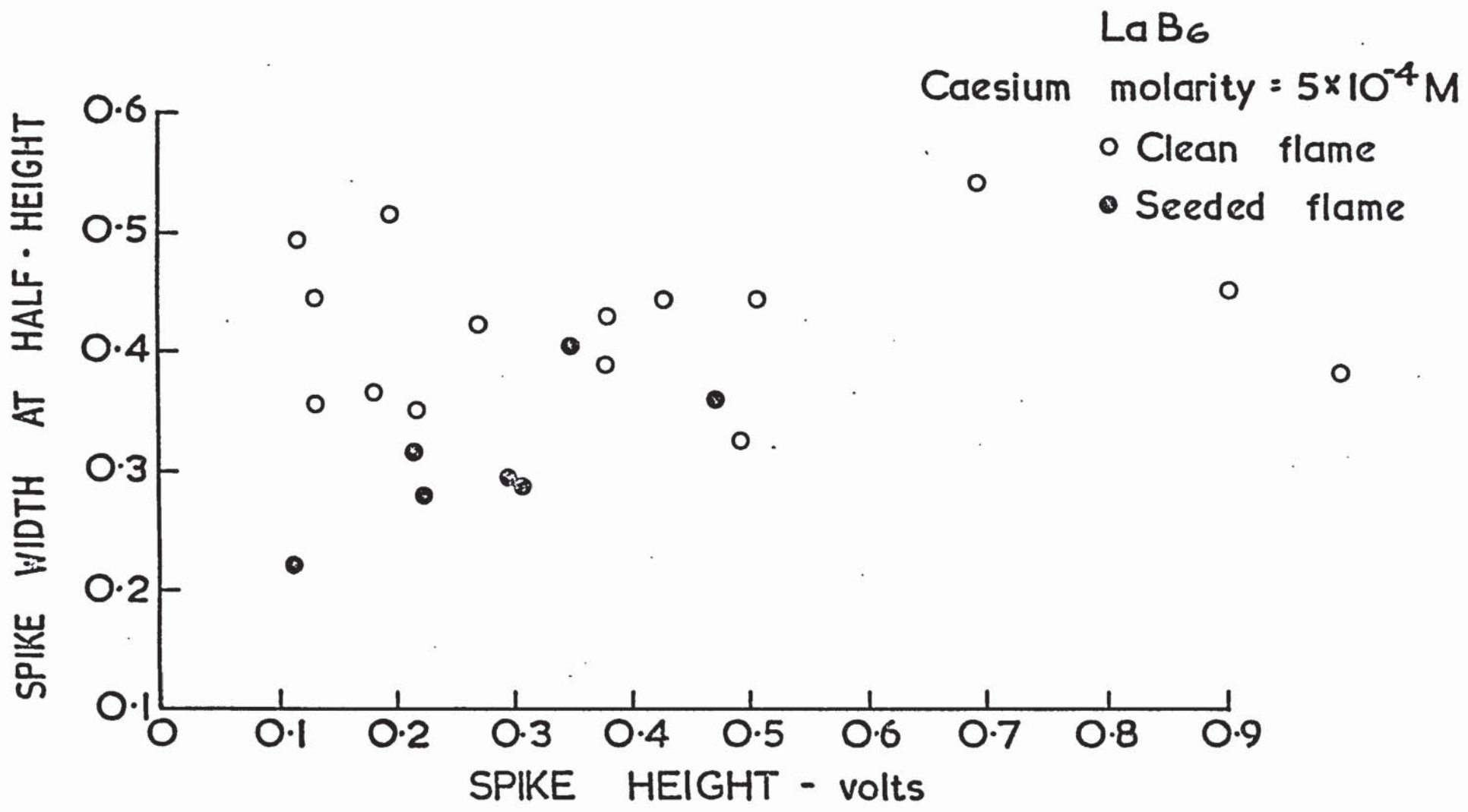

of any dependence of spike height on flame conductivity is readily understood. The reduced half-widths of the spikes may be interpreted in terms of the reduced time constant of the circuit accompanying the increase in flame conductivity. Unfortunately the reduction in half-width produced by seeding is considerably lower than predicted by the increase in flame conductivity. Using the probe calibration curve, the ion density in the seeded flame was found to be 10^{10} cm^{-3}. Reference to equation 5.2 will show that this level of ionisation should lower the time constant by more than an order of magnitude, while only a marginal effect on the spike height is observed. No explanation can be offered for this discrepancy, largely because of the lack of experimental results. More work is needed on the half-widths of spikes at a range of flame conductivities. Since the relaxation time of the positive ion sheath around the probe will be the ultimate limiting factor on the shape of the spikes, experiments of this type will furnish information on sheath conditions.

Fig. 28 The distribution of spike height

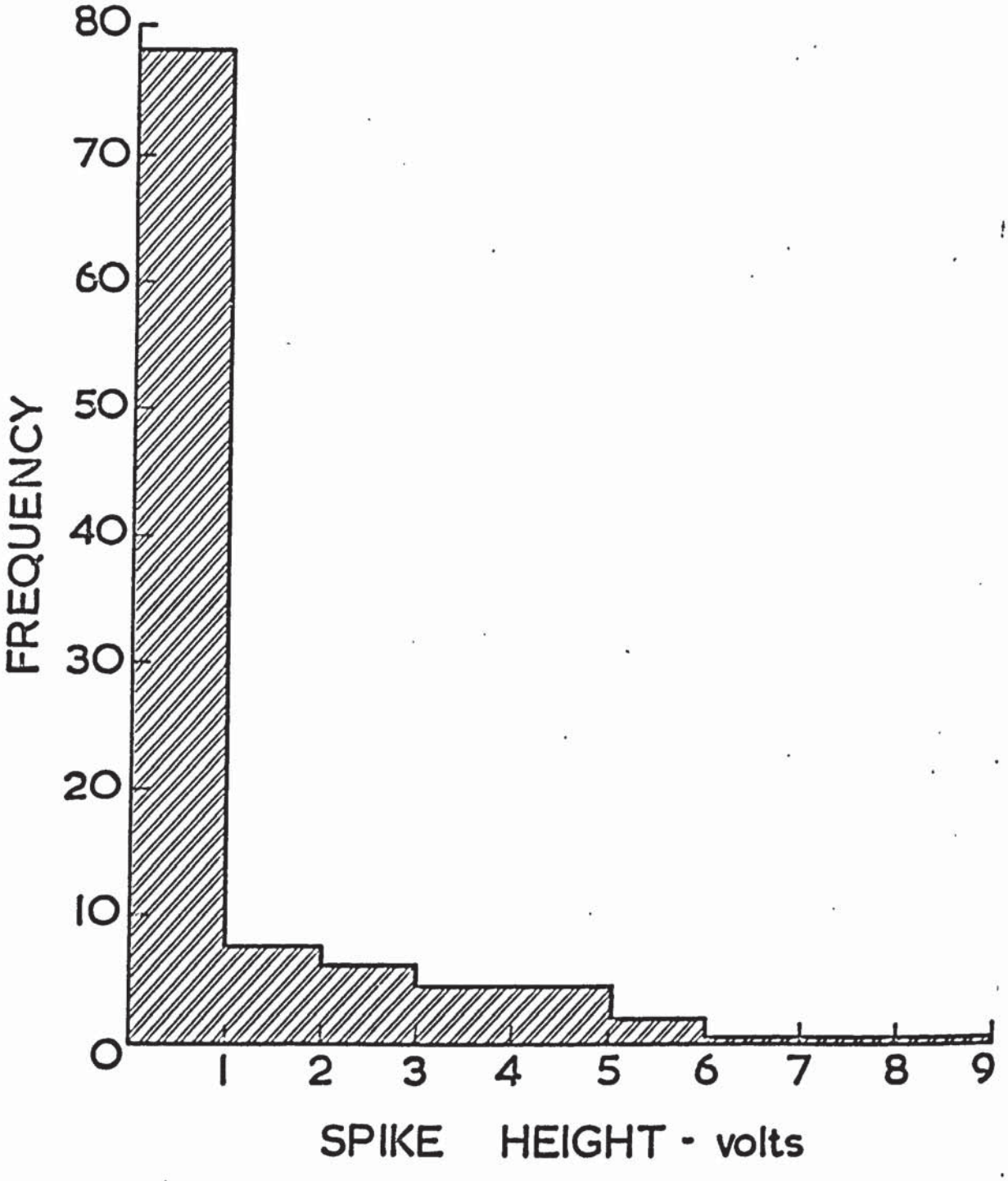

5.6. THE DISTRIBUTION OF SPIKE SIZES.

In the work reported in the previous three sections on the general properties of the spikes, the data was obtained by measuring all spikes occurring on the set number of oscillograms, which was usually twenty. However, it was not found possible to follow this procedure in the investigations of the relation of the spikes to material and flame properties. At the outset it was intended to analyse the spikes by relating the distribution of spike sizes to the particle size distribution of the powder producing them. This was prevented by the nature of the spike size distribution, which is shown for carbon in the histogram in Figure 28. It can be seen that the distribution is highly skew. More important, the majority of the spikes were small ones, and hence could not be measured with accuracy. It was therefore necessary to devise a sampling method. The procedure finally adopted was to select the top 10% of the distribution obtained at each set of experimental conditions, and measure the height of these spikes only. This sample usually amounted to between ten and thirty spikes. The arithmetic mean of the sample, termed the mean spike height, was used in the temperature plots discussed below. It is reasonable to suppose that the mean spike height at each temperature would be representative of the distribution of spike heights at that temperature, and a meaningful indication of the temperature dependence of the spikes should thus be obtained.

Two assumptions were made in the interpretation of the results. The first of these concerns the relationship between the temperature of the particles and that of the flame. Schack[57] has considered the situation in which the size of the particles is large compared with the mean free paths of the gas molecules in the flame. For soot particles in the absence of surface heating by catalytic reaction,

Fig. 29 Variation of spike height with height of probe in flame

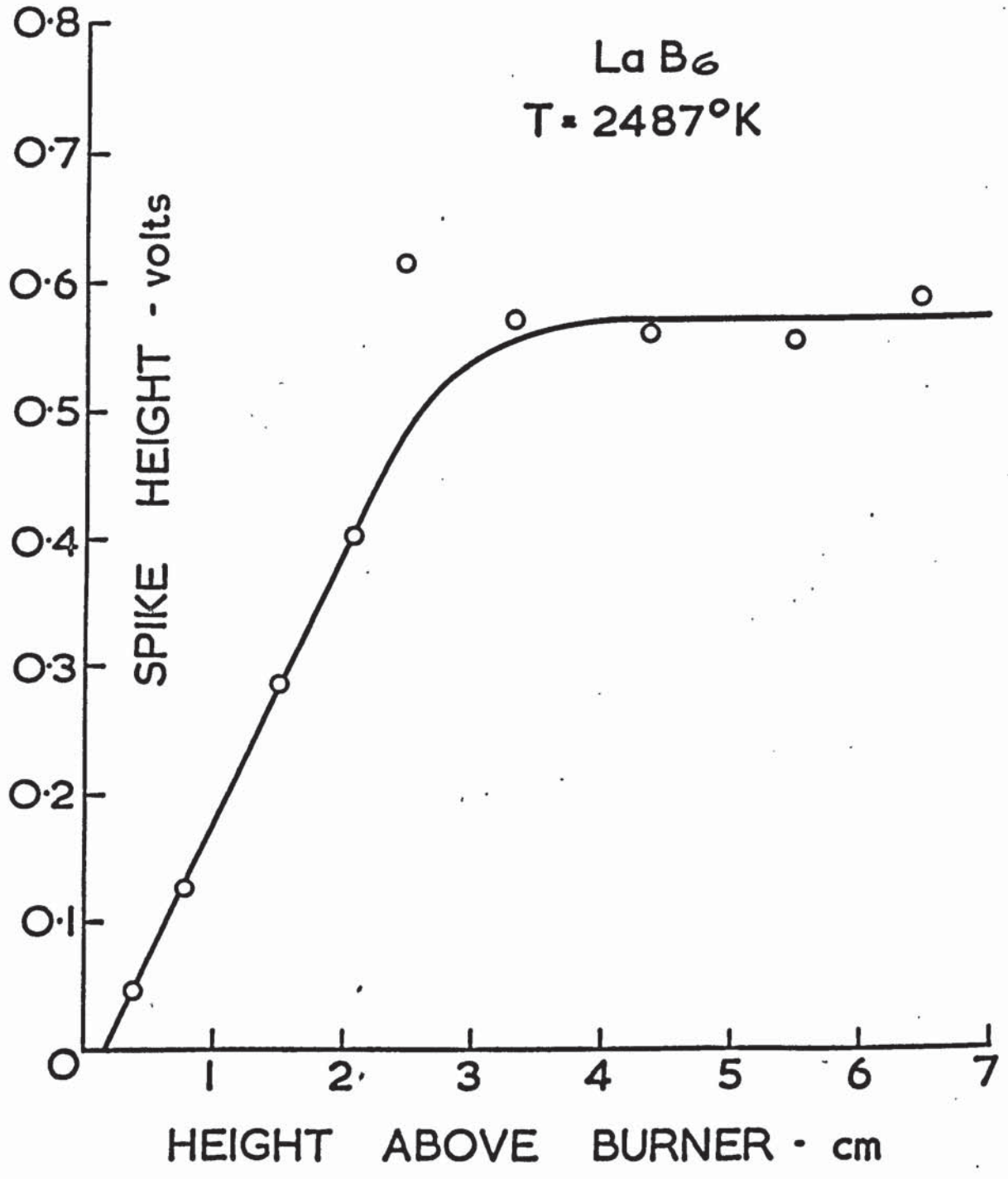

he concluded that the particles would have a temperature within $1^{o}K$ of the gas temperature. In the present work the mean free path of the gas molecules is of the order of 10^{-5} cm, and particle diameters at the upper end of the distribution are greater than 10^{-3} cm, On this basis of Schack's work it may therefore be assumed that, well removed from the reaction zone, the particles will be essentially at the flame temperature. The notable exception to this will be aluminium particles after ignition, for which the self-sustained combustion reaction may raise the temperature considerably above the flame temperature. In contrast, for materials which are evaporating rapidly, e.g. barium oxide in the hotter flames, particle temperatures may be somewhat lower than the flame temperature.

Secondly, it was assumed that the particles travelled through the flame at the velocity of the burned gases. This was valid since the gas velocity was of the order of 900 cm sec^{-1}, while the settling velocity of the particles used lay between 1 and 5 cm sec^{-1}. The assumption enabled the properties of particles at different heights in the flame to be related to residence times by means of the gas flow velocity.

5.7. THE VARIATION OF SPIKE HEIGHT WITH HEIGHT IN FLAME.

By raising and lowering the burner and elutriator relative to the probe, it was possible to determine spike heights as a function of height in the flame. A typical result for lanthanum hexaboride is shown in Figure 29, in which the mean spike height is plotted against distance along the flame. It can be seen that the spike height increases rapidly in the first 3 cm of the flame, and then levels off to an almost constant value. There are two obvious explanations for this behaviour. First, bearing in mind the dis-equilibrium near the reaction zone, it is possible that reactions

are occurring between the particles and the large numbers of free radicals in this region, resulting in a modified work function. Alternatively, the increase in spike height may be attributed to an increase in temperature of the particles with time. The curve in Figure 29 is not in good agreement with the first mechanism, which in view of the known distribution of free radicals would be expected to produce a much sharper rise in spike height initially, and a more gradual levelling off. The second suggestion is therefore more probable.

A significant contribution to the heating of small particles in hydrogen flames may result from catalytic recombination of hydrogen atoms, and an estimate of the efficiency of this process may be made using fairly simple concepts. The number of particles in a gas striking unit area per second from all directions is given by equation 3.4,

$$n = \frac{1}{4} N \bar{c} \qquad 3.4.$$

N, the total number of gas molecules per cm^3, is equal to 3×10^{18} cm^{-3} at 2500°K. Assuming that 1% of the total gas molecules are hydrogen atoms, N_H is 3×10^{16} cm^{-3}. $\bar{c}$ for hydrogen at the same temperature is 5×10^5 cm sec^{-1}. Substitution of these values into equation 3.4 gives

$$n_H = 3.75 \times 10^{21} \text{ cm}^{-2} \text{ sec}^{-1}$$

Since the heat of recombination of a pair of H atoms is 1.04×10^5 cal $mole^{-1}$, the total heat release from n_H atoms is

$$q = 3.24 \times 10^2 \text{ cal cm}^{-2} \text{ sec}^{-1}$$

The heat received by the particle in t seconds thus becomes

$$q_t = 4 \pi r^2 q t \quad \text{cal} \qquad 5.3$$

The heat required to raise the temperature of the particle to that of the flame is

$$Q = \frac{4}{3} \pi r^3 \quad C \, T \qquad \text{cal} \qquad 5.4$$

where ρ and C are the density and specific heat of the particle. Equating 5.3 and 5.4., the heating time t is given by

$$t = \frac{\rho \, C \, T \, r}{3q} \qquad \text{sec} \qquad 5.5$$

Inserting the numerical values ρ = 4.76 g cm^{-3}, C = 0.2 cal $^{o}K^{-1}g^{-1}$, T = 2200^{o}K, r = 10^{-3} cm and q = 3.24 x 10^{2} cal cm^{-2} sec^{-1}, the time to heat the particle to the flame temperature becomes

$$t = 2 \times 10^{-3} \text{ sec.}$$

The value of t given above is an upper limit to the heating time, since immediately above the reaction zone the hydrogen atom concentration may rise considerably above the 1% level assumed in the calculation. Furthermore, normal heat transfer from the flame gases will also assist in the overall process. A heating time of the order of milliseconds is supported by other evidence. Friedman and Majek[55], studying the ignition of aluminium particles by photographic techniques, found that the time taken for a 15 micron particle to reach 2300^{o}K was 0.5 milliseconds. It is therefore reasonable to assume that the particles reach the flame temperature in the first centimetre of the flame, and Figure 29 may consequently be interpreted in terms of an increase in temperature of the particles as they pass through a flame which is itself increasing in temperature with height. Indeed, comparison of Figure 29 with the temperature profile in Figure 6 for a flame of similar composition shows the essential similarity between the two curves. It can be seen that above a height of about 3 cm in the flame the spike height assumes an almost constant value, corresponding to the relatively constant temperature in this region of the flame. All of

the work on the temperature dependence of the spikes was accordingly carried out at a height of 5 cm to minimise the effects of temperature variation of the particles on the spike height.

5.8 THE TEMPERATURE DEPENDENCE OF THE SPIKES.

The results of the measurements on the spikes over the temperature range 1806 to 2630^{o}K are summarised in Table 5 below. The term "arbitrary units" refers to the height of the spikes in cm, as measured on the prints made from the oscillograms. The spike heights were converted to the same oscilloscope sensitivity, and at this setting 42 cm on the prints was equal to 1 volt on the oscilloscope. In the Table "I" signifies insufficient spikes for a meaningful result to be obtained.

TABLE 5

THE TEMPERATURE DEPENDENCE OF SPIKE HEIGHT

Flame Temperature ^{o}K	Mean Spike height P. (arbitrary units)				
	Ba O	La B_6	WC	C	Al
1806	3.70	I	I	1.14	I
1912	5.09	I	0.67	1.34	I
2135	9.22	1.29	1.05	8.42	I
2247	12.13	4.48	2.55	9.12	1.46
2336	16.36	7.0	4.38	17.80	0.93
2427	25.98	18.46	7.04	21.48	1.68
2487	31.84	17.72	8.48	21.92	1.0
2507	37.15	-	10.10	26.32	1.30
2570	39.56	17.28	42.44	-	-
2610	-	-	-	34.72	-
2630	47.69	23.87	23.28	-	-

Before proceeding to consider the compounds individually, there are a number of points to be noted from the Table. For the three materials of similar particle size, namely barium oxide, lanthanum hexaboride and tungsten carbide, the mean spike heights in most of the flames decrease in this order, which corresponds with the order in which the clean surface work functions increase, (cf Table 3). Carbon produces anomalously large spikes in view of its high work function, although in this connection the large particle size of this material must be taken into account. Finally, aluminium exhibits quite distinctive behaviour. The temperature below which no appreciable spikeproduction occurs is higher for aluminium than for any of the other materials, which is in accordance with the fact that aluminium possesses the highest work function. However, over the temperature range 2247 - 2507^{o}K where spikes are produced, spike heights for aluminium are essentially independent of temperature.

It was found that a plot of spike height P against temperature T for all of the materials except aluminium produced curves of exponential form, in agreement with the proposed thermionic emission mechanism for the spikes. The Richardson-Dushman equation, (4.24) when written in logarithmic form becomes

$$\log_{10}\left(\frac{J}{T^2}\right) = \log_{10}A - \frac{e\phi}{kT}\log_{10}e \qquad 5.6$$

In the case of the spikes, J, the saturation emission current is represented by the spike height P. Inserting the numerical values 11,600 for $^{e}/_{k}$ and o.434 for $\log_{10}e$, equation 5.6 becomes

$$\log_{10}\left(\frac{P}{T^2}\right) = \log_{10}A - \frac{5040\,\phi}{T} \qquad 5.7$$

A plot of $\log_{10}\left(\frac{P}{T^2}\right)$ against $^{1}/_{T}$ thus exhibits a slope of -5040 ϕ. This date in Table 5 was analysed by means of Richardson plots of this type, enabling values for the work functions of the materials to be obtained. The materials are considered individually below.

Fig. 30 Temperature dependence of spike height Lanthanum hexaboride

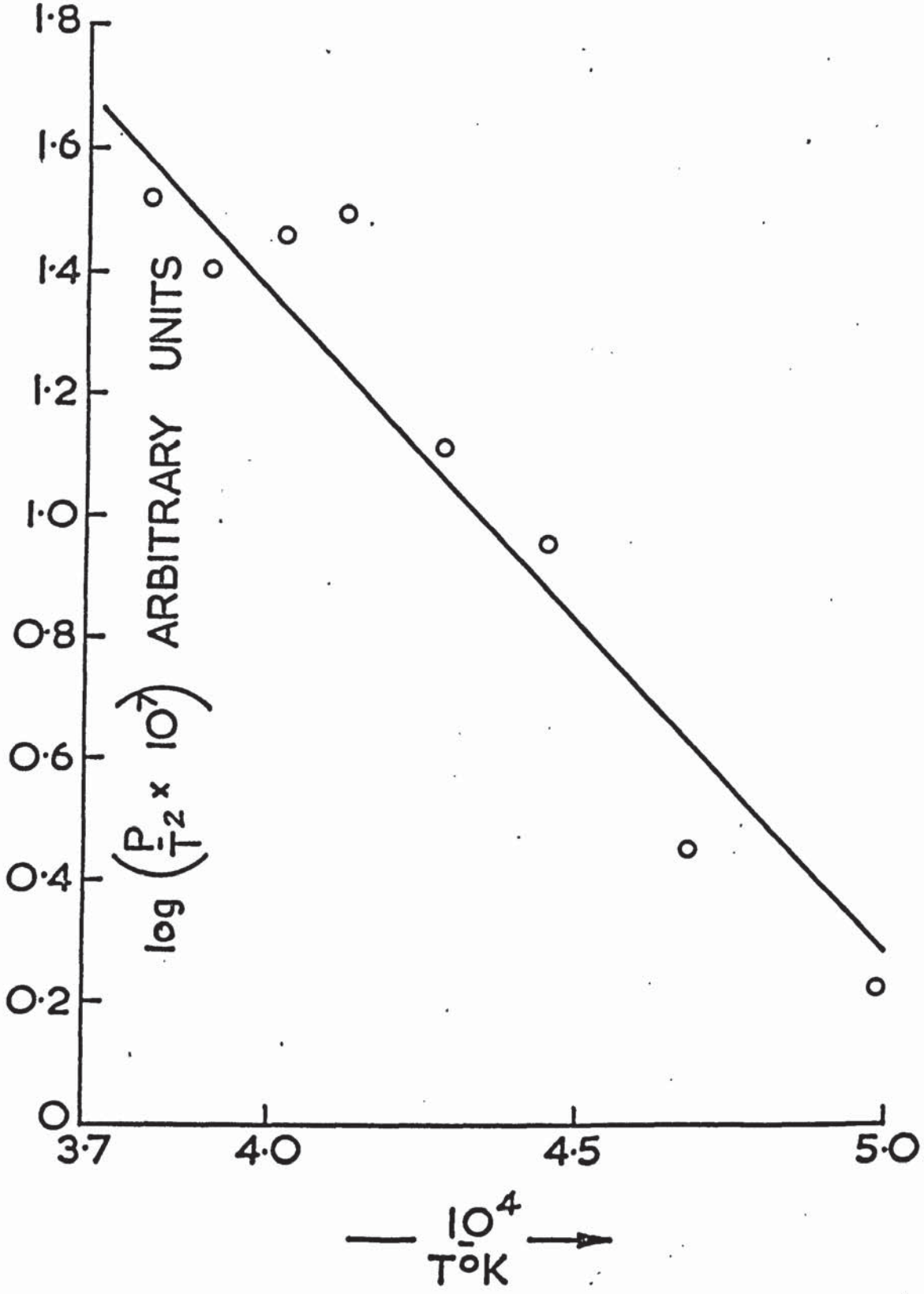

5.8. 1 LANTHANUM HEXABORIDE.

The work function of lanthanum hexaboride has been evaluated graphically by the application of equation 5.7 to the data in Table 5, and the resulting plot is shown in Figure 30. The least squares line fitted to the data gave a value for the work function ϕ of 2.20 eV. This value is slightly lower than the recommended value for ϕ of 2.66 eV[54], but values as low as 2.07 eV have been reported[54], and the divergence of the experimental result from the literature value is therefore acceptable. The factors which might lead to any modification of the work function of the particle material, notably impurities and oxidation by the flame gases will be of minimal importance in the case of lanthanum hexaboride. In the manufacture pure materials were used[59], and it is believed that the compound was essentially free from alkali metals. Only in the hotter flames would oxidation be important, when a mixed oxide coating would be established slowly over the surface of the particles. Since the effect of this would be to raise the work function relative to pure lanthanum hexaboride, it would appear that no modification of the work function from this source was occurring.

5.8. 2 TUNGSTEN CARBIDE AND CARBON.

The Richardson plots of the data in Table 5 are shown for tungsten carbide and carbon in Figures 31 and 32 respectively. Least squares treatment gave a value for ϕ of 2.5 eV for tungsten carbide, and 1.5 eV for carbon, both considerably lower than the literature values of 3.6 and 3.93 eV[54]. It can be seen from the Figures that while the experimental points for tungsten carbide lie on a good straight line, there is a large scatter in the experimental points of the carbon plot, and this casts some doubt on the reliability of the value of ϕ obtained for carbon.

Fig. 31 Temperature dependence of spike height Tungsten carbide

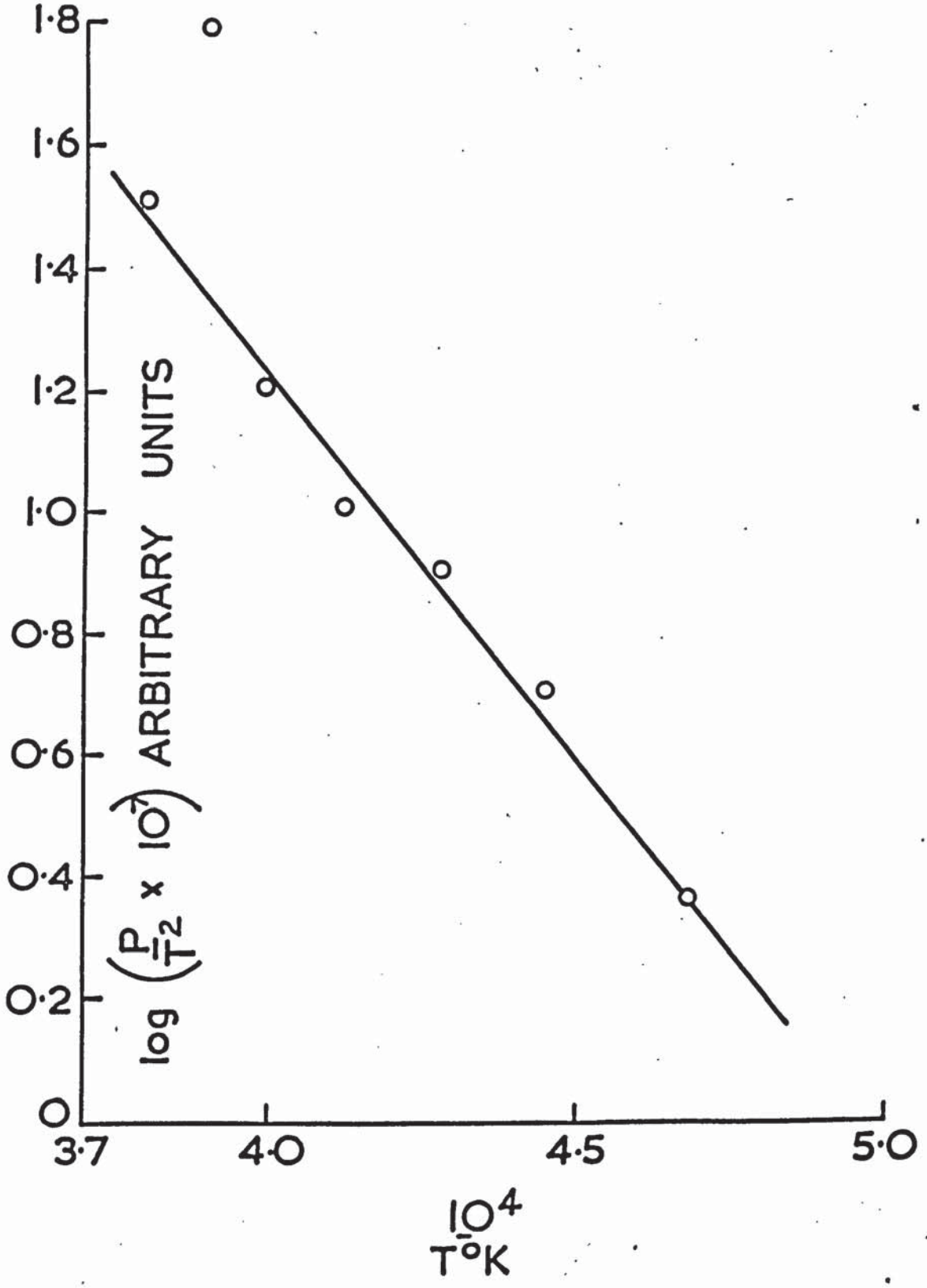

Fig. 32 Temperature dependence of spike height Carbon

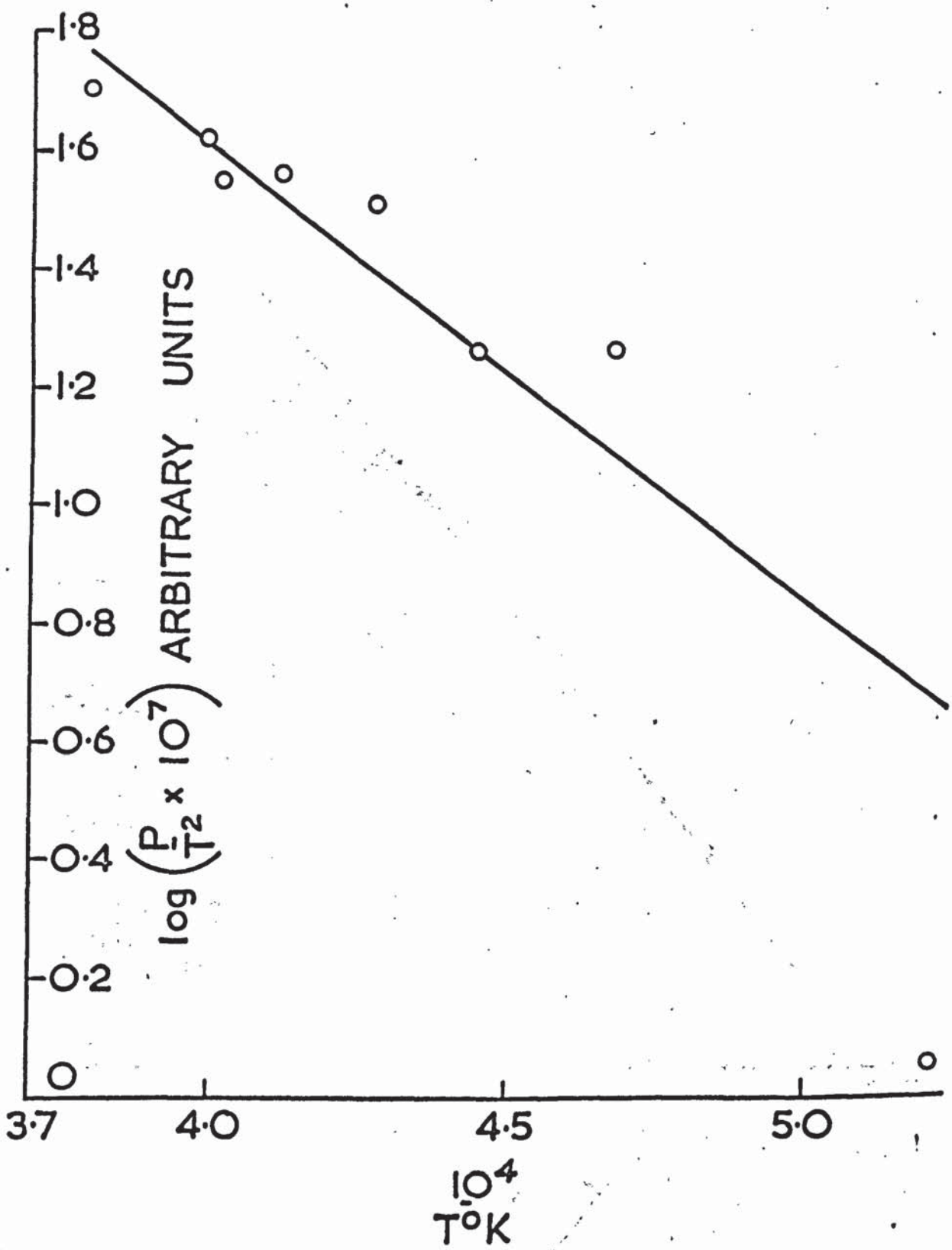

An explanation of the low work functions obtained for these materials is not immediately obvious. Kingdon[60] found that enormous increases in the work function of tungsten follow the adsorption of oxygen, although Farragher[50] has subsequently shown that a large part of the increase is an artefact, and that the true increase is no more than 1.8 eV. In any event it is unlikely that tungsten carbide will differ significantly from tungsten in this respect, and oxygen would be expected to increase the work function in this case also. While oxygen raises the work function of tungsten, it has been found that some organic compounds lowered it by 1 eV, reversibly[50]. The same work showed that the thermionic emission from a filament shown by X-ray crystallography to be tungsten carbide repeatedly gave Richardson plots whose slope corresponded to a work function of 4.5 eV. It therefore appears that the work function of tungsten carbide depends markedly on its previous history.

In both tungsten carbide and carbon significant quantities of sodium were present. Alkali metal atoms at the surface of an emitting material form an electrical double layer which reduces the work necessary to remove the electrons. In the classic case of caesium on tungsten[61], the work function of the metal is reduced from 4.52 eV to 1.5 eV. It is possible therefore that an effect of this type could be contributory to the reduced work functions obtained in this work.

5.8. 3 BARIUM OXIDE.

It can be seen from Figure 33 that the Richardson plot for barium oxide is fitted best by two straight lines of different slope, and two work functions are accordingly obtained. The lower temperature portion yields a value for ϕ of 0.6 eV, and

Fig. 33 Temperature dependence of spike height

Barium oxide

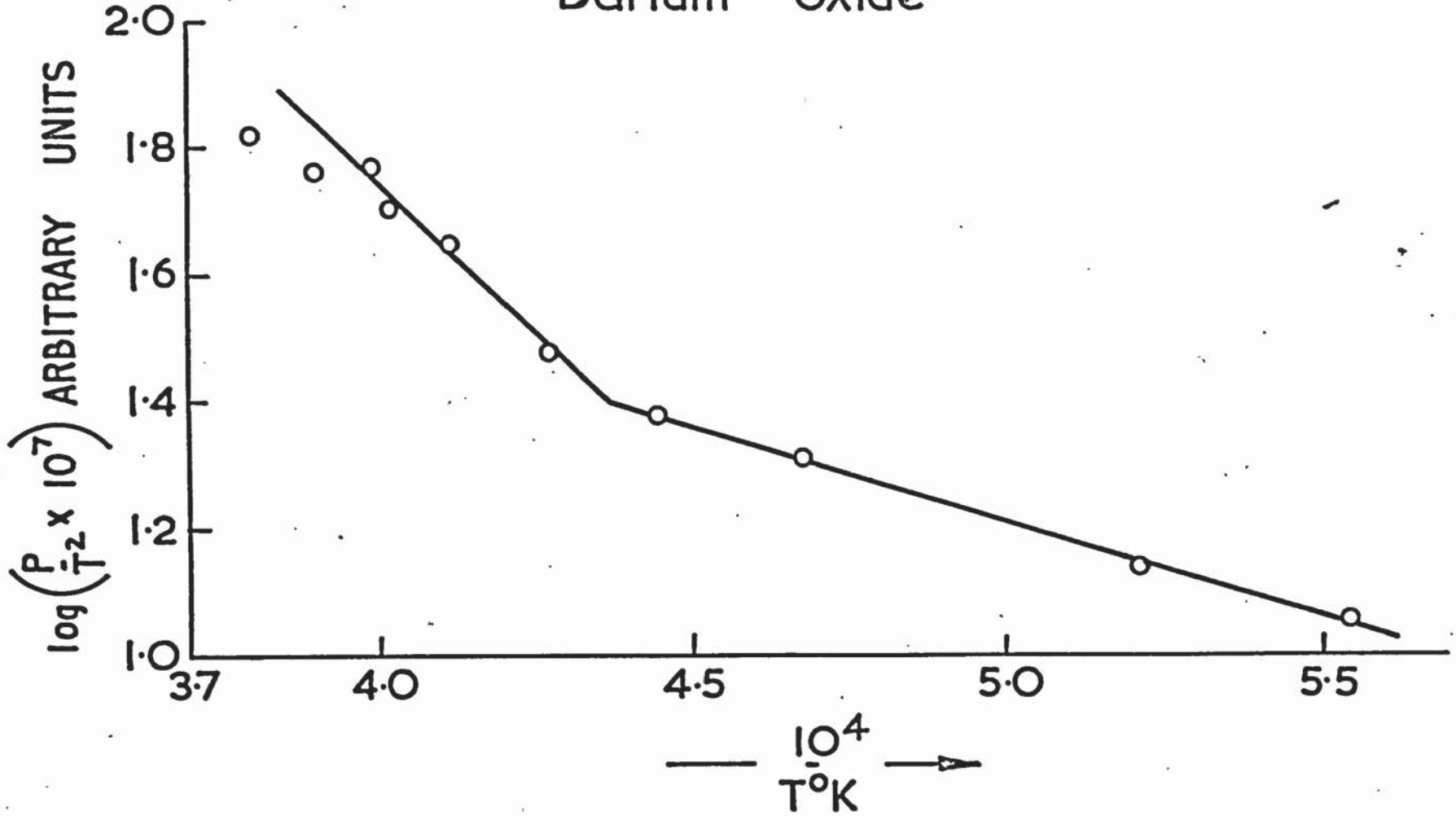

the upper portion a value of 1.94 eV. The break in the curve corresponds to a temperature of 2280°K, and it is tempting in view of the proximity of this figure to the melting point of barium oxide (2198°K) to suggest that a change of work function on melting is being detected. There is very little information available on the work functions of liquids. It is reported[62] that the increase in the interatomic distances on melting increases the barriers between the potential wells in the solid, and hence raises the work function. On the other hand Soo[63] considers that a reduction in work function will occur on melting. It is well known that an electron, distance x outside a plane conductor, experiences an attractive force by virtue of its electrical image, the force being $e^2/4x^2$. This force increases as the surface is approached, reaching a maximum at $x = x_d$, where x_d is a measure of the surface roughness of the material and is of the order of atomic dimensions. It can be shown that the work function ϕ of a material is equal to $e^2/2x_d$, and Soo suggests that for a liquid molecular agitation at the surface will increase x_d, so reducing the work function. Some support for this view is provided by the work of Toye[64] on liquid tin, in which a value for ϕ lower than the literature value for the solid was reported. Whichever theory is the correct one, it seems unlikely that there will be a difference of more than about 0.1 eV in the work functions of a liquid and solid material. It is therefore difficult to explain the magnitude of the observed increase in work function in the present work simply on the grounds of a change of phase. A factor which would have a profound effect, however, is the occurrence of non-stoichiometry in the oxide particles. This might arise, if, in the manufacture, free barium was occluded in the growing oxide particles. It is well known that the presence of small amounts of free metal in the alkaline earth oxides produces a marked increase in their efficiency as thermionic emitters. Removal

of the metal deactivates the coating. In the present case of barium oxide particles at flame temperatures, free metal atoms will diffuse to the surface and be removed. It is reasonable to suppose that in a solid particle the diffusion will be fairly slow. However, for liquid droplets the rate of diffusion will be much increased, and consequently deactivation of the particles will be more rapid. This behaviour would correlate with the observed increase in work function for molten barium oxide. More work is necessary to confirm this point. In particular it would appear that if this theory is correct a decrease in spike height with height in flame should be observed with barium oxide.

5.8. 4 ALUMINIUM.

It was shown in Table 5 that over the temperature range 2200 - 2500^{o}K no increase in the mean spike height occurred for aluminium. Accordingly no Richardson plot could be made for this material. However the small size of the spikes and the high flame temperature required before appreciable numbers of spikes were observed are both in accord with the high work function of aluminium. The constancy of the mean spike height for aluminium was attributed to the continuous reduction of particle diameter accompanying combustion of the particles. The combustion of aluminium has been studied by several workers[55,65], and the essential features of the process are now well established. When aluminium particles are injected into a flame, rapid formation of a thin oxide coating occurs and further oxidation takes place within this shell, metal vapour diffusing outwards to react with incoming oxygen. Thus the oxidation is diffusion controlled and is relatively slow below the melting point of the oxide. When melting occurs, it is accompanied by a discontinuity in the rate of oxidation, since diffusion through liquids is much more rapid than through solids. If the increased

rate of oxidation generates sufficient heat to sustain the oxidation reaction, the particles ignite. The ignition temperature in the case of aluminium is 2300°K. After ignition the particles burn by a vapour-phase diffusion flame, with a burning rate controlled by gas-phase diffusion of the oxidant.

The appearance of flames containing aluminium particles in the present work were in agreement with the combustion mechanism described above. A sharp increase in luminousity of the particles occurred when the temperature of such flames was raised above 2300°K, and a diffuse blue colouration was produced in the flame. Further increase in temperature resulted in a corresponding increase in the intensity of the light emission, coupled with a decrease in the number of particle tracks visible in the flame.

The number of spikes observed on the oscilloscope was also reduced in the hotter flames. In the light of these observations it is not surprising that no temperature dependence was demonstrated by the spikes for aluminium, since by virtue of the high rate of combustion there will be a steady reduction in the mean particle diameter. It would therefore seem that measurement of the work function of aluminium by the method applied to the materials considered earlier will only be possible using a more sensitive apparatus at temperatures below the ignition temperature of the metal.

5.9. CONCLUSIONS

The investigations of the spikes produced by solid particles on collision with an electrostatic probe, which have been described in this chapter, have clearly demonstrated the dependence of spike height on the temperature and work function of the particle material. The results thus confirm the thermionic emission mechanism proposed for the spikes. The work function values obtained from the Richardson plots are collected for comparision purposes in Table 6 below.

TABLE 6

THERMIONIC WORK FUNCTIONS

Material	Work Function ϕ eV	
	Experimental	Literature
Barium oxide	0.6 , 1.94	1.66
Lanthanum hexaboride	2.20	2.66
Tungsten carbide	2.50	3.60
Carbon	1.50	3.93

The discrepancy between the experimental and literature values for the work functions, which is particularly noticeable for carbon, have already been discussed. It is considered that in view of the marked effects on thermionic work functions which are known to occur in gaseous environments, the experimental values are reasonable ones. It can also be seen from Table 6 that, in passing from barium oxide to tungsten carbide, a similar trend in work functions is observed for the experimental results as for the literature values. This serves as additional support for the reliability of the experimental values. The relative magnitudes of the spike heights, which are shown in Table 5, are more difficult to interpret, since here the effect of particle size becomes important. The electron emission

from a particle is proportional to its surface area, and hence is related to the square of the particle diameter. From Figures 20 and 21 it can be seen that, for carbon, the largest 10% of the particles possess diameters four times as great as those of the corresponding sample of lanthanum hexaboride particles. On particle size grounds alone, therefore, assuming equal work functions, electron emission from carbon particles would be expected to be sixteen times as great as that from lanthanum hexaboride. Remembering the low value of ϕ obtained for carbon, and the fact that the actual area of the carbon particles will be markedly greater than the geometric area because of the occurrence of aggregation, this figure should be greatly increased. However, Table 5 shows that the mean spike height for carbon never exceeds that of lanthanum hexaboride by more than a factor of six. This anomaly is not restricted to carbon alone. Reference to the particle size distributions in Figure 20 shows that the particle diameter of the top 10% of lanthanum hexaboride particles exceeds that of the corresponding sample of tungsten carbide particles by a factor of two. This would indicate that, irrespective of its lower work function, the mean spike height for lanthanum hexaboride should be four times that of tungsten carbide, in a given flame. Again, Table 5 shows that this figure is not approached, and that the difference between the mean spike heights of lanthanum hexaboride and tungsten carbide is below that demanded by particle size considerations alone. It is therefore evident that the full effect of particle size is not being observed in the results. No explanation can be offered for this at the present time.

It was shown in section 4.2.4 that the initial observations on aluminium indicated that the spikes arose from emission currents much lower than those predicted by theory. This is a general feature

of the work. Taking lanthanum hexaboride as an example, Table 5 shows that the mean spike height at 2487^{o}K is 17.72 cm, or 0.42 volts. The normal 1 megohm load resister was used, and so the emission current equivalent to this spike height is 4.2×10^{-7} amps. The particle size results for lanthanum hexaboride suggest that this current should be equated with a particle diameter of 15 microns. When the theoretical emission current from such a particle is calculated using the Richardson-Dushman equation (4.25), inserting values of ϕ and A of 2.20 eV and 29 amp cm^{-2} ^{o}K^{-2}[54] respectively, a value for I of 4.18 amps is obtained. It can thus be seen that for lanthanum hexaboride the measured emission current is below that theoretically predicted by a factor of 10^{7}. Similar results are obtained for any of the other materials. These discrepancies are now understood in terms of the limitation imposed on the spike height by the contact time of the particle and the probe. It was shown in section 5.3 that the contact time is approximately constant, and is of the order of 0.2 milliseconds. It would seem that the contact time is governed by the nature of the process occurring during the collision, and it is of interest in this connection to note that the time taken for a particle moving with the flame gases to travel from the base of the probe to its equator is 1.4 milliseconds. This would indicate that a particle is rolled over the surface of the probe by the rising flame gases, a conclusion which could be confirmed by an examination of the spikes obtained with probes of differing size.

There are thus several unsolved problems, but the work has indicated that there are two aspects of the work which would repay further study. First, there are the general properties of the spikes, which if examined on suitable equipment should provide information on the conditions around the probe. Of particular relevance here is the rate at which the ion sheath reforms after the particle has left

the probe. Second, the spikes offer a means of determining thermionic work functions in flames, which to the writer's knowledge are unobtainable by any other means.

6. SUMMARY.

It can be seen that the original objective on the work, namely, the determination of the effect of solid particles on ion densities in flames, has not been realised. Indeed, one of the major achievements of the studies has been to show that meaningful measurements of positive ion densities cannot be made in flames containing solid particles. In this work, the concentration of solid particles in the flame has deliberately been minimised, to enable the behaviour of single particles to be examined. By this means a spike could be considered as an event involving one particle only. However, in investigationsof systems of practical interest, particle densities may be as high as 10^{10} cm^{-3}, and under these conditions an electrostatic probe will be effectively covered at all times by an incandescent coating. Such a probe will function as an emitting probe, and it was shown in Section 3.6 that the current drawn by a probe of this type may not be interpreted in terms of positive ion densities. In view of these considerations, recent work by Kelly and Padley[66] in which ion densities were measured in flames containing oxide smokes, is open to serious question. It would appear that reliable measurements of the level of ionisation in particulate flames will only be obtained using the microwave attenuation technique.

It has been shown that the spikes themselves are able to yield valuable information on the thermionic properties of materials in combustion systems. However, extensive work function measurements have not been possible, since a considerable amount of effort was involved in the elucidation of the process giving rise to the spikes.

This included the attempts made to scale up the process by employing ball bearings and metal wires to simulate the behaviour of solid particles, although this work was of limited usefulness in view of the fact that only qualitative results were obtained. Nevertheless, these experiments assisted in the general development of the theory of the spikes, and observations on the iridium wire served to emphasise the extent to which work functions can be modified when materials are exposed to flame gases.

Of the work functions obtained by analysis of the temperature dependence of the spikes, that for lanthanum hexaboride is considered to be the most reliable. A value for the work function ϕ of 2.2 eV was obtained, compared with a recommended literature value of 2.66 eV. This material was in many ways ideally suited for the studies, since it was substantially free from impurities, and furthermore would not be markedly affected by high temperature flame gases.

In contrast, the low experimental values for the work functions of tungsten carbide and carbon, 2.5 eV and 1.5 ev respectively; were almost certainly influenced by alkali metal impurities. Since the literature values are given as 3.6 eV and 3.93 eV for these materials, it can be seen that the discrepancy, particularly in the case of carbon, is quite large. It is clear that, in any future work, every effort must be made to obtain pure materials. Only in this way can the true effect of electropositive species be established, by independent addition of known amounts of suitable additives.

The two work functions of 0.6 eV and 1.94 eV which were obtained for barium oxide, are probably the most interesting observations arising from the work. The location of the discontinuity in the Richardson plot so near to the melting point of this material is a fair indication that

the work function change is associated with a change of phase. There is very little information available on the work functions of liquids, which is particularly unfortunate since several of the materials which are of interest in M.H.D. power generation and rocketry would be present in the liquid state. The experimental determination of the work functions of liquids is therefore very attractive.

For the fifth material investigated using the probe method, aluminium, it proved impossible to obtain a value for the work function of the metal, because of the high rate at which it was consumed by combustion. These experiments indicate that the applicability of the probe technique for determining work functions is restricted to materials which are not evaporating rapidly or subject to vigorous combustion under the conditions obtaining in laboratory flames.

In this work a phenomenon has been observed and identified. Much work still remains to be done, and a number of improvements in experimental techniques can be made, in particular with regard to the measuring system. This was designed for conventional probe measurements and was not well suited for observations on the spikes. A suitably modified electrometer which would count and measure the spikes would not only increase the accuracy of the measurements but also reduce the tedium of the analysis of the results. Concerning the general properties of the spikes, the influence of flame conductivity and particle size has yet to be established. To date the high end of the particle size spectrum has been of primary interest, while future development must be aimed at determining the smallest particle size which can be detected. This will determine the extent to which work functions can be determined for solid particles produced by liquid additives, since such particles are orders of

magnitude smaller than those used in these experiments. There can be no doubt, however, that in any event the basic technique developed in this work will be able to make important contributions to the subject of ionisation of solid particles in flames.

REFERENCES.

1. Smith F.T. and Gatz C.R.

   Progress in Astronautics and Aeronautics Vol. 12 K.E. Shuler Ed. Academic Press (1963)

2. Sodha M.S. and Bendor E.

   International Symposium on M.H.D. Electrical Power Generation 1964 No. 17

3. Honma T. and Fushimi K. Japanese Jnl. App. Phys. 5 (1966)

4. Sodha M.S., Palumbo C.J., and Daley J.T. (Brit. J. App. Phys. 14 916 (1963)

5. Sugden T.M. and Thrush B.A. Nature 168 703 (1951)

6. Einbinder H., J. Chem. Phys., 26 948 (1957)

7. Smith F.T., Proceedings of the Third Conference on Carbon, 419 Pergamon (1959)

8. Soo S.L. J. App. Phys. 34 1689 (1963)

9. Calcote H.F., 10th Symposium (International) on Combustion

10. Knewstubb P.F. & Sugden T.M. Proc Roy Soc. A255 520 (1960)

11. Sugden T.M. 5th Symposium (International) on Combustion p 406 Reinhold 1955

12. Padley P.J. & Sugden T.M. 8th Symposium (International) on Combustion p.164 Williams and Wilkins 1962

13. Shuler K.E. and Weber J. J. Chem. Phys. 22 491 (1954)

14. Su C.H. and Lam S.H. Phys. Fluids 6 1479 (1963)

15. Wheeler R.C. Dissertation Cambridge (1954)

16. James and Sugden T.M. Proc. Roy. Soc. A 227 312 (1955)

17. Kelly R. and Padley P.J. Nature 216 258 (1967)

18. Egerton A.C. and Rudrakanchana Proc. Roy. Soc. 225 427 (1954)

19. Woolley D.E. Dissertation Aston (1968)

20. Gilbert P.T. Anal. Chem. 34 1025 (1962)

21. Gaydon A.G. and Wolfhard H.G. "Flames" 2nd Edition Chapman and Hall (1960)

22. Mavrodineaunu R. and Boiteux H. "Flame Spectroscopy" John Wiley (1965)

23. Griffiths E. and Awbery J.H. Proc. Roy. Soc. A.123 401 (1929)

24. Langmuir I. General Electric Review 26 731 (1923)

25. Langmuir I. and Mott-Smith H. General Electric Review 27 449 (1924)

26. Johnson E.O. and Malter L. Phys. Rev. 80 58 (1950)

27. Calcote H.F. and King I.R. 5th Symposium (International) on Combustion p.423, Reinhold, 1955.

28. Calcote H.F. 8th Symposium (International) on Combustion p.484, Williams and Wilkins, 1962

29. Calcote H.F. 9th Symposium (International) on Combustion p.622, Academic Press 1963

30. Knewstubb P.F. and Sugden T.M. Nature 196 1312 (1962)

31. Padley P.J. 9th Symposium (International) on Combustion, Discussion p.635 Academic Press 1963

32. Travers B.E.L. and Williams H. 10th Symposium (International) on Combustion p.557 Combustion Institute 1965

33. Bohm D., Burhop E.H.S. and Massey H.S.W. "The Characteristics of Electrical Discharges in Magnetic Fields," Chapter 2, edited by A Guthrie and R.K. Wakerling, McGraw Hill 1949

34. Calcote H.F. and King I.R. J. Chem. Phys. 23 2203 (1955)

35. Boyd R.L.F. Proc. Phys. Soc. B.64 795 (1951)

36. Shultz R.G. and Brown S.C. Phys. Rev. 98 19 (1955)

37. Soundy R.G. and Williams H. 26th Agard meeting, (Pisa 1965)

38. Williams H. Private Communication

39. Langmuir I J. Franklin Inst. 196 754 (1923)

40. Saha M.N. Phil. Mag. 40 472 (1920)

41. Jensen D.E. and Padley P.J. Trans. Farad Soc. 62 2132 (1966)

42. Condon E.U. and Odishaw H. Handbook of Physics, 2nd Edition McGraw Hill 1967 4-181

43. Richardson O.W. "The Emission of Electricity from Hot Bodies" 2nd Edition Langmuir Longmans (1921)

44. Soo S.L. and Dimich R.C. Multi-Phase Flow Symposium. Am. Soc. Mech. Eng (1963)

45. Rayleigh Phil. Mag. 14 184 (1882)

46. Reid R.C. and Sherwood T.K. "The Properties of Gases and Liquids" 2nd Edition Mr.Graw Hill 1966 p.372

47. Gates D.S. and Thodos G. A.I. Ch. E. Jnl 6 50 (1960)

48. Dushman S. Phys. Rev. 21 623 (1923)

49. Langmuir I. Phys. Rev. 21 419 (1923)

50. Farragher A.L. Dissertation Aston (1966)

51. Mullaney G.J., Kydd P.H. and Dibelius N.R. J. Appl. Phys. 72 668 (1961

52. Klemperer D.F. J. Appl. Phys. 33 1532 (1962)

53. Huber E.E and Kirk C.T. Surface Science 5 447 (1966)

54. Fomenko and Samsonov "Handbook of Thermionic Properties" Plenum Press (1966)

55. Friedman R. and Majek A. Combust. Flame 6 9 (1962)

56. Cotton D.H. and Jenkins D.R. Trans. Farad. Soc. 64 2988 (1968)

57. Schack A. Z. tech. Phys. 6 530 (1925)

58. Banta H.E. Phys. Rev. 33 211 (1929)

59. Borax Consolidated Limited. Private communication.

60. Kingdon K.H. Phys. Rev. 24 510 (1924)

61. Langmuir I and Kingdon K.H. Science 57 58 (1923)

62. Page F.M. Private communication (1969)

63. Soo S.L. Private communication (1969)

64. Toye T.C. Proc. Phys. Soc. 73 807 (1959)

65. Brzustowski, T.A. and Glassman I Heterogeneous Combustion p.75 Academic Press 1964.

66. Kelly R. and Padley P.J. Trans. Farad. Soc. 65 367 (1969)